

**ESTIMATION OF PETROPHYSICAL DATA FOR ASSESSING
HYDROCARBON POTENTIAL IN WESTERN GHANA OILFIELD
(TANO BASIN)**



**A report submitted to the school of Graduate Studies, Kwame Nkrumah University of
Science and technology (KNUST), Kumasi, in partial fulfillment of the Degree of Msc.
Geophysics**

**By
OPOKU KUFFOUR
Bsc. (Hons) Physics**

(Supervisor Dr. S. K. Danuor)

May, 2008

CERTIFICATION

We certify that this thesis is the candidate's own research.

Signature

Dr. S. K. Danuor

(Supervisor)

Signature

Dr. A. B. C. Dadson

(Head of Department)

Signature.....

Opoku Kuffour

(Student)

DEDICATION

This work is dedicated to my late grandmother, Grace Tetteh Ashong for being the architect of my formal education.

ACKNOWLEDGEMENTS

This thesis work could not have been written without the support of my wife and family. For over a year now, my wife has taken care of duties I'm supposed to perform, and she also has typed a major portion of this report.

There are not enough words to express my appreciation to Ebenezer Apesegah, my Supervisor at Ghana National Petroleum Corporation (GNPC) and his colleague Gabriel Osatey, not forgetting the entire staff of G.N.P.C. for their immense contribution to this successful research. Mr. Apesegah never tried to overwhelm me, but his contributions are significant reason for my pride in this final work. Mr. Apesegah was responsible for keeping this work on track. A sweeter boss I have never had.

My academic Supervisor, Dr. S. K. Danuor, asked then most thought-provoking questions and detected the most embarrassing mistakes. His questions always led to a better explanation of a particular topic, and the mistakes he detects you will never see. Dr. Danuor is the definition of a great technical editor. He is someone who just won't let you get away with an explanation that isn't quite complete. Also many thanks go to all the lecturers at the Physics Department. Finally, my thanks go to the Almighty God who saw me through this work.

ABSTRACT

Well log data were obtained from Ghana National Petroleum Corporation for each of the six exploratory wells studied. For each well, the following logs were collected; resistivity log, sonic log, formation density compensated log, compensated neutron log and gamma ray log. These in situ well logs were subjected to well log analysis and interpretation methods. The following Petrophysical parameters; porosity, permeability, water saturation, reservoir thickness and volume of shale were estimated for each hydrocarbon-bearing zone delineated for each well. The data obtained have been analyzed and interpreted quantitatively, to assess the hydrocarbon potential of each well. The mean estimates for porosity and permeability of all the oil-bearing zones delineated, range from 23.75 % to 34 % for porosity and 65 md to 714.7 md for permeability, compared to mean porosity range of 8.5 – 23.15 % and permeability range of 6.83×10^{-2} md to 5.99 md of the gas zones. The results of the well logs interpretation suggest that oil-bearing zones are much more porous and permeable than the gas-bearing zones. This was evident throughout the wells. The estimates for the water saturation of hydrocarbon-bearing zones range from 6 % to 63.6 % indicating good hydrocarbon saturation potential. The reservoir thickness estimated for all the oil-bearing zones delineated range from 2 m to 40 m while the gas-bearing zones range from 4 m to 10 m. The Western Basin low estimated reservoir thicknesses for hydrocarbon-bearing zone suggests that reservoir reserves potentials are not sufficient, but the range 8 % to 36.8 % of volume of shale estimated for the hydrocarbon-bearing zones of the wells suggests that sandstone lithology of the Western Basin is clean. The Western Basin proved to be a high capital venture, as far as drilling is concern due to abnormal high pressure zones detected in almost all the wells studied.

TABLE OF CONTENTS

CONTENTS	PAGE
DEDICATION.....	i
ACKNOWLEDGEMENTS.....	ii
ABSTRACT.....	iii
LIST OF FIGURES.....	x
LIST OF TABLES.....	xii
NOMENCLATURE.....	xiii
CHAPTER 1 INTRODUCTION.....	1
1.1 General Introduction.....	1
1.2 Statement of the Problem.....	3
1.3 Research Purpose and Objectives.....	4
1.4 Research Hypothesis.....	4
1.5 Significance of Study.....	5
1.6 Scope of the study.....	5
CHAPTER 2 LITERATURE REVIEW.....	7
2.1 Introduction.....	7
2.2 History of Well Logging Interpretation.....	8
2.3 Location and Geological Setting.....	11
2.4 Stratigraphy Component of the Western Basin (Tano Basin).....	12
2.4.1 Aptian-Lower Albian (Kobnaswaso Formation).....	13

2.4.2 Lower-Middle Albian (Bonyere Formation or B shale).....	14
2.4.2.1 Uppermost lower Albian – middle Albian (Voltano Formation).....	14
2.4.3 Upper Albian (Domini Formation).....	15
2.4.4 Cenomanian.....	16
2.4.5 Turonian.....	16
2.4.6 Coniacian-Santonian.....	17
2.4.7 Uppermost Santonian to Intra Lower Campanian.....	17
2.4.8 Lower Campanian to Upper Campanian.....	17
2.4.9 Maastrichtian.....	18
2.4.10 Tertiary Sequences.....	19
2.5 Tectonic Component of the Western Basin.....	20
2.6 Well Logging Analysis.....	21
2.7 Well Drilling.....	22
2.8 Invasion Effects.....	22
2.9 Formation Evaluation.....	23
2.10 Costs.....	24
2.11 Types of Logs.....	25
2.11.1 The Gamma Ray Logs.....	25
2.11.1.2 Applications.....	25
2.11.1.3 Gamma Log Interpretation.....	26
2.11.1.4 Gamma Log Calibration.....	27

2.11.2 Induction logs.....	27
2.11.2.1 Principle.....	28
2.11.3 Other Resistivity Methods.....	29
2.11.3.1 Electric Log (E-Log) Interpretation.....	30
2.11.4 Neutron logs.....	32
2.11.4.1 Principle.....	32
2.11.4.2 Neutron Log Interpretation.....	33
2.11.5 Density logs	35
2.11.5.1 Principle.....	35
2.11.5.2 Density Log Interpretation.....	36
2.12 Neutron – Bulk Density Cross- Plot.....	37
2.13 Limitations.....	37
2.14 Acoustic Log Interpretation.....	38
2.15 Detection of Abnormal Pressures.....	39
2.16 Over Pressured formations of Oil and Gas Exploration.....	41
2.17 Nuclear Magnetic Resonance (NMR) Logging.....	42
2.18 The Archie Equation.....	43
2.18.1 Formation Factor - Porosity Relationships for Sandstones.....	44
2.19 Permeability.....	45
2.20 Fluid Saturation.....	47
2.21 Reserves.....	48

CHAPTER 3 METHODOLOGY.....	49
3.1 Data Preparation and Analysis.....	49
3.1.1 Picking of log values.....	49
3.1.2 Log Editing and Reconstruction.....	50
3.2 Reservoir Formation Evaluation.....	50
3.2.1 Delineation of Shale Beds and Vsh Determination.....	51
3.2.2 Porosity Determination.....	52
3.2.3 Resistivity of Formation water (Rw) from Resistivity-Porosity Logs.....	53
3.2.4 Water Saturation Determinations from Resistivity Logs.....	54
3.2.5 Selection of Irreducible Water Saturation.....	54
3.2.6 Permeability Estimation from the Wylie-Rose Method.....	55
3.3 Problems with data collection.....	55
3.4 Assumptions.....	56
CHAPTER 4 RESULTS AND DISCUSSIONS.....	57
4.1 Well Reservoir Statistics.....	57
4.2 Hydrocarbon Potential of Well 1S-1X.....	58
4.2.1 Interpretations of 1S-1X Well Results.....	59
4.3 Hydrocarbon Potential of Well 1S-3AX.....	60
4.3.1 Interpretations of 1S-3AX Well Results.....	60
4.4 Hydrocarbon Potential of Well 1S-4AX.....	61
4.4.1 Interpretations of 1S-4AX Well Results.....	61

4.5 Hydrocarbon Potential of Well ST-05.....	62
4.5.1 Interpretations of ST-05 Well Results.....	63
4.6 Hydrocarbon Potential of Well ST-06.....	64
4.6.1 Interpretations of ST-06 Well Results.....	64
4.7 Hydrocarbon Potential of Well ST-7H.....	65
4.7.1 Interpretations of ST-7H Well Results.....	65
4.8 Depth Plot of Vsh, Sw, and Ø for 1S-1X Well.....	66
4.9 Depth Plot of Vsh, Sw, and Ø for 1S-3AX Well.....	67
4.10 Depth Plot of Vsh, Sw, and Ø for 1S-4AX Well.....	68
4.11 Depth Plot of Vsh, Sw, and Ø for ST-05 Well.....	69
4.12 Depth Plot of Vsh, Sw, and Ø for ST-06 Well.....	70
4.13 Depth Plot of Vsh, Sw, and Ø for ST-7H Well.....	71
4.14 Detection of Abnormal Pressures Zones.....	72
4.14.1 Depth Plot of Well 1S-1X with Interval Transit Time.....	73
4.14.2 Depth Plot of Well 1S-3AX with Interval Transit Time.....	74
4.14.3 Depth Plot of Well 1S-4AX with Interval Transit Time.....	75
4.14.4 Depth Plot of Well ST-05 with Interval Transit Time.....	76
4.14.5 Depth Plot of Well ST-06 with Interval Transit Time.....	77
4.14.6 Depth Plot of Well ST-7H with Interval Transit Time.....	78
4.15 Problems with results and interpretation.....	79

CHAPTER 5 CONCLUSIONS AND RECOMMENDATIONS.....	80
5.1 Conclusions.....	80
5.2 Suggestions for Further Work.....	82
REFERENCES.....	83
Appendix A.....	89
Appendix B.....	96

LIST OF FIGURES

FIGURES	PAGE
Fig.2.1 Location map of the area of study.....	11
Fig 2a Schematic diagram, of a basic two coil induction system.....	28
Fig 2b Formation density logging device.....	36
Fig.4.1 Depth plot of Vsh, Sw and porosity for 1S-1X well.....	66
Fig.4.2 Depth plot of Vsh, Sw and porosity for 1S-3AX well.....	67
Fig.4.3 Depth plot of Vsh, Sw and porosity for 1S-4AX well.....	68
Fig.4.4 Depth plot of Vsh, Sw and porosity for ST-05 well.....	69
Fig.4.5 Depth plot of Vsh, Sw and porosity for ST-06 well.....	70
Fig.4.6 Depth plot of Vsh, Sw and porosity for ST-7H well.....	71
Fig.4.7 Depth plot of well 1S-1X with interval transit time.....	73
Fig.4.8 Depth plot of well 1S-3AX with interval transit time.....	74
Fig.4.9 Depth plot of well 1S-4AX with interval transit time.....	75
Fig.4.10 Depth plot of well ST-05 with interval transit time.....	76
Fig. 4.11 Depth plot of well ST-06 with interval transit time.....	77
Fig.4.12 Depth plot of well ST-7H with interval transit time.....	78
Fig.2.2 Distribution of resistivity in an invaded formation.....	98
Fig.2.3 Stratigraphic column of West Africa – Tano basin.....	99
Fig.2.4 South Tano Field 1S-1X well log response Curve.....	100
Fig.3.1 Porosity and lithology determination chart.....	101

Fig.3.2 Permeability from porosity and water saturation.....	102
Fig.3.3 Flowchart for Log Interpretation.....	103
Fig.3.4 Sonic log editing.....	104
Fig.3.5 Making log picks.....	105

LIST OF TABLES

TABLES	PAGE
Table 4.1 well reservoir statistics of each well.....	57
Table 4.2 Summary results of the hydrocarbon potential of well 1S-1X.....	58
Table 4.3 Summary results of the hydrocarbon potential of well 1S-3AX.....	60
Table 4.4 Summary results of the hydrocarbon potential of well 1S-4AX	61
Table 4.5 Summary results of the hydrocarbon potential of well ST-05.....	62
Table 4.6 Summary results of the hydrocarbon potential of well ST-06	64
Table 4.7 Summary results of the hydrocarbon potential of well ST-7H.....	65
Table 1a Well 1S - 1X reservoir section petrophysical raw data.....	89
Table 2b Well 1S - 3AX reservoir section petrophysical raw data.....	91
Table 3c Well 1S - 4AX reservoir section petrophysical raw data.....	94
Table 4d Well ST-05 reservoir section petrophysical raw data.....	95
Table 5e Well ST-06 reservoir section petrophysical raw data.....	96
Table 6f Well ST-7H reservoir section petrophysical raw data.....	97

NOMENCLATURE

A	-	Tortuosity factor
BHT	-	Bottom Hole Temperature
T_f	-	Formation Temperature
BVW	-	Bulk Volume Water
c	-	Conductivity
CNL	-	Compensated Neutron Log
C	-	Compaction factor for sonic porosity
DIL	-	Dual Induction Laterolog
DLL	-	Dual Laterolog
Δr_j	-	radius of invaded zone
t	-	Interval transit time of formation
SN	-	short normal log
t_f	-	interval transit time of fluid in borehole
t_{ma}	-	interval transit time of formation matrix
d_h	-	diameter of borehole
d_i	-	diameter of invaded zone (flushed zone)
d_j	-	diameter of invaded zone
EPT	-	Electromagnetic Propagation Tool
F	-	Formation factor
FDC	-	formation density compensated log
GR_{zone}	-	gamma ray reading from formation
V_{sh}	-	volume of shale

GR_{max}	-	gamma ray reading from shale
GR_{min}	-	gamma ray reading from clean zone
h_{mc}	-	thickness of mudcake
LDT	-	Litho-Density Tool
LN	-	long normal log
m	-	Cementation exponent
ML	-	Microlog
MLL	-	Microlaterolog
MOS	-	moveable oil saturation ($S_{xo} - S_w$)
LWD	-	Logging While Drilling
MWD	-	Measurement While Drilling
NGS	-	Natural Gamma Ray Spectrometry
NLL	-	Neutron Lifetime Log
NML	-	Nuclear Magnetism Log
PL	-	Proximity Log
k	-	Permeability
Φ	-	Porosity
PSP	-	pseudostatic spontaneous potential
ρ_b	-	bulk density of the formation
ρ_f	-	density of fluid in the borehole
ρ_h	-	hydrocarbon density
ρ_{ma}	-	density of the formation matrix
R_{SFL}	-	resistivity of spherically focused log
R_j	-	resistivity of invaded zone

R_{ILM}	-	resistivity induction log medium
R_{ILD}	-	resistivity induction log deep
R_{LLd}	-	resistivity of Laterolog deep
R_{LLS}	-	resistivity of Laterolog shallow
R_m	-	resistivity of drilling mud
R_{mc}	-	resistivity of mudcake
R_{mf}	-	resistivity of mud filtrate
R_{MSFL}	-	resistivity of Microspherically Focused Log
R_o	-	resistivity of the formation 100% water saturated (i.e. wet resistivity)
ROS	-	residual oil saturation ($1.0 - S_{xo}$)
R_s	-	Resistivity of adjacent shale
R_t	-	resistivity of uninvaded zone
R_w	-	resistivity of formation water
R_{xo}	-	resistivity of flushed zone
S_h	-	hydrocarbon saturation ($1.0 - S_w$)
SNP	-	sidewall neutron porosity
SP	-	spontaneous potential
SPI	-	secondary porosity index
SSP	-	static spontaneous potential
S_{wirr}	-	irreducible water saturation
S_w	-	water saturation of uninvaded zone
S_w/S_{xo}	-	moveable hydrocarbon index
S_{xo}	-	water saturation of flushed zone
TDT	-	Thermal Decay Time

BOPD - Barrel of Oil per Day
STB - Stock Tank Barrel
SCF - Standard Cubic Foot
MCF - Thousand Cubic Foot
MMCF- Million Cubic Foot

CHAPTER 1

INTRODUCTION

1.1 General Introduction

The word logging means recording of any information with respect to depth or time. The term 'well-logging' had a wider meaning and application in borehole geophysics, ever since its adaptation. Well-logging is a wireline study of different formations encountered in a well. In oil exploration, the interest lies mainly in identification of porous and permeable formation, their thickness and extent, and geometry of the reservoir. Well logging is exactly such a device which aims at acquiring this information, by measuring various physical, chemical and lithologically properties of the formations (Alger, 1980). This information when supplemented with other information available from core analysis, seeks to give depth, formation, its nature, fluid type, extent of fluid contact, porosity, permeability, mobility of hydrocarbon the flow rate, formation pressure and a score of other details with a high degree of precision. The advancement in electronics and instrumentation and the advent of computers have found their wide applicability in well-logging.

Thereby the well-logging has entered into the field of high technology and modernization. The transmission of down hole data through wireline cable has opened a new era in well-logging offering the scope of recording vast amount of information in the sense of real time data acquisition. Thus, presently the data acquisition and data interpretation through application of computers in well-logging has made new vistas for hydrocarbon exploration and exploitation.

Geophysical well logging, for more than a century has played a central role in the discovery and development of petroleum and natural gas resources. It tells the nature of rock formation penetrated by a drill. The drill itself does not provide unambiguous information about the formations. Rock cuttings tell us what lithologies are present but are unclear about exactly

where they occur. Even core drilling, which can be prohibitively expensive, yields incomplete information about formation fluids, and 100 percent core recovery is seldom possible. Hence the needs of an assortment of well logs for more complete evaluation of the formations.

The productivity of wells in a hydrocarbon-bearing (oil/gas) reservoir depends on Petrophysical properties. Hydrocarbon bearing reservoir rock consists of two components: the rock matrix and an interconnected pore network. The pores can have dimensions varying from sub-microns for tight sandstones to centimeter for vuggy carbonate rock (Levorsen, 1967).

The main Petrophysical properties are porosity, permeability, saturation and capillarity.

Porosity determines the storage capacity for hydrocarbons and permeability determines the fluid flow capacity of the rock. Saturation is the fraction of the porosity that is occupied, by hydrocarbons or by water.

Finally, capillarity determines how much of the available hydrocarbons can be produced. Accurate determinations of these Petrophysical properties are essential to assess the economic viability of the development of reservoirs. Lately, the geophysical well-logging technology has led to enormous developments in downhole data acquisition and interpretation techniques due to advances in science and technology particularly in the field of electronics and computerization. In the west, the logging companies are equipped with diversified advanced logging systems.

In Ghana too, these advances have found applications in oil/gas as well as in ground water and other mineral exploration. An attempt has been made here to depict the application of well logging in oil exploration in Ghana. Since the users are many and applications are wide, no claim is made to cover all spheres of applications.

1.2 Statement of the Problem

Ghana has developed over the past years; the industrial and domestic demand for power has increased as well. At the same time, drought conditions have affected Ghana's ability to generate power through its large hydro-electric facilities at Lake Volta (Troy Ikoda Group, 2001).

The search for alternative methods of generating electrical power using the potential gas reserves at south Tano has necessitated for this research to be carried out, using less expensive geophysical methods, such as well logging analysis to further enhance the prospect of oil and gas accumulation in Western Ghana oilfield.

1.3 Research Purpose and Objectives

Petrophysical data estimations and analysis for assessing the hydrocarbon potential in the western Ghana oil field is the focus of this study.

The study seeks to use the modern day industrial petrophysics methods to estimate these Petrophysical parameters; however, the research was carried out with the following specific objectives:

- I. To estimate porosity, water saturation, and permeability from the study wells.
- II. To estimate the volume of shale of the wells.
- III. To delineate hydrocarbon bearing zones of the reservoir wells.
- IV. To estimate the thickness (pay zone) of hydrocarbon bearing zones.
- V. To estimate reservoir statistics parameters such as gross reservoir thickness, net pay, and the net-gross ratio of the wells.
- VI. To predict and locate abnormal pressure zones within the wells.

Log cross plots such as compensated neutron log and formation density compensated log will be used to accurately determine the true formation porosity of the reservoir. The compensated

borehole log readings when plotted with depth of reservoir will tell us how acoustic velocity changes with depth.

Porosity determines the storage capacity for hydrocarbons and permeability determines the fluid flow capacity of the rock. Saturation is the fraction of the porosity that is occupied by hydrocarbons or by water.

This method is also used to determine pore pressure and gas zones within the reservoir. Finally, capillarity determines how much of the available hydrocarbons can be produced. Accurate determinations of these Petrophysical properties are essential to assess the economic viability of these reservoir wells in the Western Ghana oilfield. These are some of the petrophysics methods going to be employed in the estimations and analysis of this study.

1.4 Research Hypothesis

Oil was discovered in an Upper Albian age reservoir by Phillips Petroleum with the drilling of the 1S – 1X exploratory well in 1978. This reservoir is structural feature contained by a major rift fault to the south and west and by either a dip closure or series of ramped faults to the north and east.

This discovery well tested about 1600 BOPD of 32° API oil, with about 8 MMCFD gas from the cretaceous upper Albian sand. Phillips Petroleum attempted to delineate the field with an additional three wells (the 1S – 1X, 1S – 3AX and 1S – 4AX). Only the 1S – 4AX was drilled in the main reservoir closure and encountered oil in Upper Albian Sand where rates of up to 1500 BOPD were achieved. Phillips decision was that the reservoir potential was not sufficient and abandoned the prospect (Troy Ikoda Group, 2001).

In 1984, Petro Canada attempted two locations on the very crest of the main South Tano structure. The two wells drilled, ST – 05 and ST – 06, both tested hydrocarbons. The ST – 05 indicated the presence of a gas cap by testing gas and condensate (21.5 MMCFD with 389

BOPD of 66° API condensate). PetroCanada, considering the results of these two wells, also decided that reservoir potential was insufficient to warrant further development.

From the above results, it could be hypothesized that “Tano basin now called the Western basin has insufficient potential for hydrocarbon”. This stands to be proved or disproved based on the results of this study.

1.5 Significance of Study

In the past, much emphasis was given to geochemistry, core analysis and seismic survey in the exploration work with little or no work in petrophysics analysis.

The necessary components for the existence of a hydrocarbon bearing reservoir at Tano Basin have been proved through the drilling of wells and the acquisition of seismic data. There is a reservoir quality rock, which is in the presence of structural trap and is charged with hydrocarbon (Williams, 1995).

However because of the complex nature of the structural and stratigraphy of the reservoir, and the cost associated with developing an offshore resource, it is yet to be established that this oil resource can be exploited.

With advent of modern well logging tools with enhanced data acquisition the need of petrophysics analysis of reservoir wells cannot be over emphasized. Therefore this study has the tendency to enhance the hydrocarbon potential of the Western basin.

1.6 Scope of the study

Since the early 1970s few wells have been drilled in and around South Tano offshore basin.

In this study, in situ raw well log data is reviewed from a total of six wells. Wells were grouped according to geographical location and stratigraphy. Cross plots such as compensated neutron log and bulk density trends were used to estimate effective porosity of

zone of interest. Compaction trend curves were also used to indicate over-pressured zones as shown in figure 4.7.

From the well groupings, representative wells were chosen for detailed well log analysis. These analyses included log editing and reconstruction, standard formation evaluation, and rock properties interpretation.

CHAPTER 2

LITERATURE REVIEW

2.1 Introduction

The evolution of well log analysis methods over the past 50 years is fascinating and illuminating subject because obsolete but traditional definitions, abbreviations, symbols, and methods still pervade the industry. Although well logging is a relatively young science, initial work in the field dates back over 100 years, as early as 1869, about the same time as Drake made the first discovery of oil in the U.S., Lord Kelvin in Great Britain was making interpretation of heat flow in shallow wellbores by measuring temperature vs. depth (Crain, 1986). Segesman (1980) published a 50 year historical review of well logging in the 50th Anniversary Issue of GEOPHYSICS. Johnson (1962) and Allaud and Martin (1977) also published historical reviews of well logging. Because well logging is a broad subject, a limit is placed on the scope of this review to only petrophysical measurements made in a borehole. Archie (1942) defined the term “petrophysics” as the science wherein the physicochemical and petrological relationships of rocks and their geologic significance are studied. Since well logging employs geophysical measurements in a borehole, many use the term “borehole geophysics” interchangeably with the term “well logging.” [Ed. Note: Some scientists reserve the term “borehole geophysics” to borehole-to-surface, surface to-borehole, and cross-borehole techniques.]

It is believe that well logging is the application of borehole geophysics and other measurements to petrophysics. Borehole geophysics may also be applied on a larger scale, possibly involving transducers on the surface or in other boreholes.

Today, the detailed analysis of a carefully chosen suite of wireline services provides a method of deriving or inferring accurate values for the hydrocarbon and water saturations, the porosity, the permeability index, and the lithology of the reservoir rock.

The purpose of any Geophysical Log is to provide meaningful information about the geological and physical conditions in and around a borehole (Asquith and Gibson, 1982). Many books have been written on the subject of log interpretation. Fundamental Log Interpretation has not changed in decades and will probably not change. Almost all oil and gas produced today come from accumulation in the pore spaces of reservoir rocks –usually sandstones, limestones, or dolomites (Allen, 1989). The conditions necessary for a commercial accumulation of oil and gas are: a mature source rock, a reservoir rock with a migration route between source and reservoir, an impermeable seal, or cap rock, above the reservoir; finally, the source, reservoir and seal must be arranged so that the oil is trapped (Hobson, 1984).

The amount of oil or gas contained in a unit volume of the reservoir is the product of its porosity by the hydrocarbon saturation. In addition to the porosity and the hydrocarbon saturation, the volume of the formation containing hydrocarbons is needed in order to estimate total reserves and to determine if the accumulation is commercial. Knowledge of the thickness and the area of the reservoir are needed for computation of its volume.

2.2 History of Well Logging Interpretation

The first recognizable technical paper on log interpretation was published in 1934 by Schlumberger brothers and E.G Leonardon. The paper describes the electrical resistivity log. Since then, great advances have been made, particularly the last 25 years, in logging techniques and acquisition and interpretation of wireline log data and now sophisticated science. Log analysis at this time involved curve-shaped recognition- still a valid and commonly used qualitative approach to interpretation. Log curve shapes were determined visually from the recorded data when plotted vs. depth. These curves shapes were related to

rock sample and core description data to determine general rule of thumb for separating permeable, porous, oil-bearing beds from nonproductive zones.

Today, a four-arm dipmeter tool records 10 micro resistivity curves simultaneously, and a triaxial accelerometer and magnetometers provide highly accurate information on tool deviation and azimuth. The processing of these data into formation dip information is now done exclusively with electronic computers.

The gamma ray (GR) and neutron tools represented the first use of radioactive properties in well logging and the first use of down hole electronics. Unlike spontaneous potential (SP) and resistivity tools, they are able to log formations through steel casing, as well as in air- or gas-filled holes or in oil based mud. The neutron log was described by Pontecorvo in 1941.

In combination with the GR log, a neutron log enhances lithologically interpretations and well-to-well stratigraphy correlations. After about 1949, attention was given to the neutron log as a porosity indicator. However, the early neutron logs were greatly influenced by the borehole environment. It was not until the introduction of the sidewall neutron porosity tool in 1962 and the compensated neutron tool in 1970, that the neutron gained acceptance as a porosity measurement (Johnson, 1960).

The Dual Porosity neutron tool combines those two neutron measurements into a single tool. Early attempts at porosity determination employed micro resistivity measurements. The Microlog tool, introduced in the early 1950's, uses a miniature linear array of three electrodes imbedded in the face of an insulating pad, which is applied to the borehole wall. A borehole caliper is provided by the arm carrying the electrode pad and an opposite backup arm. The Microlog recording is also useful to delineate permeable beds, and other micro resistivities devices help establish the resistivity profile from the invaded zone near the borehole to the non invaded virgin formation.

The Microlaterolog tool was developed for salt mud in 1953. The MicroProximity log and MicroSFL log have followed. In 1951, the laterolog tool, the first focused deep investigating resistivity device, was introduced. It uses a focusing system to constrain the surveying current (emitted from a central electrode) to substantially a horizontal disc for some distance from the sonde. Focused resistivity logs are well adapted for investigation of thin beds drilled with low-resistivity mud. The laterolog device quickly supplanted conventional resistivity logs in salt mud and highly resistive formations (Snyder, Donald and Fleming, 1985).

Over the years, several laterolog tools were developed and used commercially. Today, the DLL dual laterolog tool, which consists of deep laterolog and shallow laterolog measurements, is the standard. It is usually run with a MicroSFL device as well. In freshwater mud, the original electrical log has been replaced by the induction log. The induction log was developed in 1949, as an outgrowth of wartime work with mine detectors, for use in oil-base mud. However, its superiority over the electrical log in freshwater mud was soon recognized. Other logging measurements include nuclear magnetic resonance, nuclear spectrometry (both natural and induced), and numerous cased hole parameters.

Today, logging is most often performed using digital data acquisition platforms. The data stored in a data file may have extensive statistical computation applied to it. Intelligent systems apply the same and sometimes better algorithms than their human counterparts once did. The result is faster and often times “smarter” interpretation (Doveton 1994). Taking the additional steps required to apply corrections to raw data and perform ‘sanity’ checks on results adds confidence to any interpretation.

2.3 Location and Geological Setting

The area under investigation is the Western Basin, (as defined by GNPC) comprising Tano, Cape Three Point sub-basin in Ghana, which is part of the larger Ivory Coast Basin located in the Gulf of Guinea, West Africa. It is located in about 75 m of water, 35 km offshore of Ghana. The location is about 4° 46' north latitude and about 3° west longitude. It is East-West onshore-offshore structural basin (Davies, 1986).

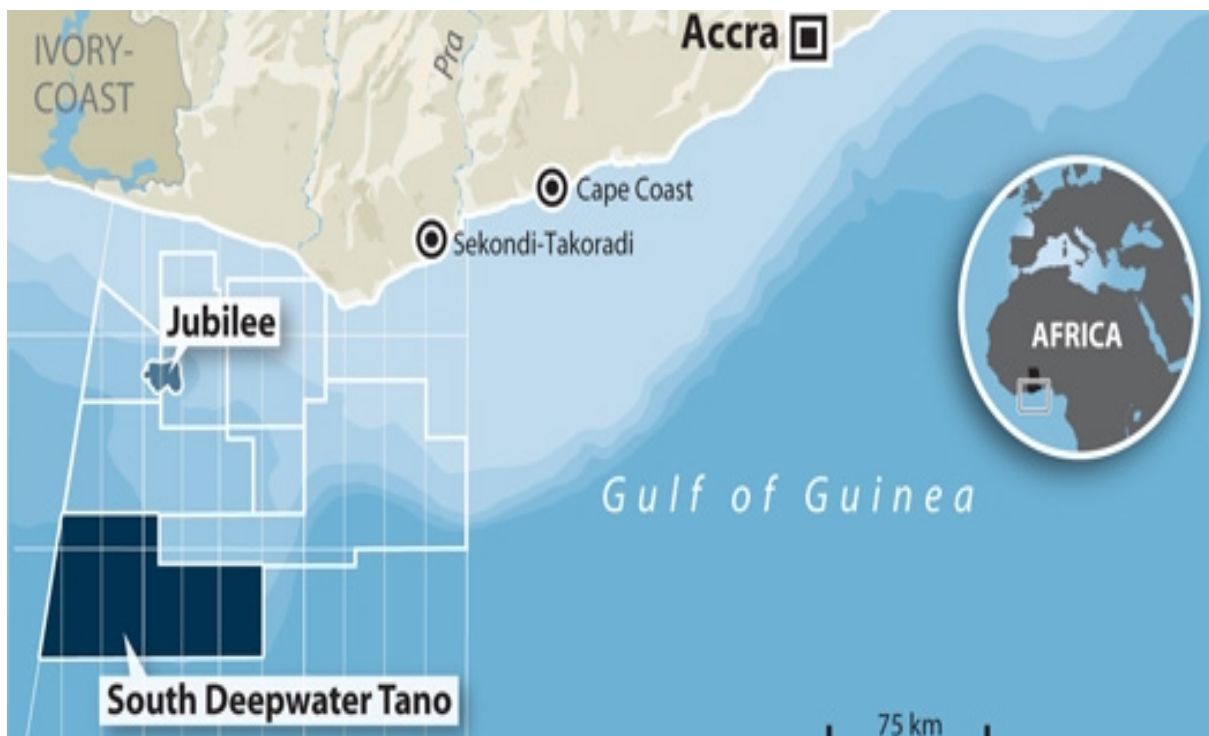


Fig 2.1 above shows the location of the study area. Courtesy G.N.P.C

It occupies an area of at least 3000 square kilometers in offshore and narrow onshore segment of the southwestern corner of the Republic of Ghana (fig.2.1). It includes the narrow Mesozoic coastal strip of southwestern Ghana, the continental shelf, and steep submarine Ivory coast-Ghana ridge which form the continental slope (Mah, 1987).

In August 2007, Kosmos Energy announced that the Mahogany-1 exploration well offshore Ghana on the West Cape Three Points Block has discovered a significant oil accumulation based on the results of drilling and wireline logs and sample of the reservoir fluid. The well has encountered to date a gross hydrocarbon column of 270 m with 95 m of net stacked pay

in the cretaceous sandstone reservoir. The well, which is drilling in water depths of 1320 m, is targeted to reach a total depth of 4200 m and opens a new play fairway in the Tano Basin. This is the first exploration well to be drilled under the block's seven-year exploration agreement.

2.4 Stratigraphy Component of the Western Basin (Tano Basin)

The information summarized in this section is in large part the result of the study conducted by Petro-Canada International Assistance Corporation on behalf of Ghana National Petroleum Corporation (1988-89).

Sedimentary infill of the initial rift phase of the Western basin consists of more than 4000 m of lower cretaceous (Aptian to lower Albian) sandstone and shale, mainly non-marine in the lower section but increasing marine- influenced in the upper part, where thick sandstone units form oil and gas reservoirs in three wells in the offshore North of the Western basin area. This thick rift-fill unit, the Kobnaswaso formation, surrounds and buries a large tilted block, the central Tano structure, which may be cored either by early cretaceous or Paleozoic (including Devonian) rocks.

Middle and Upper Albian sedimentation in the Western Basin (Tano) was characterized by shallow marine shelf to shore face sandstones and shales in several depositional units, including newly-named Bonyere, Voltano, and Domini and Tano formations. The north Tano fault-bounded tilted structural block is a product of early Albian tectonics.

Final separation of West African and Northern Brazil continental plates and opening of equatorial Atlantic ocean south of Ghana occurred at the of Early Cretaceous (Albian) or earliest Cenomanian time, and resulted in faulting, uplift and erosion along the outer margin of the Tano basin and creation of south Tano structural trend. Subsequent Upper Cretaceous sedimentation was dominantly open marine in character, with porous sandstones in the near

shore and onshore settings. The end of Cretaceous time was marked by widespread deposition of very porous shelf and shoreline sands. A series of marine tertiary sediment wedges completed the sedimentary fill of the Western Basin.

Earlier the oldest drilled section in the western basin was found to be Aptian to lower Albian Kobnaswaso formation, penetrated for more than 2 km in 1N-1X and Kobnaswaso #1. The oldest drilled rocks are early cretaceous (Aptian) in age, but older cretaceous and possibly Triassic to late Paleozoic rocks may be present in the basal western basin. In the onshore section, the Kobnaswaso consists of mainly thinly interbedded lithic and feldspathic sandstones and shales, and is interpreted to be dominantly fluvial plain and braided stream in origin. The formation is thick sequence of sandstones, shales and other intermixed lithologies that has been partly penetrated three or four of the deep Gulf onshore wells, and seven of the nine offshore western basin wells. The sandstones are fine grained to conglomeratic poorly sorted and sub-angular to sub-rounded.

In offshore where the focus of this study is, a complete section of Kobnaswaso formation penetrated by well CTS-1 has a thickness of 1997 meters. The formation shows a more distal environment of deposition with lower sand/shale ratios and finer grain size and better sorting. Recent deep drilling has revealed older rocks which are carboniferous in age. The sandstones are well cemented and have poor porosity. The sequence was deposited in a terrestrial environment.

2.4.1 Aptian-Lower Albian (Kobnaswaso Formation)

The lower Aptian sediments of the Kobnaswaso formation overlie the carboniferous with an angular unconformity. Two mega-sequences are identified in the North (1N-1X well) and the South Tano (1S-1X well) areas. The lower mega-sequence in 1N-1X consists of thin to medium interbedded sandstones. The sandstones are generally fine to occasionally coarse

grained, poorly sorted with poor porosity probably due to diagenesis. The unit is characterized by olive grey to dark grey, very carbonaceous and micaceous shales. The interbedded sandstones, shales and siltstones are gradational showing soft-sediment deformation (Davies, 1986).

The upper Kobnaswaso mega-sequence is characterized by shale units about 200 metres thick with interbedded coarsening upward sequences of sandstones siltstones and shales. The sandstones are fine to medium grained, poorly sorted, variably argillaceous, calcareous and dolomatic, (Davies, 1986). The shales are medium dark grey, sub fissile to fissile, silty and occasionally calcareous (RRI, 1998). Marginal marine conditions are indicated in 1N-1X and 1N-2X wells for the upper mega-sequence. Part of the upper mega-sequence is truncated due to uplift and subsequence erosion in the area.

2.4.2 Lower-Middle Albian (Bonyere Formation or B shale)

This formation represents the first major long -term open marine transgression in Tano Basin. The Bonyere formation is described as dark grey, micro-micaceous, non-calcareous, fissile and variably silty and sandy. Three wells (1N-1X, 1X-2X and VT-1) in North Tano have penetrated this formation with thickness of 84 m, 262 m and 181 m respectively, (Davies, 1986). Marginal to shallow marine conditions with strong terrestrial influence were prevalent during the deposition (RRI, 1998).

In south Tano the shale is medium to dark grey, blocky to sub fissile, micro-micaceous, variably silty to sandy.

2.4.2.1 Uppermost lower Albian – middle Albian (Voltano Formation)

A study conducted by RRI (1998) assigned this formation an uppermost early Albian to middle Albian age. The thickness section (819 metres) in North Tano is penetrated by VT-1 while 1N-1X and 1N-2X intersected thickness of 431 metres and 436 metres respectively. The shales in this formation are dark grey, micro-micaceous, occasionally silty to very finely sandy and non-calcareous. The sandstones are medium grained, calcareous with dark grey shaly partings also present in lower part of the formation in the wells. A shallow, near shore marine to intertidal depositional setting is attributed to these sediments. However, the presence of plank tonic foraminifera in the wells suggests occasional open marine influence, at inner neritic water depths.

2.4.3 Upper Albian (Domini Formation)

This formation consists of thinly interbedded sandstones, siltstones, carbonates and shales. The sandstones are light grey to grey, generally fine to medium grained, moderate to well sorted, micaceous calcareous and pyretic. Calcite cement is common, yielding poor porosities. Limestone interbeds are white to buff, micritic to chalky in texture. According to RRI (1998), the depositional environment of the Domini formation in the North Tano area was fluvial to near shore becoming more marines towards the later period of deposition.

In the North Tano area, the base of the Domini formation is placed at the top of the B shale in the 1N-1X and 1N-2X wells in a prominent sandstone marker that can be correlated with other wells in the sub-basin (Davies, 1986). The thickness of the Upper Albian is 431 m, 436 m and 432 m in 1N-1X, 1N-2X and VT-1 respectively.

An angular unconformity exists between the top of the formation and the base of the Cenomanian. The Domini formation has been identified in all the South Tano wells analyzed by RRI.

2.4.4 Cenomanian

The Cenomanian interval shows a wide variation in lithology and thickness across the Tano sub-basin with a condensed carbonate-dominant section above the Cenomanian unconformity in the South Tano area. The base Cenomanian, in the North Tano, is picked at the top of sequence of interbedded limestone and sandstones overlain by a thin sequence of black shale.

Two limestone Facies of the Cenomanian are indicated in the Tano sub-basin: deeper shelf oligostigmoid limestone that overlies shallow-water shoal limestones. Both sub formations are late cretaceous in age (Davies 1986 and RRI 1998). In the North Tano (1N-1X and 1N-2X) area, the lower to middle Cenomanian is characterized by interbedded fine to coarse grained sands with occasional calcite cement and grey, variably silty mudstone RRI, (1998). This unit was deposited under shallow, near shore and fully marine inner neritic conditions though slight open marine influence was also noticed (RRI, 1998).

In the South Tano area the unit represents a condensed sequence that overlies an eroded Upper Albian section. The middle to Upper Cenomanian sequence is characterized by thinly inter-bedded tan to brown oligostigmoid limestones, shales and sandstones. The sandstones are fine to very coarse grained, sometimes calcareous and carbonaceous. Mudstones and minor limestones of the Middle-Upper Cenomanian age in the South Tano wells represent low energy, offshore marine conditions.

2.4.5 Turonian

In the North Tano area, the top of the Turonian is picked at the top of series of thinly interbedded sandstones, limestones and shales. The Turonian shale in the 1N-1X well is about 90 m thick reducing to about 45 m in VT-1 and is overlain by coarsening-up sandstones (Davies, 1986 and RRI, 1998). In South Tano, the Turonian is picked at the top of a shale section overlying the Cenomanian limestones.

2.4.6 Coniacian-Santonian

This formation extends from the Turonian to the Campanian (or the basal Maastrichtian sandstone) and is about 412 m thick in VT-1 well, but thinner in 1N-1X and 1N-2X wells. The sediments are predominantly dark grey shales alternating with medium grey siltstones. Occasional unconsolidated sand horizons are noted particularly towards the base of the formation. The sequence shows a major fining upwards succession indicating an increasing marine deposition.

2.4.7 Uppermost Santonian to Intra Lower Campanian

This unit corresponds to a sandstone unit with two thick shale sequences. Davies, (1986) has reported six distinct Para-sequences below the Campanian. According to RRI (1998), the sequence is well developed in the offshore Tano area and the sediments comprise of mudstones with occasional thin carbonate stringers. They are generally olive grey to brown sub fissile, black and occasionally silty or glauconitic. The deposition environment throughout the latest Santonian to early Campanian times according to RRI (1998), were marine shelf in both the South and North Tano areas.

2.4.8 Lower Campanian to Upper Campanian

Sediments of this formation are predominantly composed of mudstones with minor carbonate-rich layers. The Upper unit found in the Tano North well 1N-1X, is characterized by the presence of sandstone (RRI, 1998).

In the 1N-1X well, initial short-lived transgressive episodes attaining outer neritic water depths were followed by deposition in a mainly middle to inner neritic setting. In the South Tano area however, deposition was under low energy conditions in a mainly distal shelf setting at outer neritic water depths (RRI, 1998).

2.4.9 Maastrichtian

The thickness of the Maastrichtian sequence is variable in the Tano area. It ranges from about 138m in 1N-1X well to 154m in 1N-2X and 178m in VT-1 well. Two sub-divisions of the Maastrichtian, into lower and upper units, have been reported by both Davies (1986) and RRI (1998). The lower Maastrichtian unit consists predominantly of coarse grained, unconsolidated and well to poorly sorted sandstone with mudstone interbeds.

The mudstones are mostly fossiliferous and glauconitic. A general down hole decrease in gamma values is observed as compared with the upper unit. Depositionally, an inner neritic environmental setting prevailed at the 1N-1X North Tano well, while low energy conditions existed in the South Tano.

According to Davies (1986), the uppermost Maastrichtian sub-unit lies at the top of the sandy Maastrichtian sequence and is composed of shales or claystones. In the Middle to Upper Maastrichtian unit a prominent gamma spike is identified at the base of the upper unit in contrast to the lower gamma values in the lower sandier unit.

This prominent gamma spike is interpreted to represent a possible highly condensed section, (Davies, 1986). The Middle to Upper Maastrichtian is generally characterized by the presence of glauconitic mudstones, which records high gamma values. Based on logs, the top is picked at the top of a coarsening up sequence in contrast to the overlying shale unit. Very fine to fine grained sandstones are also present in the North Tano 1N-1X well. The depositional environment, as stated by RRI for the Middle to Upper Maastrichtian at the 1N-1X North Tano well, is an offshore, fully marine setting at middle neritic water depth.

2.4.10 Tertiary Sequences

These sediments range in age from the Paleocene to Upper Miocene. The Paleocene is unconformable on the Cretaceous, which accounts for the absence of the Lower Paleocene in the Tano area (RRI, 1998). Upper Paleocene sediments have been identified in the RRI study of the 1N-1X well and most of the South Tano wells.

The top of the Paleocene is marked by a down hole increase in gamma ray and resistivity and is composed of mainly glauconitic shales and are abundant in the South Tano area. Mudstones are generally brownish grey to brownish black, moderately organic rich, slightly pyritic and micro-micaceous.

These sediments, according to RRI (1998) represent the first tertiary transgressive-regressive cycle of sedimentation initiated during Thanetian times mainly in the South Tano and South Dixcove areas. They represent offshore, generally deep marine low energy settings at inner neritic to bathyal water depths.

Lower and Middle Eocene sediments have been identified in the RRI study. The Upper Eocene is absent as a result of a major regional unconformity in the area. The Lower Eocene consists of predominantly mudstones, which are light olive grey to occasionally brownish grey slightly waxy, rarely glauconitic, organic-rich and slightly pyretic. Minor stringers of very fine grained sandstones also occur (RRI, 1998).

The sediments indicate outer neritic water depths throughout the interval studied and across the study area; however, slightly deeper marine conditions were believed to have existed at the 1S-1X well. Lower to Middle Eocene sediments are brownish grey, organic rich mudstones with occasional chert layers and thin horizons of slightly glauconitic limestones.

According to RRI (1998), the sediments were deposited in deep offshore waters at inner neritic water depths. Due to a regional unconformity, the Lower Oligocene is absent in the North Tano wells studied by RRI, but is present in the South Tano 1S-1X and ST-7H wells.

The lithology consists of brownish grey, glauconitic and pyritic mudstones with thinly interbedded argillaceous limestones.

The Upper Oligocene interval is thinly developed in the wells. These sediments were deposited under moderately deep water, offshore marine conditions at possibly outer neritic water depths.

Lower Miocene sediments are absent in both the North and South Tano area due to a major regional unconformity in the area. However, Middle and Upper Miocene sediments have been identified in the Tano area by RRI (1998).

The Middle Miocene interval as seen in the South Tano 1S-1X and 1S-2X wells is made up of light to medium grey, fossiliferous, slightly calcareous and glauconitic mudstones which were deposited in moderately deep open marine waters.

The Upper Miocene interval, as identified by RRI in the South Tano ST-8 well, is composed predominantly of mudstones. The mudstones are light brownish grey, occasionally silty to very finely sandy, slightly calcareous and sometimes glauconitic with minor thin sandstone layers and carbonate stringers. These sediments were deposited in probably deep, open marine conditions at outer neritic to upper bathyal water depths.

2.5 Tectonic Component of the Western Basin

The African and South American continents were once joined to form the super continent called the Gondwana. As much as 500 MA, a rift valley had formed in the region between what is now the separate continent (Trompette, 1994). The basin was formed initially by extension and subsidence of thinned continental crust in a rift system between diverging continental plates of West Africa and Northern Brazil.

This stage followed by development of a marginal sag basin by thermal contraction (cooling) as plate separation continued along major east-west oceanic transform faults including the

Romance fracture zone. It is thought that the strike slip fault movement between the St. Paul fracture zone to the northwest, and the Romanche zone to the southeast, created a transtensional basin, the West Basin (Tano Basin). Prior to onset of the continental separation in early cretaceous time, the west African and Northern Brazilian continental plates were contiguous within the Pangaea super continent, and a large part of the area was occupied by a continental interior sag basin filled progressively, by lower and upper Paleozoic to probable Triassic sediments. The eroded remnants of this Paleozoic – dominant interior basin are recorded in the Parnaiba, Amazon and other basins of northern Brazil.

2.6 Well Logging Analysis

Petrophysical characteristics of the subsurface can be estimated using information from geophysical logs. The diversity and accuracy of the estimates depends upon the number of logs available. As logging tools are being pulled up in the well, their sensors are measuring certain physical properties of formations (Welex, 1978). These measurements recorded on long strips of paper and, digitally, on magnetic tapes-are called well logs. A few dozen different logs can be run today, including such measured properties as resistivity or conductivity of the rocks, intensity of natural radioactivity, electrical potentials existing in the well, and velocity of sound waves.

The task of the log analyst, after all measurements have been collected, is to determine the presence and amount of hydrocarbons in the well. It is also important to determine various characteristics such as permeability and the types of minerals present in the producibility of hydrocarbons. Thus, many parameters can be computed from well logs.

In this project, the well logs for the selected wells are analyzed in order to estimate the gas reserves. Several logs have run through the six selected well (such as gamma ray log, density log, resistivity log, and temperature log).

2.7 Well Drilling

Most modern well drilling is done with rotary drills and percussion drills. The rotary can be used for both shallow and deep wells. The record drill reached with rotary drill is more than 40,000 feet. A percussion drill is faster, but cannot be operated if the well becomes flooded with ground water while drilling is in progress (Robinson, 1988). This problem restricts its use for most part to the depths of less than a few thousand feet.

2.8 Invasion Effects

Invasion is the results of the rotary drilling process which involves the pumping of a fluid (usually water – or an oil based mud) down the inside of the drill pipe and its return to the surface through the annular space between the drill pipe and the sides of the boreholes. Invasion affects only the porous and permeable zones; tight formations permit little or no invasion (Doveton, 1986).

Drilling fluids serves several purposes, apart from carrying rock cuttings out of the well; the fluid also lubricates the rotating column of the pipe, and cools the drill bit. Another important function of the mud fluid is to seal the rock surface so that pore fluids cannot seep into the well. During drilling the mud pressure in the annulus must be kept greater than the hydrostatic pressure of the fluid in the formation pores, to prevent a blowout. The differential pressures between the mud and the pore fluids, which is typically a few hundred (psi), forces drilling fluid into the formation (Schlumberger, 1989).

The zone surrounding the well in which drilling fluid has infiltrated is called the zone of invasion; its structure is shown in figure 2.2. As the mud filters into the porous layers, it displaces some of their content, replaces them with mud filtrate, and creates a cylindrical fluid distribution pattern. At the same time, the filtration effects of the process causes the deposition of some of the material suspended in the mud of the porous faces surrounding the

borehole wall. As the mud cake thickens, its low permeability causes it to form a barrier and eventually the flow of filtrate into the porous layers virtually ceases.

Thickness of the mud cake is generally between one-eighth and three-quarters of an inch. In the immediate vicinity of the borehole, almost all the formation water and some of the hydrocarbons, if present, are displaced. This is referred to as the flushed zone, the width of which is usually between 3 and 4 inches. Away from the borehole the effect of the flushing becomes progressively less marked. The flushed zone is therefore surrounded by a transition zone beyond which lies the uninvaded part of the porous layer. The width of the invaded zone ranges from less than 1ft to perhaps 10 to 15 ft.

Factors that determine the depth of invasion include the type of mud used, the differential pressure between the mud in the borehole and the formation, and the porosity and permeability of the formation (Chapman, 1983). The depth of invasion is minima at high porosity where plenty of pore space is available for the invading fluid and maximum at low porosity where little room is available.

2.9 Formation Evaluation

Formation evaluation is the *raison d'être* of wireline logging. Virtually all other digital processing, with the possible exception of dipmeter logging, is done in support of and as an adjunct to formation evaluation (Bloch, 1993). The central problem of formation evaluation is the determination of porosity and water saturation. Resistivity logs have always been the primary tools for determination of water saturation, and despite the advent of sophisticated logs such as Carbon- Oxygen, Nuclear-Magnetic-Resonance and Neutron Lifetime logs, resistivity continues to be of utmost importance (Labo, 1986).

The rather unique role of the resistivity logs has been a major factor in the evolution of the science of formation evaluation. Although most rock-forming minerals are essentially

insulators, electrically, the clay minerals cause a saturated or partially saturated rock to exhibit anomalous conductivity (Dresser, 1982).

The ultimate goal of formation evaluation is to help determine the size of a reservoir, the quantity of hydrocarbons in place, and the reservoir's producing capabilities (Worthington, 1985). The initial discovery of a reservoir lies squarely in the hands of the exploration department, using seismic, gravity and magnetic studies, and other geologic tools. Formation evaluation presupposes that a reservoir has been located, and is to be defined by drilling the least number of wells possible (Sengel, 1983). Enough data should be gathered from those wells to extrapolate reservoir parameters field-wide, and to arrive at realistic figures for both the economic evaluation of the reservoir and the planning of the optimum recovery method. Formation evaluation offers a way of gathering the data needed for both economic analysis and production planning.

2.10 Costs

The amount spent on running wireline logs, cutting cores, evaluating the logs, and analyzing the core samples depends very much on the total cost of the well, the importance of the data (do we get another chance to collect similar data in another well?) and the risks involved in obtaining the data (can we afford to lose the well if a logging tool gets stuck?). The evaluation costs usually amount to 6 -12 % of the total well cost. For an offshore exploration well drilled from a floating rig in deep water, the total well cost can easily be 20 million dollars. Maximizing the information obtained from this "one time" effort is essential. Evaluation costs for such ventures can reach several million dollars.

2.11 Types of Logs

This section provides a catalog of tools available to the log analyst. Included are: lists of the measurements made, units of measurements, major uses, and tool resolution.

2.11.1 The Gamma Ray Logs

The GR is a measurement of the natural radioactivity of the formation. In sedimentary formation the log normally reflects the shale content of the formations. This is because the radioactive elements tend to concentrate in clay and shale. Clean formations usually have a very low level of radioactivity, unless radioactive contaminant such as volcanic ash or granite wash is present or the formation waters contain dissolved radioactive salts (Heslop, 1974).

The GR log can be recorded in cased wells, which makes it very useful as a correlation curve in completion and work over operation. It is frequently used to complement the SP log and as substitute for the SP curve in wells drilled with salt mud, air, or oil-based mud.

In each case, it is useful for location of shales and nonshaly beds and, most importantly, for general correlation.

2.11.1.2 Applications

The GR is particularly useful for defining shale beds when the SP is distorted (in very resistive formations), when the SP is featureless or when the SP cannot be recorded (in nonconductive mud, empty or air-drilled holes, cased holes). The bed boundary is picked at a point mid way between the maximum and minimum deflection of the anomaly.

The GR log reflects the proportion of shale and, in many regions, can be used quantitatively as a shale indicator. It is also used for the detection and evaluation of radioactive minerals, such as potash or uranium ore. Its response, corrected for borehole effect, is practically proportional to the K_2O content, approximately 15 API units per 1 percent of K_2O . The GR log can also be used for delineation of non- radioactive minerals (Schlumberger, 1989).

This traditional correlation log is part of most logging programs in both open and cased hole. Furthermore, because it is readily combinable with most other logging tools, it permits the accurate correlation of logs made on one trip into the borehole with those made on another trip.

2.11.1.3 Gamma Log Interpretation

Natural gamma radiation occurs in rock formations in varying amounts. Uranium, Thorium, Potassium, and other radioactive minerals are associated with different depositional environments. Sedimentary sandstone and Carbonate environments are low in gamma radiation. Clay and Shale formations exhibit greater amounts of gamma radiation. A log of gamma radiation in “counts” or API units will give a positive indication of the type of lithology. Interpretation of gamma log data is done based on the relative low and high count rates associated with respective “clean” and “dirty” environments. Composition of formations having more clay or shale as indicated by higher gamma count rates generally are more tightly compacted with fine particles and therefore have less porosity and permeability. Formations having high gamma count rates even though they may exhibit low water saturation are generally unfavorable for production in oil and water well environments.

It is important to be aware that certain areas are known to have sandstone formations with higher than normal levels of radiation (Schlumberger, 1989).

These formations are sometimes erroneously interpreted. Information from an SP log can be used for correlation. Coal formations normally have very low (almost zero) gamma radiation and contrast quite well with surrounding formations. Knowledge of local “exceptions” is an important aspect of accurate interpretation.

2.11.1.4 Gamma Log Calibration

Gamma radiation is detected differently in every logging tool. Due to variation in detector types, tool design, detector efficiency and overall tool response, the American Petroleum Institute (API) standard of API Units is commonly used for calibration (Crook, 1975). A Test well located in Houston, Texas has been used for many years as the API reference test well. The well is designed with three layers of concrete. The top 8 feet of concrete is low radiation, the middle 8 feet is a mix of radioactive elements designed to closely match a radiation level of twice the mid-continent US shale, and the bottom 8 feet is a low activity concrete zone. A tool is calibrated in the test well by first measuring the gamma radiation counts in the low radioactivity zone which is considered to be 0 API units. A second measurement of gamma counts is the made with the detector centered in the high radioactivity zone. The high radioactivity zone corresponds to 200 API units. Secondary reference calibration jigs containing a low-level gamma radiation source are often used in the field to establish detector calibration. Operation of the detector is confirmed by placing the source at a specified distance from the detector, and then at a distance sufficiently far away to obtain background counts.

2.11.2 Induction logs

The induction-logging tool was originally developed to measure formation resistivity in boreholes containing oil-base mud and in air-drilled borehole. Electrode devices did not work in the nonconductive mud, and attempts to use wall-scratchier electrodes were unsatisfactory. Experience soon demonstrated that the induction log had many advantages over the conventional ES log when used for logging wells drilled with water-base mud.

Designed for deep investigation, induction logs can be focused in order to minimize the influences of the borehole, the surrounding formations, and the invaded zone (Schlumberger, 1989).

2.11.2.1 Principle

Today's induction tools have many transmitter and receiver coils. However, the principle can be understood by considering a sonde with only one transmitter coil and one receiver coil

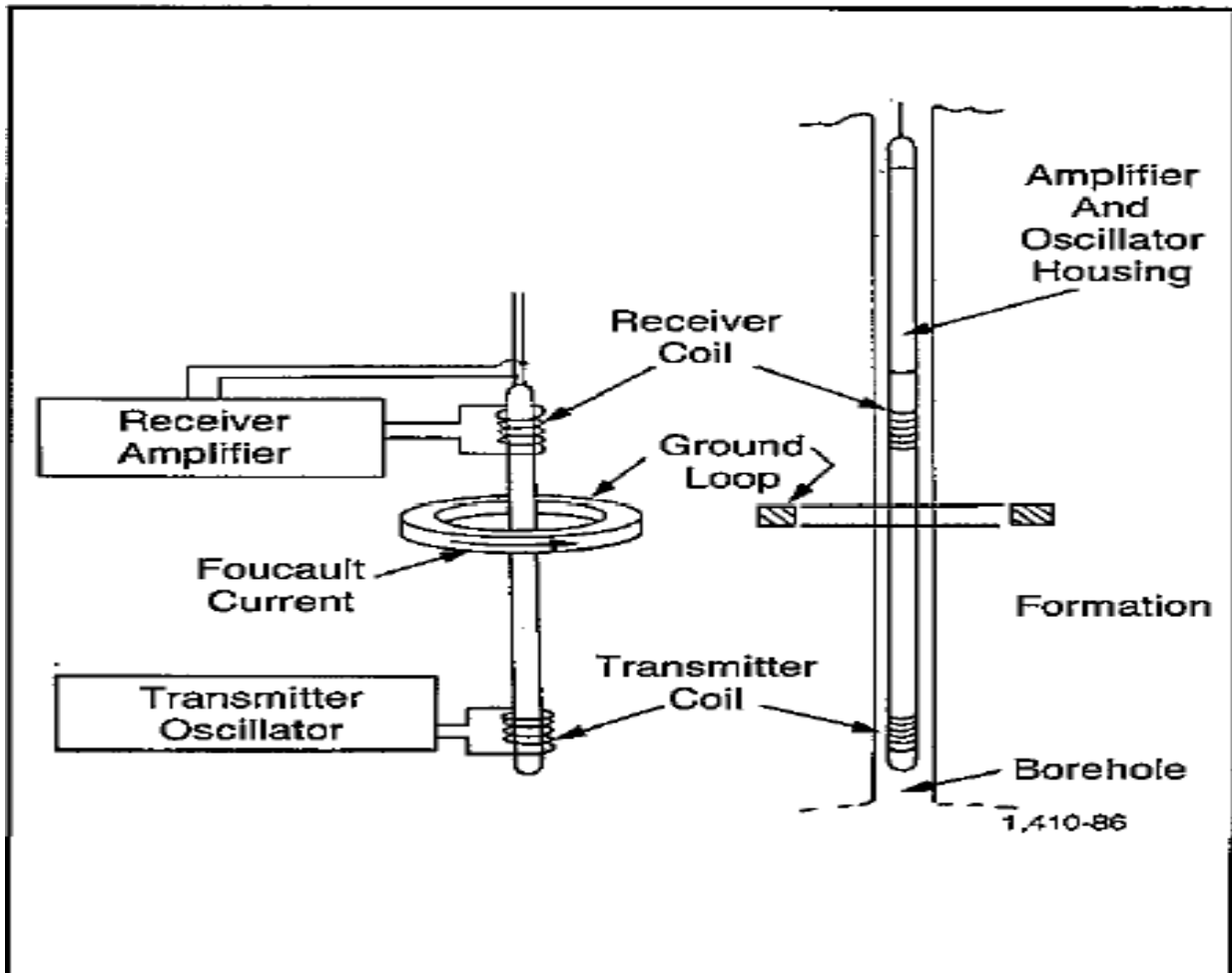


Fig 2a - Schematic diagram, of a basic two coil induction system.

A high-frequency alternating current of constant intensity is sent through a transmitter coil. The alternating magnetic field created induction currents in the formation surrounding the borehole. These currents flow in circular ground loops coaxial with the transmitter coil and create, in turn, a magnetic field that induces a voltage in the receiver coil (Schlumberger, 1989).

Because the alternating current in the transmitter coil is of constant frequency and amplitude, the ground loop currents are directly proportional to the formation conductivity. The voltage

induced in the receiver coil is proportional to the ground loop currents and, therefore, to the conductivity of the formation.

There is also a direct coupling between the transmitter and receiver coils. Using “bucking” coils eliminates the signal originating from this coupling. The induction tool works best when the borehole fluid is an insulator-even air or gas. The tool also works well when the borehole contains conductive mud unless the mud is too salty. The formations are too resistive, or the borehole diameter is too large.

2.11.3 Other Resistivity Methods

The discussion thus far has been related to resistivity using a “normal” electrode array. Several other tools are available for the purpose of measuring resistivity. Each tool is designed to provide an accurate determination of formation resistivity in various borehole environments.

Lateral resistivity measurements are used when it is necessary to obtain deep formation resistivity measurements. Deep formation resistivity is a close approximation of true resistivity where invasion is small (Hansen and White, 1991). In cases of deep invasion, interpretation must include a correction for the invading borehole fluid. Note: Due to the larger spacing of electrodes used in this method, thin formations are less noticeable on the log.

Focused electrode resistivity tools are used in boreholes that have low resistivity mud or other drilling fluids. Normal and lateral logging tools tend to conduct current through the borehole fluid in this case. Focused electrode systems are designed to reduce or eliminate borehole fluid conduction. The current emanating from the tool therefore flows into the surrounding formation and provides a more accurate measurement of formation resistivity.

Micro electrode resistivity tools have small electrodes attached to a non conductive pad that is pressed against the borehole wall while logging. These tools are designed to measure the resistivity of the combined mud filtrate (R_{mf}) and resistivity of the flushed zone (R_{xo}). The objective is to obtain information about formation porosity and permeability. The small spacing used in the electrodes make this tool very accurate in establishing bed boundaries.

Induction resistivity tools use electromagnetic induction as a method of measuring formation resistivity. It is important to know that all other resistivity measurements require fluid in the borehole. Induction logging tools provide resistivity measurements in oil/water and air.

Corrections are applied to all of the above resistivity methods (Misk, Mowat, Goetz and Vivet, 1977).

2.11.3.1 Electric Log (E-Log) Interpretation

The exploratory phase of oil production does not necessarily end with the location of the wildcat drilling site but rather when the wildcat well has been drilled and proved conclusively to be productive or dry. There have been cases in the past of an operator drilling through an oil reservoir, logging the well, and plugging it without testing or making a decisive test of the zone which was later proven to be productive. The development of quantitative electric log interpretation techniques during the past several years has provided a valuable exploration tool for the oil industry. The electric log is not only useful for formation correlations but also provides the resistivity data which permit quantitative calculations of the water and oil content of the zones penetrated by the borehole.

A properly calibrated E-log will provide important information about formation Electrical Resistivity. In addition to resistivity, Spontaneous Potential (SP) is obtained. SP shows lithology and type of lithology in terms of sand/carbonate or shale/clay and relative proportion of each.

Electrical Resistivity provides information about the fluid that is in the pore spaces within the rock matrix in oil and water wells. Because electrical resistivity is controlled by ion flow in liquids, the E-log will provide confirmation of the existence of water, water quality, and/or hydrocarbon content of the rock matrix (Merkel, 1979). The electrode spacing (A to M) used on the E-log tool is directly related to the depth of measurement. When multiple spacings are used, resistivities of different depths are measured. It is possible to form conclusions on invasion and permeability based on resistivity measurements made at two or more different depths into the formation. If no invasion has occurred, then both shallow and deep curves will read the same resistivity. If invasion has occurred, then the shallow resistivity will reflect the resistivity of the invading mud filtrate and the deep resistivity will reflect the formation fluid resistivity. Resistivity curves should read the same and depart only where invasion occurs.

In water well, higher resistivity in a saturated zone implies higher quality water. Total dissolved solids in water are related to the resistivity of water. Although certain conditions apply, as total dissolved solids decrease, water resistivity increases (Turcan, 1966).

In wells having hydrocarbons, increasing resistivity in sandstone or carbonate zones may be an indication of increasing hydrocarbon content.

The amount of fluid contained in a formation is directly related to porosity. Porosity affects formation resistivity. In water filled-pore spaces, as the volume of water increases, the capacity for more ions increases. More ions mean more conductivity (Pachett and Coalson 1979) and (Pirson 1983). Conductivity and Resistivity are inversely related. Conductivity is expressed in units of micro-mhos per centimeter. Conductivity (C, in micro-mhos/cm) = 10,000/ Resistivity (in ohm-meters)

In the SI system of units, Siemens are used to replace mhos. 1 Siemens = 1 Mho.

Formation resistivity is affected by three factors: Salt Concentration, Temperature, Pore volume (porosity). Formation Resistivity Factor (F) is a fundamental concept in log

interpretation and analysis. The formation resistivity factor is defined as the ratio of the electrical resistivity of a rock 100 percent saturated with water to the resistivity of the water with which it is saturated, (Archie, 1942). The equation is: $F = R_o/R_w$ (Referred to as Archie's Equation)

2.11.4 Neutron logs

Neutron logs are used principally for delineation of porous formation and determination of their porosity. They respond primarily to the amount of hydrocarbon in the formation. Thus, in clean formation whose pores are filled with water or oil, the neutron log reflects the amount of liquid-filled porosity.

Gas zones can often be identified by comparing the neutron log with another porosity log or a core analysis. A combination of the neutron log with one or more porosity logs yield even more accurate porosity values and lithology identification-even an evaluation of shale content.

2.11.4.1 Principle

Neutrons are electrically neutral, each having a mass almost identical to the mass of a hydrogen atom. High-energy (fast) neutrons are continuously emitted from a radioactive source in the sonde. These neutrons collide with nuclei of the formation materials in what may be thought of as elastic "billiard-ball" collision. With each collision, the neutron loses some of its energy (Schlumberger, 1989).

The amount of energy lost per collision depends on the relative mass of the nucleus with which the neutron collides. The greater energy loss occurs when the neutron strikes a nucleus. Collisions with heavy nuclei do not slow the neutron very much. Thus, the slowing of neutrons depends largely on the amount of hydrogen in the formation.

Within a few microseconds the neutrons have been slowed by successive collisions to thermal velocities, corresponding to energies of around 0.025 eV. They then diffuse randomly, without losing more energy, until they are captured by the nuclei of atoms such as chlorine, hydrogen, or silicon.

The capturing nucleus becomes excited and emits a high-energy gamma ray of capture. Depending on the type of neutron tool, either these capture gamma rays or the neutrons themselves are counted by detector in the sonde.

When the hydrogen concentration of the material surrounding the neutron source is large, most of the neutrons are slowed and captured within a short distance of the source.

On the contrary, if the hydrogen concentration is small, the neutrons travel farther from the source before being captured. Accordingly, the counting rate at the detector increases for decreased hydrogen concentration, and vice versa.

2.11.4.2 Neutron Log Interpretation

A Neutron Log when properly calibrated (usually to an API standard) will provide important information about the content of the pore spaces within a rock matrix. Neutrons emitted from a neutron source are slowed down and eventually captured through interaction with hydrogen atoms. Once captured, a gamma ray of capture is created.

Neutron Logging tools are designed to respond to slow Thermal Neutrons or Gamma Rays of Capture. Since hydrocarbons and water (H₂O) contain hydrogen a neutron log will provide knowledge of the hydrogen in the pore spaces of the matrix. When more hydrogen is present, more neutrons are captured, and fewer neutrons reach the neutron detector. Conversely, lower porosity, neutrons travel farther and reach the detector, increasing neutrons counted at the detector. In other words, increased fluid filled porosity is indicated by lower neutron

count. Neutron porosity is calculated based on neutron tool response in known lithologies having known porosity (Ransom, 1977).

Tool response is specified in terms of American Petroleum Institute (API) units. The standard unit for neutron logging tools is the "API Neutron Unit". 1000 API units are assigned to any neutron tool in a water filled hole having 7 - 7/8 inch diameter in Indiana Limestone of 19 percent porosity. One API Neutron Unit is 1/1000 of the difference between tool instrument zero and the log deflection in the Indiana Limestone section. The API test well is located at the University of Houston, Houston, Texas.

When a tool is calibrated at the API test well, its response to a standard neutron calibrator is also determined. The differential deflection produced by this two environment device is compared to the API test well deflection representing 1000 API Units. A definite number of API units can then be assigned to a tools calibrator deflection. This calibration figure must be determined for each model or series of tool.

Each tool supplier develops a transform from API units to porosity for the neutron tools they produce. Neutron Porosity is based on a Limestone matrix (Indiana Limestone).

The combination of density and neutron logs is now used commonly as a means to determine porosity that is largely free of lithology effects. Each individual log records an apparent porosity that is only true when the zone lithology matches that used by the logging engineer to scale the log. A limestone-equivalent porosity is a good choice for both neutron and density logs, because calcite has properties that are intermediate between dolomite and quartz. By averaging the apparent neutron and density porosities of a zone, effects of dolomite and quartz tend to cancel out.

2.11.5 Density logs

Density logs are primarily used as porosity logs. Other uses include identification of minerals in evaporate deposits, detection of gas, determination of hydrocarbon density, evaluation of shaly sands and complex lithologies, determinations of oil-shale yield, calculation of overburden pressure and rock mechanical properties.

2.11.5.1 Principle

A radioactive source, applied to the borehole wall in a shielded sidewall skid, emits medium-energy gamma rays into the formations. These gamma rays may be thought of as high-velocity particles that collide with the electrons in the formation. At each collision a gamma ray loses some, but not all, of its energy to the electron, and then continues with diminished energy. This type of interaction is known as Compton scattering. The scattered gamma rays reaching the detector, at a fixed distance from the source, are counted as an indication of formation density. The number of Compton scattering collisions is related directly to the number of electrons in the formation (Schlumberger, 1989).

Consequently, the response of the density tool is determined essentially by the electron density (number of electrons per cubic centimeter) of the formation. Electron density is related to the true bulk density, which, in turn, depends on the density of the rock matrix material, the formation porosity, and the density of the fluids filling the pores.

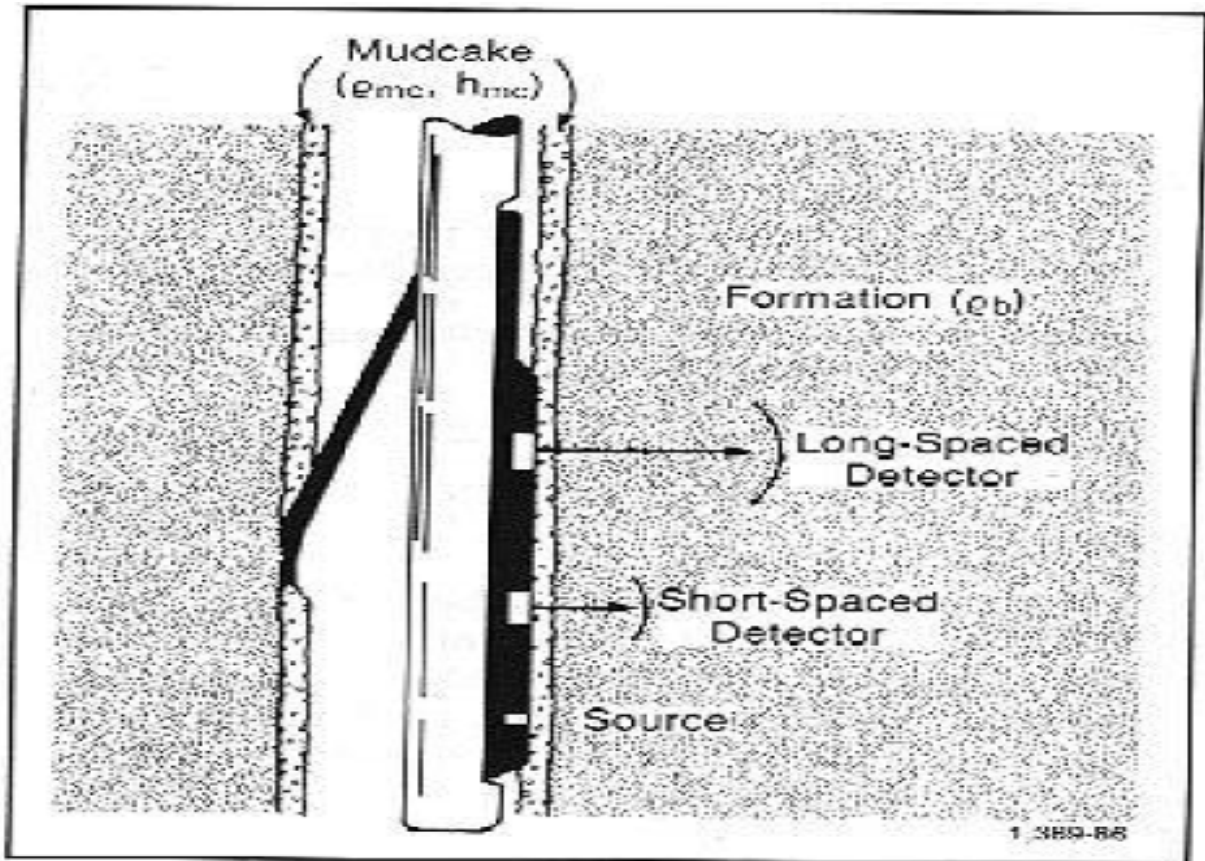


Fig 2b - Formation density logging device.

2.11.5.2 Density Log Interpretation

A Density Log when properly calibrated will provide reliable information about matrix bulk density. When density is known and a specific matrix is assumed then porosity of the matrix may be determined. A mathematical relationship exists between measured density, assumed matrix density with no porosity and the density of the material filling the pore space (Jenkins, 1960). Water has a density of 1 gram per cubic centimeter. Sandstone with no porosity has a density of 2.65 grams per cubic centimeter. If a sandstone matrix is assumed for example, then a given density of 2.00 grams per cubic centimeter allows calculation of 40 percent porosity.

For reference, Sandstone has a density of 2.65 gm/cc, Limestone is 2.71 gm/cc, Dolomite 2.87 gm/cc.

2.12 Neutron – Bulk Density Cross-Plot

Combination of data from a Neutron Porosity Log and Bulk Density log can be helpful in identification of Lithology. A chart is used that has the known relationship between Neutron Porosity and Bulk Density for three matrices; Sandstone, Limestone, and Dolomite. It is possible to determine ratio of Sandstone/Limestone and obtain a more accurate porosity using the cross-plot chart. Results from the cross-plot chart should be correlated with known lithological information.

Neutron porosity and density porosity are often presented in an overlay on the same scale on a log for shale and gas identification. Formation resistivity is affected by three factors: Salt Concentration, Temperature, Pore volume (porosity).

Formation Resistivity Factor (F) is a fundamental concept in log interpretation and analysis. The formation resistivity factor is defined as the ratio of the electrical resistivity of a rock 100 percent saturated with water to the resistivity of the water with which it is saturated, (Archie, 1942). The equation is: $F = R_o/R_w$ (Referred to as Archie's Equation).

2.13 Limitations

All logging methods have limitations to consider. Bed thickness effect: The curves produced by the normal devices are affected by bed thickness and resistivity (Lynch, 1962). Where the resistive bed is more than 6 AM spacings thick, logging up hole, there is a gradual increase in resistivity until the M electrode on the sonde enters the bottom of the bed. This level of resistivity is maintained until the A electrode enters the bed. As the sonde continues there is a gradual increase in resistivity until the midpoint of the bed is reached.

Thereafter a gradual reduction occurs in resistivity, which is symmetrical with the curve below the midpoint of the bed, until the sonde passes out of the bed. The recorded resistivity approaches but does not fully equal the true resistivity of the bed. The bed also appears to be

1 AM spacing thinner than it actually is, the major resistivity deflections occurring $\frac{1}{2}$ AM above the bed bottom and $\frac{1}{2}$ AM spacing below the bed top. As the bed thickness decreases, the resistivity peak at the center decreases in amplitude. Further thinning to AM or less than AM causes the resistivity deflection to disappear entirely, and the curve actually reverses. The resistive bed now appears to be more conductive than the surrounding formations. Although the radius of investigation increases as the electrode spacing increases, the use of AM spacing greater than 64 inches is not practical because thinner beds are not only shown at less than true resistivity but may be recorded as conductive beds if their thickness is less than or equal to the AM spacing. Focused resistivity tools overcome this limitation (Elliott, 1983). Recently, software has been developed for improving resistivity log interpretation. Old logs and new are being subjected to inversion processing that removes the effect of surrounding formations. These techniques will make electrical resistivity a more accurate viable logging method well into the future.

2.14 Acoustic Log Interpretation

An Acoustic Log (sometimes referred to as a sonic log) when properly calibrated, will provide important information about the physical structure of a rock matrix. The ability of sound to travel within and through rock or sand and gravel depends on the physical structure of the matrix. The amplitude, speed and phase relationships of a transmitted sound wave that returns to an acoustic receiver is a function of all of the combined matrix densities, interconnections, cementation, fracturing, and porosities within the matrix (Thomas, 1977). Because the total transit time from the transmitter to the receiver includes the path through the borehole fluid, Borehole compensated (two or four receiver) logging tools are used. Borehole compensation is accomplished mathematically by subtracting the borehole transit time.

Acoustic waveforms provide information related to transit time (density) and amplitude (interconnection) of the material comprising the rock matrix. Surface Geophysics has for many years used seismic reflection and refraction for determination of subsurface structure. Transit time (Δt) through sandstone, limestone, water, and other materials have been determined in the laboratory. Relationships between porosity and transit time are known. It is possible to determine porosity of a given matrix if the transit time is known.

2.15 Detection of Abnormal Pressures

Overpressured formations exhibit several of the following properties when compared with a normally pressured section at the same depth:

- Higher porosities,
- Lower bulk densities,
- Lower effective stresses,
- Higher temperatures,
- Increase interval transit times.

Borehole data measure several of these properties and can be used to determine overpressures. Interval transit time's determination is the key to pore-pressure prediction.

Changes in pore pressure can be recognized on regular formation evaluation tools such as sonic, resistivity, porosity, and density logs. These logs show the effects of pore pressure because of the relationship between compaction, porosity, density, and the electrical and acoustic properties of sediments (Fertl 1976).

As rock compacts, the porosity is reduced and the density increases, which also causes the bulk modulus and shear modulus to increase because of increase in grain contact area and grain contact stress. This process continues until the mechanical process of compaction is

slowed by either the stiffness of rock frame or by increases in pore pressure that resist further compaction (Mario, Neil and Brent 2006).

In cases where the sealing rocks allow fluid pressures to counteract the vertical stress and undercompaction occurs, the result of this is to slow down the decrease of porosity and decrease in interval transit time (or the increase in acoustic velocity) and density, but not to stop it totally. As such, under compacted intervals will still follow the normal compaction pathway but the rocks in such a condition will show higher porosities and lower velocities than a normally compacted rock at the same depth of burial (Raymer, Hunt and Gardner, 1980).

This effect can be seen on log display (Figure 4-1). When unloading pressure mechanisms occur in the subsurface, the increase in fluid pressure causes the compaction process to stop, which causes the porosity and density to cease changing with depth of burial. As the fluid pressure increases and the effective stress drops, the rock is not able to increase its porosity because the compaction process is irreversible. Therefore, the grain contact area also is essentially unchanged. However, the increase in the pore pressure does cause a reduction in the grain contact stress, which causes the velocity to drop as the grain stress is lowered by the increase in pore pressure.

2.16 Over Pressured formations of Oil and Gas Exploration

Overpressures in the subsurface pose major problems for safety and cost-effective well design. Furthermore, geopressures impact prospect and play appraisal and economics in a number of ways. A partial list of the issues associated with subsurface geopressures includes:

- Drilling safety and cost: rig selection; well kicks and blowouts; lost wells; wellbore stability problems; mud expense and mud loss; stuck pipe; formation damage; extra casing runs.
- Environmental risks.
- Prospectively and trap analysis: hydrocarbon retention and column height; sealing/nonsealing faults; top seal capacity; aquifer continuity/pressure support during production; volumetrics and economics.
- Impact on rock and fluid properties: reservoir quality; sediment and fluid acoustic properties and quantitative seismic interpretation.

Consequently, the prediction of the occurrence and magnitude of overpressures and the associated trap integrity (difference between the minimum horizontal stress and the pore pressure) are of considerable importance in hydrocarbon exploration (Chopra and Huffman, 2006).

2.17 Nuclear Magnetic Resonance (NMR) Logging.

No review of well logging would be complete without mention of the nuclear magnetic resonance logging method. The NMR method, described in Brown and Gamson (1960), uses a periodically pulsed dc magnetic field to realign some of the atomic nuclei with magnetic moment (principally hydrogen) in a direction different from that of the Earth's magnetic field. While the polarizing field is off, the receiving circuitry measures both the amplitude and rate of decay of the Larmor precession frequency which is produced as the polarized nuclei precess about the Earth's magnetic field (Brown and Gamson, 1960).

The amplitude of the received signal at the beginning of precession is related to the amount of fluid (hydrogen) in the pore space which is free to polarize in the direction of the applied field. Hence, the log produced is called the Free Fluid Index (FFI) log. The rate of signal decay may be used to infer something about the type of fluid saturating the rock. Parameters measured by laboratory and borehole NMR apparatus (i.e., FFI and relaxation time) were related to movable fluid and to permeability in sandstone reservoir rock (SeEVERS, 1966; Timur, 1969).

For this reason, there continues to be great interest in NMR. Unfortunately, realization of a completely satisfactory borehole NMR measurement has been elusive. At present, only Schlumberger offers an NMR log. The Schlumberger probe, called the Nuclear Magnetism Log is a second generation probe.

Operationally, the NML log must be run in a drill hole in which the borehole fluid has been doped with magnetic additives to eliminate the NMR effect of the borehole. Moreover, the general consensus is that, an S/N ratio problem which limits the quality of the data remains (at least at tolerable logging speeds). An NMR technique based on a somewhat different measurement principle was recently described in Jackson (2001).

This technique, called the “inside out” technique, uses a static magnetic field in conjunction with a radio frequency magnetic field to generate an NMR signal in a toroidal-shaped region concentric with the borehole. Although the technique eliminates the borehole effect without the need for doping the mud, it is limited to static mode measurements. Improvements in the “inside out” NMR method must await development of substantially stronger permanent magnets.

2.18 The Archie Equation

In his classic paper, Archie (1942) proposed two equations that described the resistivity behavior of reservoir rocks, based on his measurements on core data. The first equation governs the resistivity of rocks that are completely saturated with formation water. He defined a “formation factor”, F , as the ratio of the rock resistivity to that of its water content, R_w , and found that the ratio was closely predicted by the reciprocal of the fractional rock porosity (a) powered by an exponent, he denoted as “ m ”. The value of m increased in more consolidated sandstones and so was named the “cementation exponent”, but seemed to reflect increased tortuosity in the pore network. For generalized descriptors of a set of rocks with a range of m values, workers after Archie introduced another constant, “ a ”. In a second equation, Archie described resistivity changes caused by hydrocarbon saturation. Archie defined a “resistivity index”, I , as the ratio of the measured resistivity of the rock, R_t , to its expected resistivity if completely saturated with water, R_o . He proposed that “ I ” was controlled by the reciprocal of the fractional water saturation, S_w , to a power, “ n ”, which he named the “saturation exponent”.

The two equations may be combined into a single equation, which is generally known as “the Archie equation”. Written in this form, the desired, but unknown, water saturation (S_w) may be solved.

Although “rule-of-thumb” numbers for the cementation exponent, **m**, and the saturation exponent, **n**, are often quite adequate for estimates of water saturation when making a decision whether to run a drill-stem test, they may be poor for reserve estimations, particularly for a major field. They can also be misleading when applied to a carbonate unit that has (for example) significant oomoldic porosity, or fractures. The errors can lead one into being either too pessimistic or too optimistic. Similar concerns apply to the value of the saturation exponent, **n**. For water-wet formations, **n** is approximately equal to two, but will be much higher in formations that are oil-wet. Some background to “**m** and “**n**” in sandstones is given in the following section.

2.18.1 Formation Factor - Porosity Relationships for Sandstones

Archie (1942) measured the formation factor of a variety of sandstones (a simple laboratory procedure involving a Wheatstone bridge) and compared these with their porosities to deduce the variation of **m** with type of sandstone. He found that **m** was 1.3 for unconsolidated sands and ranged between 1.8 and 2.0 for consolidated sandstones. However, a useful rule-of-thumb comparative scale is widely quoted as:

m

1.3	unconsolidated sandstones
1.4 - 1.5	very slightly cemented
1.6 - 1.7	slightly cemented
1.8 - 1.9	moderately cemented
2.0 - 2.2	highly cemented

In 1952, Winsauer and other workers measured formation factors and porosities in 29 samples of a highly varied suite of North American sandstones. They generalized Archie’s equation to: $F = a / \Phi^m$

Since low porosity sandstones are more highly cemented than higher porosity sands, the constant 'a' functions as a slippage element which automatically incorporates the cementation exponent changes associated with sandstones of differing porosities. By taking logarithms of both sides, this can be transformed to a straight line relationship:

$$\mathbf{Log F = log a - m log \Phi}$$

On fitting log F to log Φ , they came up with a relationship for sandstones:

$$\mathbf{F= 0.62 / \Phi^{2.15}}$$

Which is known as the "Humble equation" (since they worked for the Humble Oil Company) and is the most widely used equation for sandstones in the world.

2.19 Permeability

Reservoir characterization is a very important domain of petroleum engineering. An effective management strategy can be applied only after obtaining a detailed and close-to-reality "image" of spatial distribution of rock properties. Among these, the most difficult to determine and predict is permeability (Coats and Dumanoir, 1974).

All these studies give a better understanding of the factors controlling permeability, but they also show that it is an illusion to look for a "universal" relation between permeability and other variables. To evaluate the producibility of a reservoir, it is necessary to know how easily fluid can flow through the pore system. This property of the formation rock, which depends on the manner in which the pores are interconnected, is its permeability. Permeability is a measure of the ease with which fluids can flow through a formation (Desbrandes, 1985). For a given sample of rock and for any homogeneous fluid, the permeability will be a constant provided the fluid does not interact with the rock itself. The unit of permeability is the Darcy; it is very large; so the thousandth part is generally used: the millidarcy (md). The symbol for permeability is **k** (Wycoff et al, 1934).

Just as with porosity, the packing, shape, and sorting of granular materials control their permeability. Although a rock may be highly porous, if the voids are not interconnected, then fluids within the closed, isolated pores cannot move. The degree to which pores within the material are interconnected is known as effective porosity (Osborne, 1992). Rocks such as pumice and shale can have high porosity, yet can be nearly impermeable due to the poorly interconnected voids.

In contrast, well-sorted sandstone closely replicates the example of a box of marbles cited above. The rounded sand grains provide ample, unrestricted void spaces that are free from smaller grains and are very well linked. Consequently, sandstones of this type have both high porosity and high permeability.

The range of values for permeability in geologic materials is extremely large. The most conductive materials have permeability values that are millions of times greater than the least permeable. Permeability is often directional in nature. The characteristics of the interstices of certain materials may cause the permeability to be significantly greater in one direction. Secondary porosity features, like fractures, frequently have significant impact on the permeability of the material (Wiener, 1991). In addition to the characteristics of the host material, the viscosity and pressure of the fluid also affect the rate at which the fluid will flow.

2.20 Fluid Saturation

The saturation of a formation is the fraction of its pore volume occupied by the fluid considered. Water saturation, then, is the fraction (or percentage) of the pore volume that contains formation water. If nothing but water exists in the pores, a formation has a water saturation of 100%. The symbol for saturation is S_w , various subscripts are used to denote saturation of a particular fluid (S_w for water saturation, S_o , for oil saturation, S_h , for hydrocarbon saturation, etc.). Oil, or gas, saturation is the fraction of the pore volume that contains oil, or gas. The pores must be saturated with some fluid. Thus, the summation of all saturations in a given formation rock must total to 100%. Although there are some rare instances of saturating fluids other than water, oil, and gas (such as carbon dioxide or simply air), the existence of a water saturation less than 100% generally implies a hydrocarbon saturation equal to 100% less the water saturation (or $1 - S_w$) (Pirson, 1963).

The water saturation of a formation can vary from 100% to a quite small value, but it is seldom, if ever, zero. No matter how “rich” the oil or gas reservoir rock may be, there is always a small amount of capillary water that cannot be displaced by the oil; this saturation is generally referred to as irreducible or connate water saturation.

Similarly, for an oil- or gas-bearing reservoir rock, it is impossible to remove all the hydrocarbons by ordinary fluid drives or recovery techniques. Some hydrocarbons remain trapped in parts of the pore volume; this hydrocarbon saturation is called the residual oil saturation (England, 1975).

In a reservoir that contains water in the bottom and oil in the top the demarcation between the two is not always sharp: there is a more or less gradual transition from 100% water to mostly oil. If the oil-bearing interval is thick enough, water saturation at the top approaches a

minimum value, the irreducible water saturation, (S_{wi}). Because of capillary forces, some water clings to the grains of the rock and cannot be displaced.

A formation at irreducible water saturation will produce water free hydrocarbons. Within the transition interval, some water will be produced with the oil, the amount increasing as S_w increases. Below the transition interval, water saturation is 100%. In general, the lower the permeability of the reservoir rocks the longer the transition interval. Conversely, if the transition interval is short, permeability will be high (Serra, 1986).

2.21 Reserves

Reserves are those quantities of petroleum which are anticipated to be commercially recovered from known accumulations from a given date forward. All reserve estimates involve some degree of uncertainty. The uncertainty depends chiefly on the amount of reliable geologic and engineering data available at the time of the estimate and the interpretation of these data.

The main petrophysical parameters needed to evaluate a reservoir, then, are its porosity, hydrocarbon saturation, thickness, area, and permeability (Dewan, 1983). In addition, the reservoir geometry, formation temperature and pressure, and lithology can play important roles in the evaluation, completion, and production of a reservoir. In the reservoir rock, temperature and pressure control the viscosities and the mutual solubilities of the three fluids – oil, gas, and water (Hilchie 1982).

CHAPTER 3

METHODOLOGY

This chapter deals with a variety of concepts necessary for handling the quantitative analysis aspect of this study. Definitions of the log analysis model and its components are presented, along with step-by-step procedures. Selection of analysis parameters and basic mathematics for this study are also presented.

3.1 Data Preparation and Analysis

Log data acquisition for these wells spans three decades and exhibit a wide range of data quality due to advancements in wireline tool engineering, drilling techniques, and mud systems. Geophysical curve data – considered here are compression sonic, resistivity logs, gamma ray logs, compensated neutron log (CNL) and formation density compensated log – were carefully checked for quality and completeness prior to its use in this petrophysical analysis.

3.1.1 Picking of log values

In order to perform a log analysis it is necessary to pick log values in the various zones of interest. In this study, selection of values was made on a consistent basis from day to day to assist reproducibility of results.

To select a log value, it is helpful to “box the log”; a horizontal line was drawn at each bed boundary at the inflection points on each curve. Then a vertical line was also drawn on each curve at the peaks and valleys, thus transforming the log into a series of individual beds with a single specific log reading. This concept is shown in figure 3.5. Values were not selected on slopes. Slopes indicate transition from one condition to the other, such as porosity or

hydrocarbon content (Crain, 1986). Also no selection of values was made on thin beds. This concept of hand picking log values was used for the entire well log data collected.

3.1.2 Log Editing and Reconstruction

Cycle skips and noise are normally related to sonic logs. Borehole conditions (e.g. washouts, rugosity, mud invasion), and tool problems all contribute to the generally poor log data quality (Threadgold, 1971). In 1S-1X well sonic log, cycle skips were observed at interval depths of 2740 ft to 2760 ft and also at 3540 ft to 3560 ft. producing high spikes. To edit, a smooth log curve was drawn ignoring the spikes, following an imaginary base log located beneath the noise. This concept is shown in figure 3.4. The edit gave a sonic interval transit times of 160 us/ft and 120 us/ft instead of 200 us/ft and 160 us/ft respectively, indicating a major difference and was more probable for these particular zones. Log editing and reconstruction of sonic log particularly was necessary for nearly all the wells studied.

3.2 Reservoir Formation Evaluation

Another important contribution of the log analyst is using the log data to provide an understanding of the subsurface geology at the well location. Clearly we must know something about insitu lithology, porosity, and fluids before we can evaluate the formation response to these reservoir qualities. Standard formation evaluation techniques were used to derive lithology (Vsh), porosity (phia), and water saturation (Sw).

The flushed zone method was used to pin point hydrocarbon bearing zone within the reservoirs of all the wells studied except well ST-7H. This is because its header log has no data value for the resistivity of the mud fluid.

A combination of GR log and the induction resistivity curves were used to delineate the hydrocarbon bearing zones in the ST-7H well. The GR log was first used to mark clean

zones. In hydrocarbon bearing zones the deep induction log resistivity curve will read a high resistivity because hydrocarbons are more resistant than saltwater in the formation. Medium induction log resistivity curves (ILM) measure the resistivity of the invaded zone and reads a high resistivity value which is normally equal to or slightly more than the deep induction curve (ILD). This concept was used to pick the hydrocarbon-bearing zones for ST-7H well.

The ratio S_w/S_{xo} was used to pin point the hydrocarbon bearing zones for the rest of the wells. The ratio is valuable in itself as oil moveability. If $S_w/S_{xo}=1$, then no hydrocarbons have been moved out, whether or not the formation contains hydrocarbons.

If S_w/S_{xo} is about 0.7 or less, moveable hydrocarbons are indicated (Schlumberger, 1989). The ratio S_w/S_{xo} is calculated from this empirical equation:

$$S_w/S_{xo} = [(R_{xo}/R_t) / (R_{mf}/R_w)]^{1/2} \dots\dots\dots (Eq 3-1)$$

3.2.1 Delineation of Shale Beds and Vsh Determination

The GR log is particularly useful for defining shale beds when the SP is distorted. Since there was no SP log data, GR log came in handy in defining the shale beds. The GR log reflects the proportion of shale and, in many regions, can be used quantitatively as a shale indicator. The bed boundary is picked at a point midway between the maximum and minimum deflection of the anomaly.

There are many different ways of determining Volume of Shale (Vsh) in a shaly formation (Schlumberger, 1987). In a shaly porous and permeable zone, the volume of shale (Vsh) can be estimated from the deflections of the GR curve.

The steps involved are as follows:

- I. Read the gamma ray activity associated with the zone of interest (GR_{zone}).
- II. Select a clean shale-free zone, and read GR_{clean} .
- III. Select a 100% shale zone and read GR_{shale} .

The fraction of shale in the zone of interest will be:

$$V_{sh} = (GR_{zone} - GR_{clean}) / (GR_{shale} - GR_{clean}) \dots\dots\dots (Eq 3-2)$$

This is the method used to estimate the volume of shale within every zone of interest.

3.2.2 Porosity Determination

Crossplots are a convenient way to demonstrate how various combinations of logs respond to lithology and porosity. They also provide visual insight into the type of mixtures that the combination is most useful in unraveling. Charts CP-1 (Schlumberger, 1987), through -21 present many of these combinations.

The Density-Neutron crossplot which is the most effective combination for porosity determination was used to determine the true porosity of the South Tano oil field's wells. Figure 3.1 shows a Density-Neutron crossplot chart, on which the Φ_N and ρ_b values of a given zone were cross-plotted. For a clean, gas-free and monomineralic formation a point will fall on one of the lithology lines shown, and the true porosity of the formation is indicated by the graduations along this lines.

Also, the most common evaporites (rock salt, anhydrite) are easily identified. Since the lithology of the reservoir formation is sandstone, matrix line for the sandstone is chosen for porosity graduations. The chart includes also provision for gas correction (top left-hand corner of figure 3.1).

In the presence of gas, Φ_N is lowered, and consequently gas-bearing zones tend to plot above the sandstone matrix line. This effect was corrected by projecting the points, parallel with the gas correction arrow, onto the appropriate sandstone matrix line for its porosity determination.

3.2.3 Resistivity of Formation water (R_w) from Resistivity-Porosity Logs

Formation water, sometimes called connate water or interstitial water, is the water, uncontaminated by drilling mud that saturates the porous formation rock. The resistivity of this formation water, **R_w**, is an important interpretation parameter since it is required for the calculation of saturations (water and/or hydrocarbon) from basic resistivity logs (Wyllie and Rose 1950). There are several sources for formation water resistivity information. These include water catalogs, chemical analyses, the spontaneous potential (SP) curve, and various resistivity-porosity computations and cross plots. Since there was no data on water resistivity, for the area, it has to be computed from the apparent water resistivity log (**R_{wa}**).

R_{wa} log is computed as $R_{wa} = R_t / F$ (Eq. 3-3)

Where **R_t** is from a deep-investigation resistivity log, and **F** is computed from a porosity log reading. For clean, water-bearing zones, **R_t = R_o = FR_w** and the **R_{wa}** value derived from (Eq. 3-3), is equal to **R_w**. A continuous plot of **R_{wa}**, values over many potential reservoir formations should reveal a rather consistent lower limit to this computed **R_{wa}**, value. If it does, that **R_{wa}**, value is probably the formation water resistivity **R_w**.

This technique works best over intervals in which the formation water resistivity remains constant or changes only gradually (Morris and Brigg, 1967). Fortunately, in most oil-producing provinces this is usually the case, particularly at deeper depths. Water saturation is the fraction (or percentage) of the pore volume of the reservoir rock that is filled with water. It is generally assumed, unless otherwise known that the pore volume not filled with water is filled with hydrocarbons. Determining water and hydrocarbon saturation is one of the basic objectives of well logging (Rider, 1996).

3.2.4 Water Saturation Determinations from Resistivity Logs

All water saturation determinations from resistivity logs in clean (non shaly) formations with homogeneous intergranular porosity are based on Archie's water saturation equation, or variations thereof.

The equation is $(S_w)^n = FR_w / R_t$ (Eq 3-4).

Where R_w , is the formation water resistivity R_t is the true formation resistivity and F is the formation resistivity factor. The saturation exponent 'n' is usually taken as 2.

F is usually obtained from the measured porosity of the formation through the relationship.

$$F = a/\Phi^m \text{ (Eq. 3-5)}$$

For Sandstone formation as occurred in South Tano oil fields the Humble formula is used to compute formation resistivity factor F where $a = 0.61$ and $m = 2.15$

Fluid properties such as water saturation S_w were calculated using Archie's water saturation equation (Eq. 3-4).

3.2.5 Selection of Irreducible Water Saturation

Most quantitative permeability calculations require a value for the irreducible water saturation (S_{wi}) at each level in a zone, even if the zone is not hydrocarbon bearing.

If porosity were constant, this would be the minimum value of water saturation in a zone.

However porosity is seldom constant, so the product of porosity and water saturation is usually used (Threadgold, 1971).

The $(\Phi \times S_w)$ product is found by plotting porosity (Φ) vs. water saturation S_w from log data and finding the best fit hyperbola to the data. Data from the transition zones and water zones are excluded. Once a $(\Phi \times S_w)$ product has been chosen, the irreducible water saturation for any zone can be found by entering effective porosity on figure 3.2 (schlumberger, 1989). For

clean sandstone reservoir, the recommended parameter for the product ($\emptyset \times S_w$) lies within 0.08 to 0.12 (Crain, 1986). In this investigation the product was found to be 0.1.

3.2.6 Permeability Estimation from the Wyllie-Rose Method

In their thorough analysis of the theoretical basis of quantitative log interpretation, Wyllie & Rose expanded the empirical relationship proposed by (Tixier, 1949), based on the following assumptions: -tortuosity, T, applicable to fluid flow of the wetting phase in a porous media is the same as the tortuosity affecting electrical conductivity through the fluid in the same media.

Based on the general expression of Wyllie and Rose 1950, several investigators have proposed various empirical relationships with which permeability can be estimated from porosity and irreducible water saturation derived from well logs. In this study, one of such empirical relations is used to estimate the intrinsic (absolute) permeability, these empirical relations are:

$$K = (79 \chi \emptyset^3/S_{WI})^2 \text{ for GAS}$$

$$K = (250 \chi \emptyset^3/S_{WI})^2 \text{ for OIL}$$

Where K is absolute permeability, \emptyset is the true porosity and S_{WI} is the irreducible water saturation.

3.3 Problems with data collection

One major problem confronted with was the absence of individual data value of the reservoir area of each well. It is one of the most valuable sources of information in the estimation of oil/gas reserves in place. The absence of these data led to the failure to estimate the hydrocarbon reserves in place of the studied wells. Quantitative calculations of oil and gas saturation are predicated on the knowledge of the formation water resistivity. Since there was

no water catalogs for the studied area it has to be computed from the apparent water resistivity log.

3.4 Assumptions

A thorough analysis of the theoretical basis of the quantitative log interpretation of this study is based on the following assumptions:

- Reservoir formation considered is lithologically clean (no clay minerals)
- Reservoir formation rocks do not have an excessively high surface area.
- Formation water (connate water) is saline.
- For partially saturated rocks $S_w > 0.15$.
- Reservoir formation rock is water-wet.
- Medium gravity oil is assumed for a hydrocarbon bearing zone.
- Beds less than 1 m thick is considered to be thin not considered in the analysis.
- Pore fluid is either hydrocarbon (gas/oil), water or both.

CHAPTER 4

RESULTS AND DISCUSSIONS

This chapter deals with the results and interpretation of the well log analysis carried on all the six exploratory wells studied. The detailed results for each well's hydrocarbon potential are presented in tabular form. Also depth plots of porosity, water saturation, and volume of shale of all wells and sections of reservoir abnormal pressure zones are also presented in graphical form.

4.1 Well Reservoir Statistics

Using reservoir statistics, the following reservoir parameters for all the wells studied were computed. Table 4-1 below shows the results of well reservoir statistics of all the six wells.

Table 4.1 shows well reservoir statistics of each well.

WELL RESERVOIR STATISTICS						Location	
Wells	Formation Top / Meters	Formation Bottom / meters	Gross Reservoir thickness / meters	Net Reservoir Thickness / meters	Net / Gross	Latitude	Longitude
1S - 1X	1841.60	1958.04	116.43	89.00	0.76	04° 45' 21.514" N	02° 58' 29.914" W
1S - 3AS	2021.00	2713.00	692.00	291.00	0.42	04° 43' 22.030" N	02° 58' 44.300" W
1S - 4AX	1832.76	1905.00	72.24	61.00	0.84	04° 44' 58.710" N	02° 57' 31.125" W
ST - 05	1794.97	1859.00	64.03	61.00	0.95	04° 45' 26.880" N	02° 57' 48.780" W
ST - 06	1811.12	1850.12	39.00	32.00	0.82	04° 45' 14.880" N	02° 57' 54.900" W
ST - 7H	2011.68	2157.68	146.00	76.00	0.52	04° 45' 26.000" N	02° 58' 09.000" W

From table 4.1, it shows that four of the wells, namely 1S-1X, 1S-4AX, ST-05, and ST-06 have a net-gross ratio greater than 0.70, meaning more than 70% of their formation is sandstone with the rest being shale, shaly sands and calcite. This is an indication of good reservoir quality compared to 1S-3AS and ST-7H wells.

Data from six potential reservoir wells of the western basin (Tano basin) were collected and analyzed.

In each case, distribution of porosity, water saturation, reservoir thickness, permeability was developed with the help of wireline logs.

Below are the summary results and interpretations of each well in detail.

4.2 Hydrocarbon Potential of Well 1S-1X

Table 4.2 is summary results of the hydrocarbon potential of well 1S-1X

ZONES	Depth / Meters	Reservoir Thickness / M	Ø	Sw	Vsh GR	Sxo	Sw / Sxo	Swi	K / md	Hydrocarbon predicted
1	1838 - 1841	3.00	12.50	0.36	0.10	0.97	0.37	0.80	0.04	Gas
5	1850 - 1853	3.00	26.50	0.39	0.34	0.69	0.56	0.38	149.90	Oil
8	1856 - 1857	1.00	27.00	0.33	0.40	0.72	0.46	0.37	176.87	Oil
9	1857 - 1859	2.00	27.00	0.38	0.40	0.91	0.42	0.37	176.87	Oil
10	1859 - 1861	2.00	28.00	0.31	0.30	0.53	0.58	0.36	232.39	Oil
11	1861 - 1864	3.00	17.00	0.37	0.20	0.84	0.44	0.59	0.43	Gas
12	1864 - 1867	3.00	28.00	0.34	0.40	0.75	0.45	0.36	232.39	Oil
13	1867 - 1868	1.00	17.00	0.40	0.40	0.70	0.57	0.59	0.43	Gas

4.2.1 Interpretations of 1S-1X Well Results.

The GR log of 1S-1X gave estimated clean zone of 25 API and shale zone of 75 API. Resistivity of water saturation (R_w) was estimated to be 0.098 Ohm.m while the resistivity of mud fluid was 0.178 Ohm.m. From table 4-2, a total of eight hydrocarbon-bearing zones were delineated, with total pay zone of 18 m. The first hydrocarbon zone encountered was gas zone at interval depths of 1838-1841 m. The estimated values of porosity and permeability for the oil zones were much higher than the gas zone; from table 4-2 the mean estimated values for porosity, permeability and water saturation of 27.3 %, 193.68 md, and 37.6 % compared to porosity of 15.5 %, permeability of 0.3 md and water saturation of 37.6 % of the gas zones, suggest that the oil zones were much more porous and permeable. Zones 10 and 12 proved to be the most porous and highly permeable of all the delineated hydrocarbon zones of the entire reservoir well.

The water saturation (S_w) estimated, range from 31 % to 40 %, suggesting over 60 % of hydrocarbon saturation of the reservoir. Oil and gas were detected alright but the total pay suggests that, the reservoir potential is not sufficient.

4.3 Hydrocarbon Potential of Well 1S-3AX

Table 4.3 is summary results of the hydrocarbon potential of well 1S-3AX

ZONE	Depth / Meters	Reservoir Thickness / m	Ø	Sw	Vsh GR	Sxo	Sw / Sxo	Swi	K/md	Hydrocarbon predicted
2	2034 - 2035	1.0	30.50	0.50	0.18	0.79	0.64	0.33	462.00	Oil
8	2042 - 2043	1.0	29.00	0.58	0.55	1.02	0.57	0.34	321.60	Oil
22	2158 - 2164	6.0	36.00	0.58	0.18	0.94	0.62	0.28	1735.32	Oil
38	2223 - 2225	2.0	32.00	0.16	0.04	0.41	0.38	0.31	698.32	Oil
67	2360 - 2363	3.0	29.50	0.61	0.18	1.16	0.52	0.34	356.33	Oil
69	2364 - 2365	1.0	20.00	0.86	0.18	1.37	0.63	0.50	1.60	Gas
71	2366 - 2367	1.0	24.20	0.75	0.18	1.44	0.52	0.41	7.46	Gas
72	2367 - 2370	3.0	24.20	0.73	0.18	1.24	0.58	0.41	7.46	Gas
73	2370 - 2371	1.0	24.20	0.73	0.18	1.24	0.58	0.41	7.46	Gas

4.3.1 Interpretations of 1S-3AX Well Results

Estimations from 1S-3AX well GR log, 20 API of clean zone and 75 API of shale zone. Resistivity of water saturation R_w was estimated and found to be 0.3071 Ohm.m. The first hydrocarbon-bearing zone which is oil was detected at interval depths of 2034-2034 m. Total of nine hydrocarbon-bearing zones were delineated, with total reservoir thickness (pay zone) of 19 m.

Of the nine zones delineated, five of them predicted oil, with total reservoir thickness of 13 m, while the rest showed gas. All the oil pay zones indicated both high estimated porosity and permeability values compared to the gas-bearing zones, as to be expected. Porosity and permeability values of 36 % and 1735 md respectively, were estimated at interval depths of 2158-2164 m. This also happened to be the thickest of the entire hydrocarbon-bearing zones,

with reservoir thickness of 6 m. This zone proved to be the most porous and permeable, but it was less saturated with oil and bit shaly than zone 38, which recorded a water saturation value of 16 % and a volume of shale (Vsh) of 4 %, suggesting more clean zone and high hydrocarbon saturation. The first gas zone was picked at interval depths of 2364 m to 2365 m. Though the gas zones were clean and show better promised in terms of porosity and permeability their water saturation value between 73 % and 86 % leave much to be desired, suggesting low hydrocarbon saturation.

4.4 Hydrocarbon Potential of Well 1S-4AX

Table 4.4 is summary results of the hydrocarbon potential of well 1S-4AX.

Zone	Depth /Meters	Reservoir Thickness / M	Ø	Sw	Vsh GR	Sxo	Sw / Sxo	Swi	K/md	Hydrocarbon predicted
11	1865 - 1867	2.00	28.50	0.59	0.06	0.70	0.84	0.35	273.41	Oil
16	1878 - 1879	1.00	23.50	0.51	0.07	0.86	0.59	0.43	56.93	Oil
18	1881 - 1885	4.00	28.50	0.81	0.29	0.90	0.89	0.35	273.41	Oil

4.4.1 Interpretations of 1S-4AX Well Results

From the GR log of Well 1S-4AX, the clean zone was estimated to be 35 API and shale zone of 70 API. Resistivity of water saturation estimated was 0.5721 Ohm.m. The header log recorded mud fluid resistivity of 0.27 Ohm.m. Total of three hydrocarbon-bearing zones were delineated. All the zones predicted oil. The first oil-bearing zone was picked at interval depths of 1865-1867 m. Total reservoir thickness estimated was 7 m, which suggests a poor reservoir quality in terms of reserves. Zone 11 and 18 had the same porosity and permeability estimates which proved to be comparatively higher than zone 16. This suggests that, zone 11 and 18 were more porous and permeable than zone 16. But with water saturation of 51 %

zone 16 was much better in terms of oil saturation. Though zone 18 was more promising its water saturation estimate of 81 % makes it worse off, in terms of hydrocarbon saturation.

4.5 Hydrocarbon Potential of Well ST-05

Table 4.5 is summary results of the hydrocarbon potential of well ST-05.

ZONE	DEPTH / M	Reservoir Thickness /m	Ø	S _w	V _{SH} GR	S _{xo}	S _w / S _{xo}	S _{wi}	K/md	Hydrocarbon predicted
1	1795 - 1797	2.00	15.00	0.24	0.14	0.73	0.33	0.67	0.16	Gas
3	1798 - 1799	1.00	8.00	0.59	0.11	1.78	0.33	1.25	1.05E-03	Gas
7	1802 - 1804	2.00	5.00	0.80	0.06	2.06	0.48	2.00	2.43E-05	Gas
9	1805 - 1807	2.00	5.00	0.40	0.17	2.06	0.19	2.00	2.43E-05	Gas
10	1807 - 1810	3.00	26.00	0.17	0.28	0.52	0.33	0.38	133.71	Oil
11	1810 - 1815	5.00	25.00	0.11	0.16	0.37	0.30	0.40	95.37	Oil
12	1815 - 1819	4.00	23.50	0.19	0.26	0.57	0.34	0.43	56.93	Oil
13	1819 - 1821	2.00	25.00	0.17	0.26	0.52	0.33	0.40	95.37	Oil
14	1821 - 1822	1.00	28.10	0.24	0.26	0.65	0.37	0.36	237.42	Oil
15	1822 - 1823	1.00	26.00	0.26	0.29	0.70	0.37	0.38	133.71	Oil
16	1823 -1825	2.00	22.00	0.22	0.29	0.66	0.33	0.45	35.00	Oil
19	1828 - 1829	1.00	9.10	0.23	0.19	1.08	0.21	1.10	3.54	Gas
20	1829 - 1830	1.00	24.50	0.08	0.22	0.37	0.21	0.41	80.41	Oil
21	1830 -1832	2.00	26.00	0.17	0.29	0.52	0.33	0.38	133.71	Oil
22	1832 -1834	2.00	24.00	0.01	0.22	0.29	0.04	0.42	67.71	Oil
23	1835 -1837	2.00	24.00	0.15	0.14	0.54	0.27	0.42	67.71	Oil
24	1837 - 1842	5.00	24.50	0.08	0.22	0.33	0.24	0.41	80.41	Oil
27	1852 - 1854	2.00	12.80	0.35	0.22	1.08	0.33	0.78	0.05	Gas

4.5.1 Interpretations of ST-05 Well Results

From the header log of ST-05 well, the resistivity of the mud fluid (R_{mf}) was 0.223 Ohm.m. A clean zone of 10 API and shale zone of 100 API were estimated from the GR log. This well proved to be the most promising of all the wells studied, in terms of hydrocarbon potential. A total of eighteen zones of hydrocarbon beds were delineated. Twelve out of the 18 zones predicted oil, with the rest being gas. The total reservoir thickness for the entire hydrocarbon bearing zones of the reservoir was 40 m. All the oil-bearing zones were more porous and permeable than the gas zones. Gas was first encountered at interval depths of 1795-1797 m. zone 14 at an interval depths of 1821-1822 m was found to be the most porous and permeable of all the oil-bearing zones with porosity and permeability estimates of 28 % and 237.42 md respectively, with water saturation of 24 % indicating hydrocarbon saturation of 76 %, the zone proved to be potentially good in oil.

Zone 11 and 24, at depths 1810 m and 1837 m respectively, had the highest pay zone of 5 m. both zone were highly porous and permeable. The average water saturation of 25.88 % suggests fairly good hydrocarbon saturation of over 70 % for the reservoir. The entire hydrocarbon column delineated, were highly clean of shales.

4.6 Hydrocarbon Potential of Well ST-06

Table 4.6 is summary results of the hydrocarbon potential of well ST-06.

ZONE	DEPTH / m	Reservoir Thickness /m	Ø	S _w	V _{SH} GR	S _{xo}	S _w / S _{xo}	S _{wi}	K/md	Hydrocarbon predicted
20	1832 - 1833	1.00	10.50	0.33	0.03	0.43	0.77	0.95	0.01	Gas
21	1833 - 1834	1.00	16.50	0.20	0.11	0.27	0.77	0.61	0.34	Gas
23	1834 - 1837	1.00	24.50	0.40	0.08	0.57	0.71	0.41	80.41	Oil
24	1837 - 1838	1.00	19.00	0.14	0.06	0.29	0.49	0.53	1.05	Gas
25	1838 - 1839	1.00	23.00	0.11	0.09	0.23	0.49	0.43	50.04	Oil
26	1841 - 1842	1.00	17.00	0.64	0.09	0.82	0.78	0.59	0.43	Gas

4.6.1 Interpretations of ST-06 Well Results

Clean zone of 15 API and shale zone 180 API were estimated from ST-06 GR log. The estimate for the resistivity of the water saturation was 0.1353 Ohm.m. The header log recorded 0.230 Ohm.m as resistivity of the mud fluid. A total of six hydrocarbon-bearing zones were delineated, with four of them predicting gas. The first hydrocarbon-bearing zone was delineated at the depths of 1882- 1833 m. The oil-bearing zones recorded a high porosity and permeability estimates than the predicted gas zones. The estimated porosity and permeability values for the oil zones are; 24.5 %, 80.41 md for zone 23 and 23%, 50.04 md for zone 25.

Proving that, the oil zones were much more porous and permeable than the gas zones. Zone 25 proved to be the most saturated zone of hydrocarbon, with water saturation (S_w) of 11 %, indicating a hydrocarbon saturation of 89 %.

4.7 Hydrocarbon Potential of Well ST-7H

Table 4.7 is summary results of the hydrocarbon potential of well ST-7H

ZONE	DEPTH / Meters	Reservoir Thickness/m	Ø	S _w	V _{SH}	S _{wi}	K /md	Hydrocarbon predicted
1	2012 - 2014	2.00	7.5	0.14	0.06	1.33	6.3E-04	Gas
3	2016 - 2017	1.00	9.0	0.15	0.22	1.11	2.7E-03	Gas
5	2021 - 2022	1.00	27.4	0.05	0.34	0.36	204.06	Oil
7	2024 - 2026	2.00	21.0	0.07	0.30	0.48	23.27	Oil
10	2029 - 2031	2.00	1.8	0.89	0.20	5.56	6.9E-09	Gas
21	2048 - 2049	1.00	16.0	0.12	0.40	0.63	0.27	Gas
24	2053 - 2057	4.00	25.0	0.06	0.30	0.40	95.37	Oil
29	2076 - 2083	7.00	26.0	0.06	0.30	0.38	133.71	Oil

4.7.1 Interpretations of ST-7H Well Results

GR log of ST-7H well, gave estimated value of the clean zone and shale zone as 25 API and 75 API respectively. The estimated value for the water saturation resistivity (R_w) was 0.003 Ohm.m. Data on mud fluid resistivity was not provided on the header log. A total of eight hydrocarbon-bearing zones were delineated, with the first hydrocarbon being picked at interval depths of 2012-2014 m, and predicted gas. This well also recorded low estimates of porosity and permeability for gas zones and high estimates for oil zones.

Total reservoir thickness for the hydrocarbon column was 20 m, with zone 29 an oil-bearing zone recording 7 m of pay zone alone. Zone 5 and 29 proved to be the most porous and permeable zones.

4.8 Depth Plot of Vsh, Sw, and \emptyset for 1S-1X Well

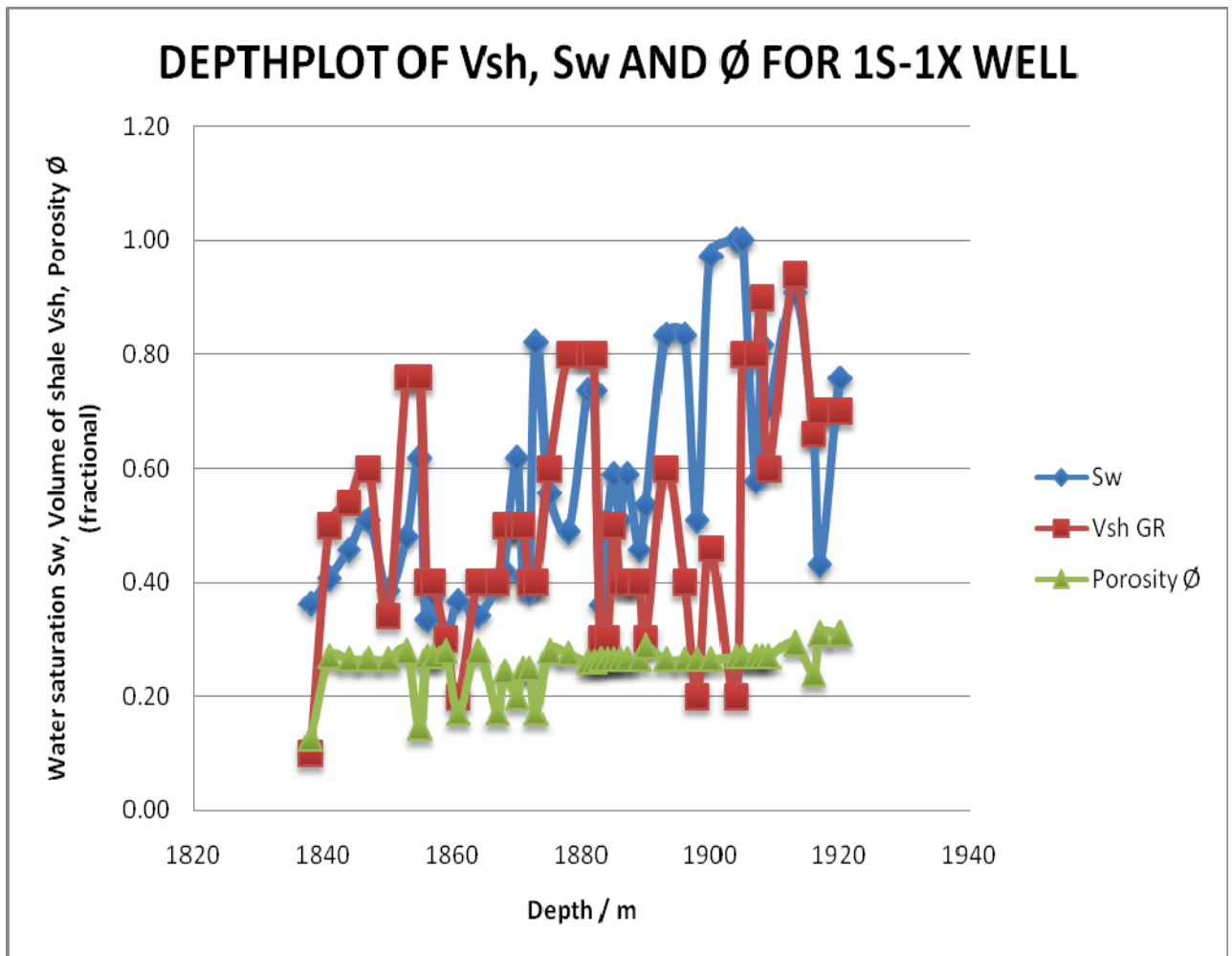


Fig.4.1 shows the depth plot of Vsh, Sw and porosity for 1S-1X well

The 1S-1X well has a total pay zone of 18 m of which 11 m is oil pay zones. It has an average porosity of 22.88%, average water saturation 36% suggests 64 % of hydrocarbon saturation. The water saturation S_w tends to increase as the depth increases. Between 1900 m and 1920 m both Vsh and water saturation S_w are so high indicating shale content as shown in figure 4.1 above.

4.9 Depth Plot of Vsh, Sw, and Ø for 1S-3AX Well

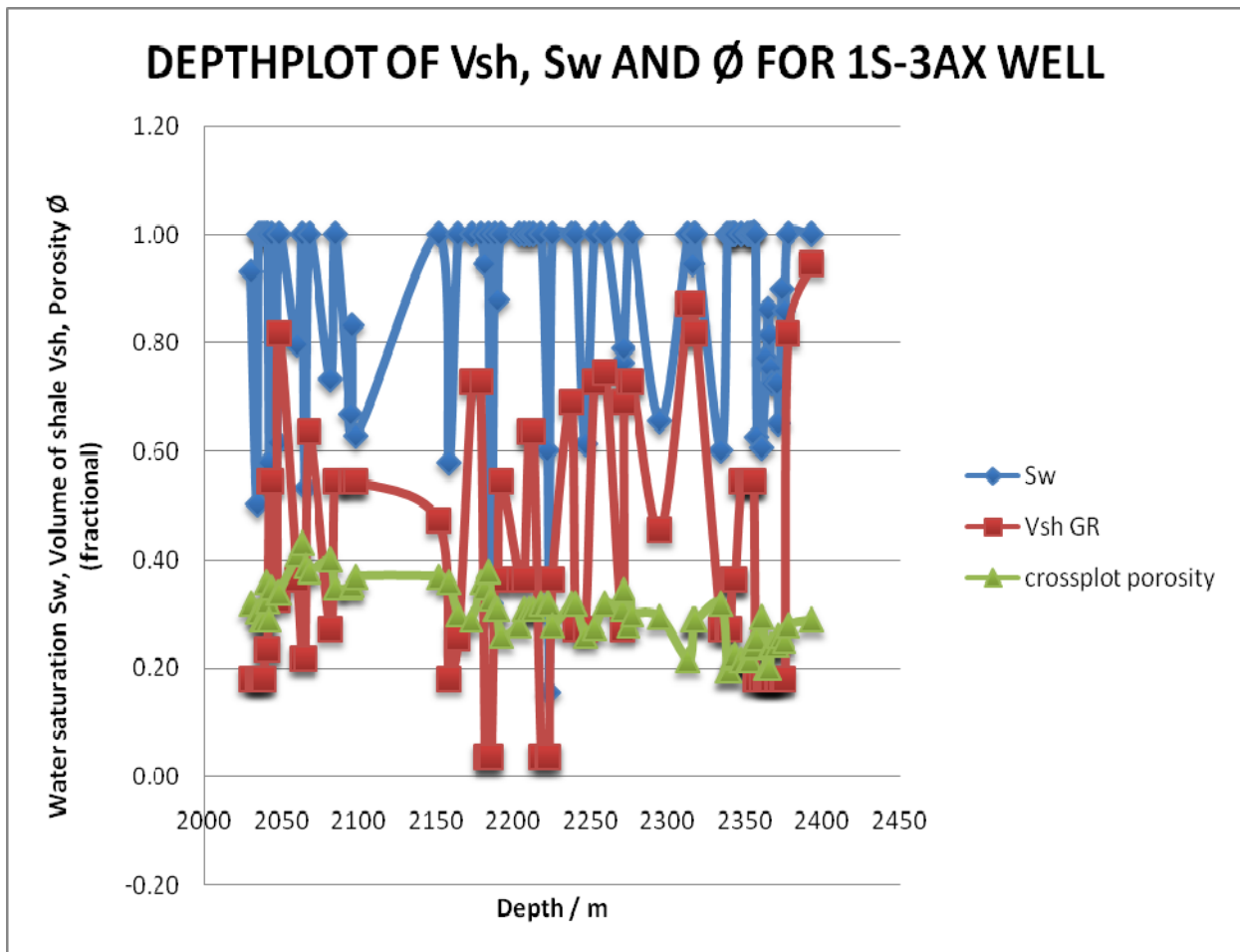


Fig.4.2 shows the depth plot of Vsh, Sw and porosity for 1S-3AX well

A total pay zone of 19 meters is estimated in the 1S-3AX well. This well recorded both oil and gas. Its highest net pay zone of 6 meters is recorded at the depth of 2158 m and 2164 m. The average porosity is 27.73% and the average water saturation is 61% suggesting a more water bearing zones and shales and 39 % of hydrocarbon saturation. From figure 4b, it shows that most part of the reservoir is 100% saturated with formation water and most of the formation section were clean. Porosity decreases as the depth increases. It happens to be the well with the highest gross reservoir thickness but the least net- to- gross ratio.

4.10 Depth Plot of Vsh, Sw, and ϕ for 1S-4AX Well

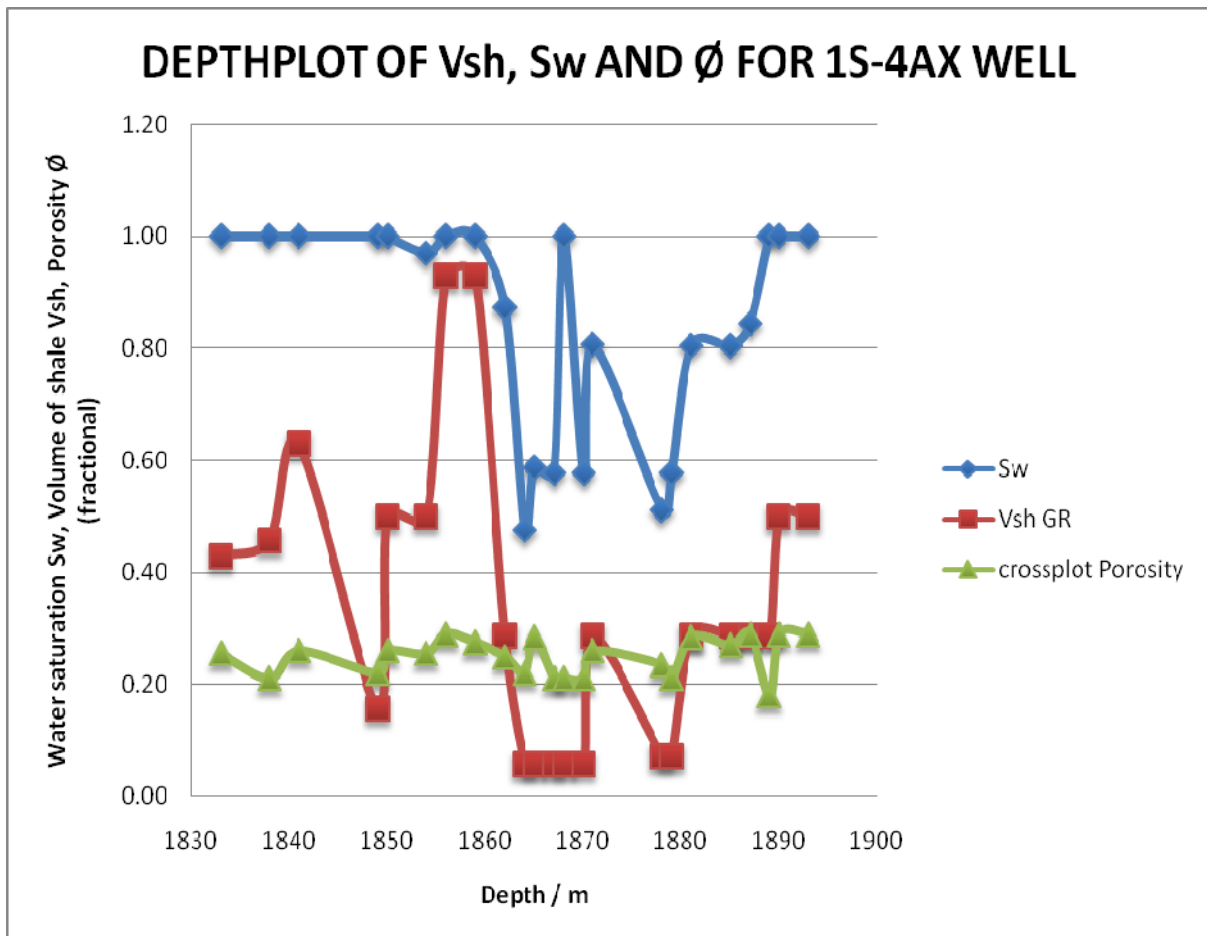


Fig.4.3 shows the depth plot of Vsh, Sw and porosity for 1S-4AX well

Only three pay zones are estimated in this 1S-4AX well. These total 7 m of which 4 m alone is recorded at a depth of 1881 m to 1885 m. Only oil was encountered in this well. The average porosity is 26.83% and average water saturation is 63.66%.

From figure 4.3, porosity appears to be constant throughout the formation. From the depth 1830 to 1860 m the water saturation Sw, remains constant at 100% suggesting no moveable hydrocarbon, within this same range of depth, the volume of shale Vsh, increases and peaks at 1860 meters. This trend then reverses rapidly for both Sw and Vsh up to 1890 meters suggesting clean formation and moveable hydrocarbon.

4.11 Depth Plot of Vsh, Sw, and ϕ for ST-05 Well

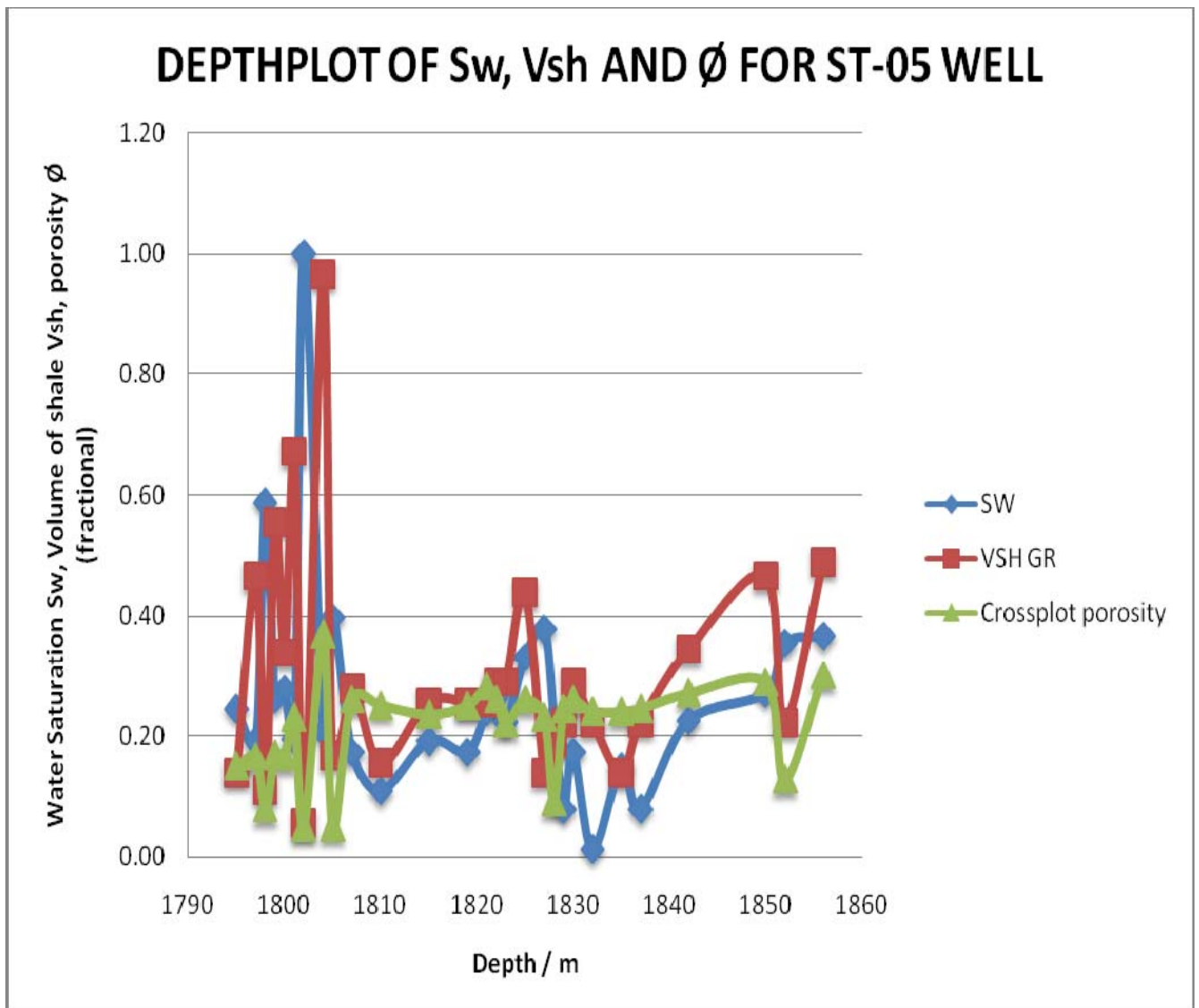


Fig.4.4 shows the depth plot of Vsh, Sw and porosity for ST-05 well

ST-05 well recorded the highest number of pay zones. As many as 27 is estimated, with total thickness of 40 m. The well encountered both oil and gas. The average porosity is 19.64% and the average water saturation Sw is 25.88%, suggesting more moveable hydrocarbons. Both water saturation Sw and volume of shale Vsh increase between 1795 m to 1805 meters suggesting zones of shaly sands to more shales and almost no moveable hydrocarbons. This trend reverses rapidly at depth 1805 meters and remain relatively low for both Sw and Vsh throughout the rest of the reservoir formation as shown in figure 4.4 above.

4.12 Depth Plot of Vsh, Sw, and \emptyset for ST-06 Well

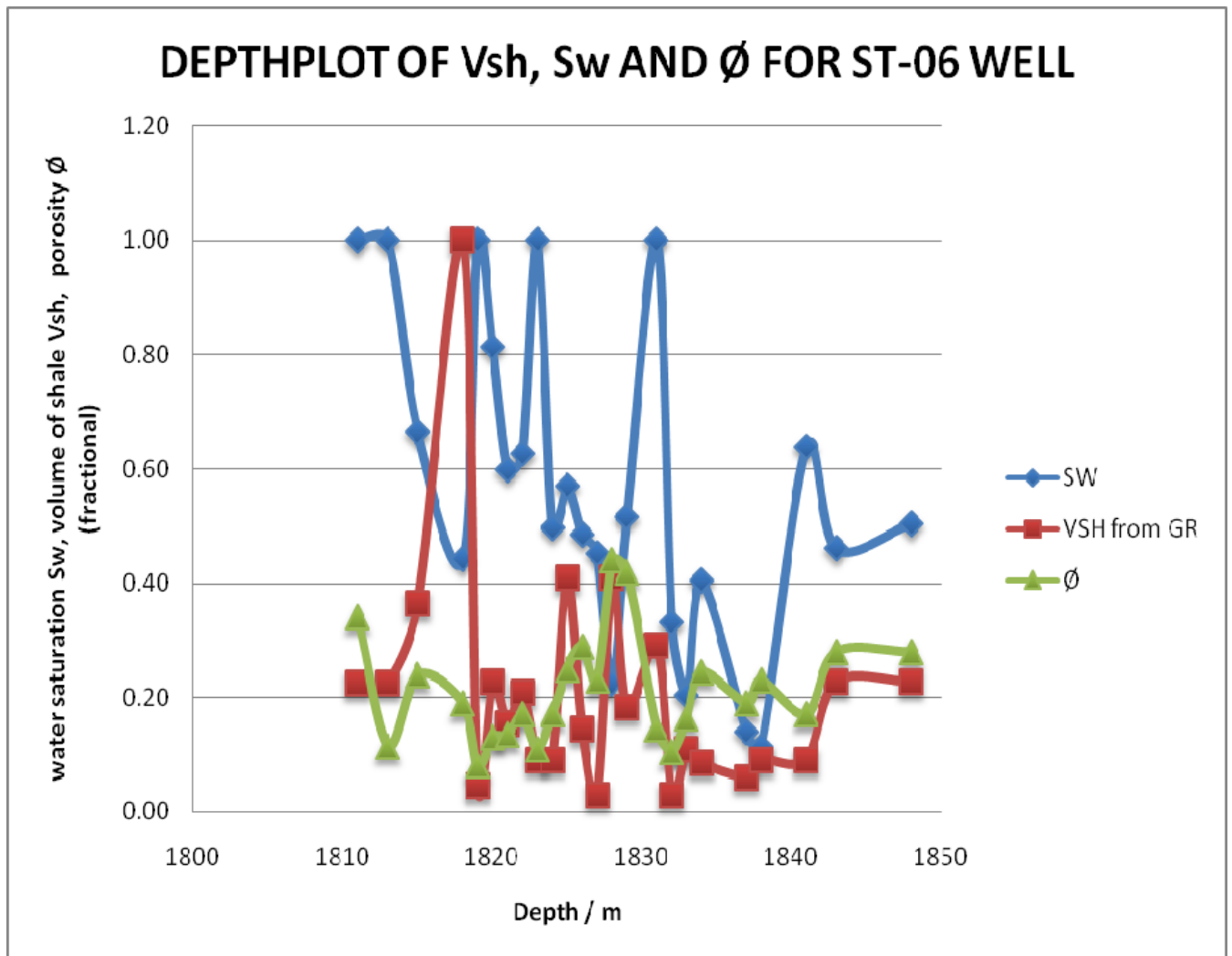


Fig.4.5 shows the depth plot of Vsh, Sw and porosity for ST-06 well

A total of six pay zones was estimated with total thickness of 6 meters. Only two of the pay zones encountered oil, with the rest being gas. The average porosity is 18.42%, the average water saturation Sw is 30% indicating good moveable hydrocarbons. Figure 4.5 shows that water saturation Sw generally decreases with depth. The highest Vsh estimated occurred at the depth of 1818 meters, the rest of it lies between 0 to 40% throughout the entire formation indicating clean formation.

4.13 Depth Plot of Vsh, Sw, and Ø for ST-7H Well

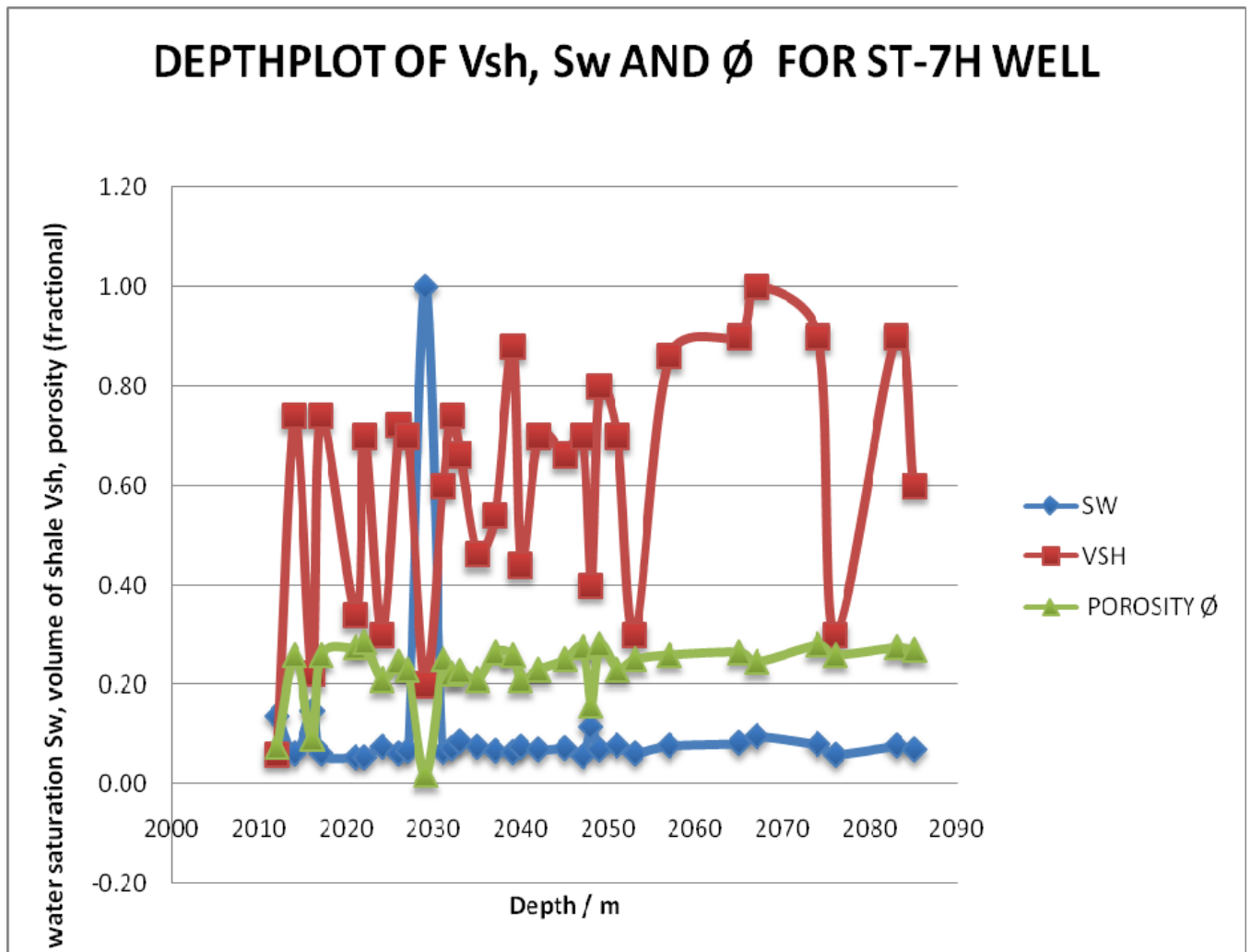


Fig.4.6 shows the depth plot of Vsh, Sw and porosity for ST-7H well

The pay zones thickness is 20 meters. The average porosity is 16.7% and the average water saturation Sw is 20.6% which looks good for moveable hydrocarbons. From the figure 4.6, at the depth of 2029 meters, the estimated water saturation Sw is about 100%, at the same depth the lowest porosity is also estimated with a low Vsh as well. This suggests that the zone in question is clean alright but may contain cementing materials such as calcite, which causes its porosity to reduce significantly.

4.14 Detection of Abnormal Pressures Zones

Formations having abnormally high fluid pressures are often overlain by over pressured shales, which have an excess of pore water. Abnormal pressures develop when a shale body becomes isolated and therefore unable to lose water. This inability to lose water arrests the compaction process, which means that shale body remains under-compacted and contains more water. As the depth of burial increases, the trapped water begins to exert a pore pressure to balance the weight of the increasing overburden (Dullien, 1992).

Sonic transit time is greater in these shales than in normally compacted shales. Thus sonic log may be used to predict the possibility of over pressured formations. The sonic travel time in shales normally decreases with increasing burial depth. Departures from this trend towards higher values of interval transit times suggest an abnormal over pressured section (Dullien, 1992).

This phenomenon is evident in almost all the wells studied except well ST-05 and ST-06.

4.14.1 Depth Plot of Well 1S-1X with Interval Transit Time

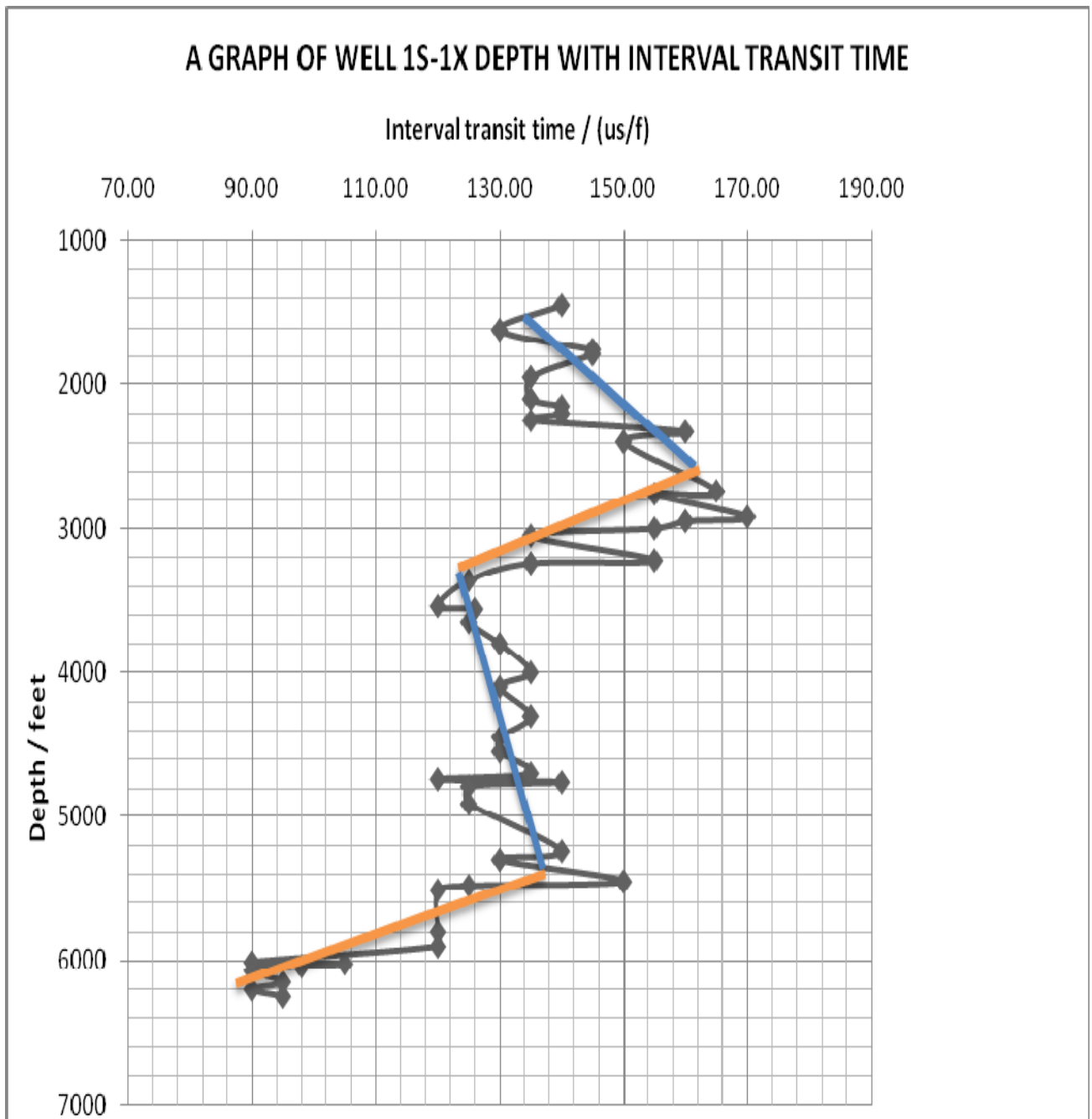


Fig.4.7, shows the depth plot of well 1S-1X with interval transit time

From figure 4.7 the blue trend lines suggest an overpressures section of the 1S-1X well.

While the orange trend lines indicate normal compaction trend.

Over pressured sections lies between, 1000-3000 ft and tends to repeat between the intervals 3500-5500 ft. Drilling through these sections comes with a high cost to the drilling company.

More additives have to be added to the mud fluid to make it denser for a high increase in its hydrostatic pressure, to hold borehole walls from collapsing in when drilling through.

4.14.2 Depth Plot of Well 1S-3AX with Interval Transit Time

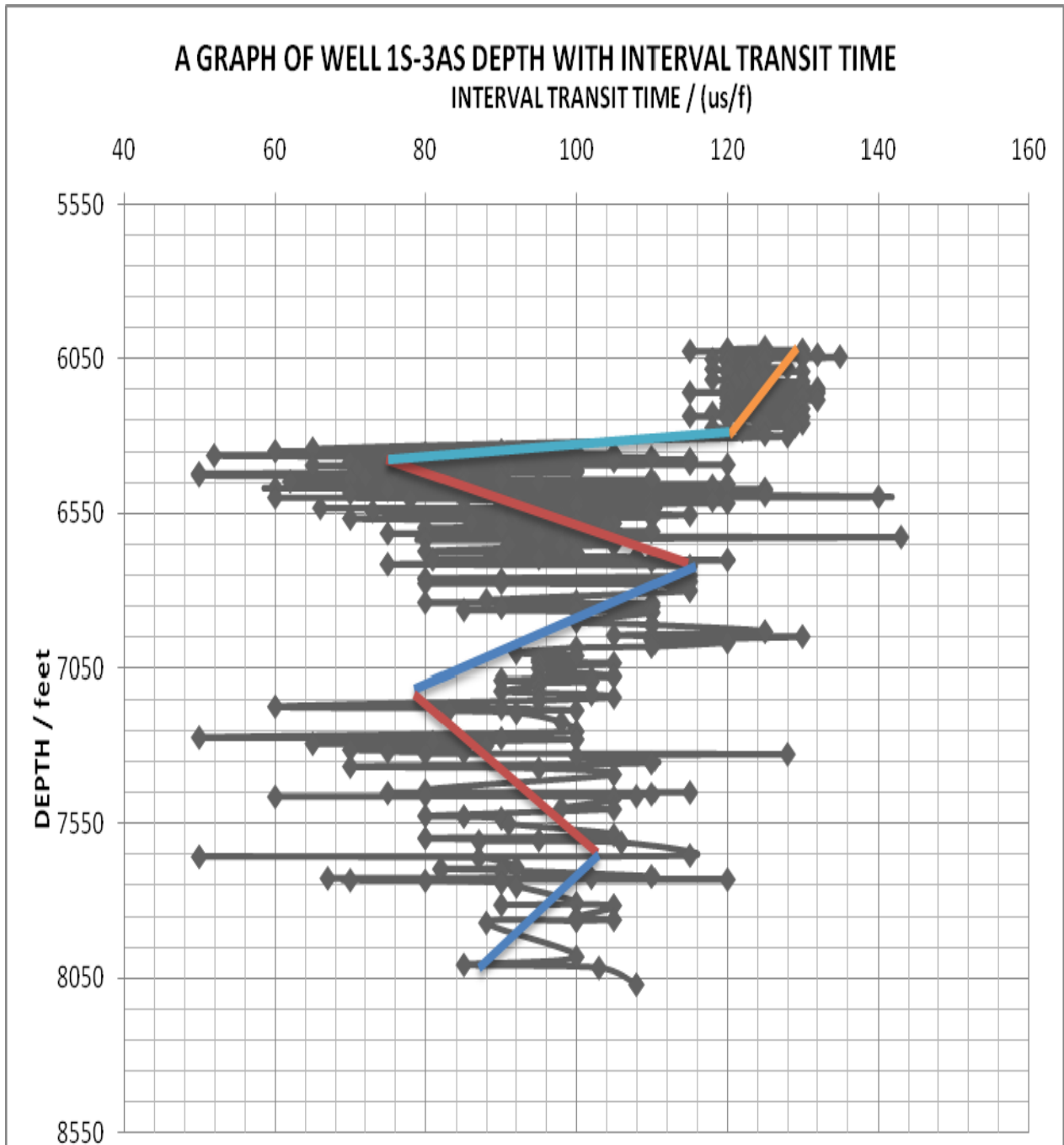


Fig.4.8, shows the depth plot of well 1S-3AX with interval transit time

From figure 4.8, the two dark red trend lines suggest over pressured formation sections and are detected between interval depths of about 6000 – 7000 ft and 7050 – 7550 ft. in the 1S-3AX well.

4.14.3 Depth Plot of Well 1S-4AX with Interval Transit Time

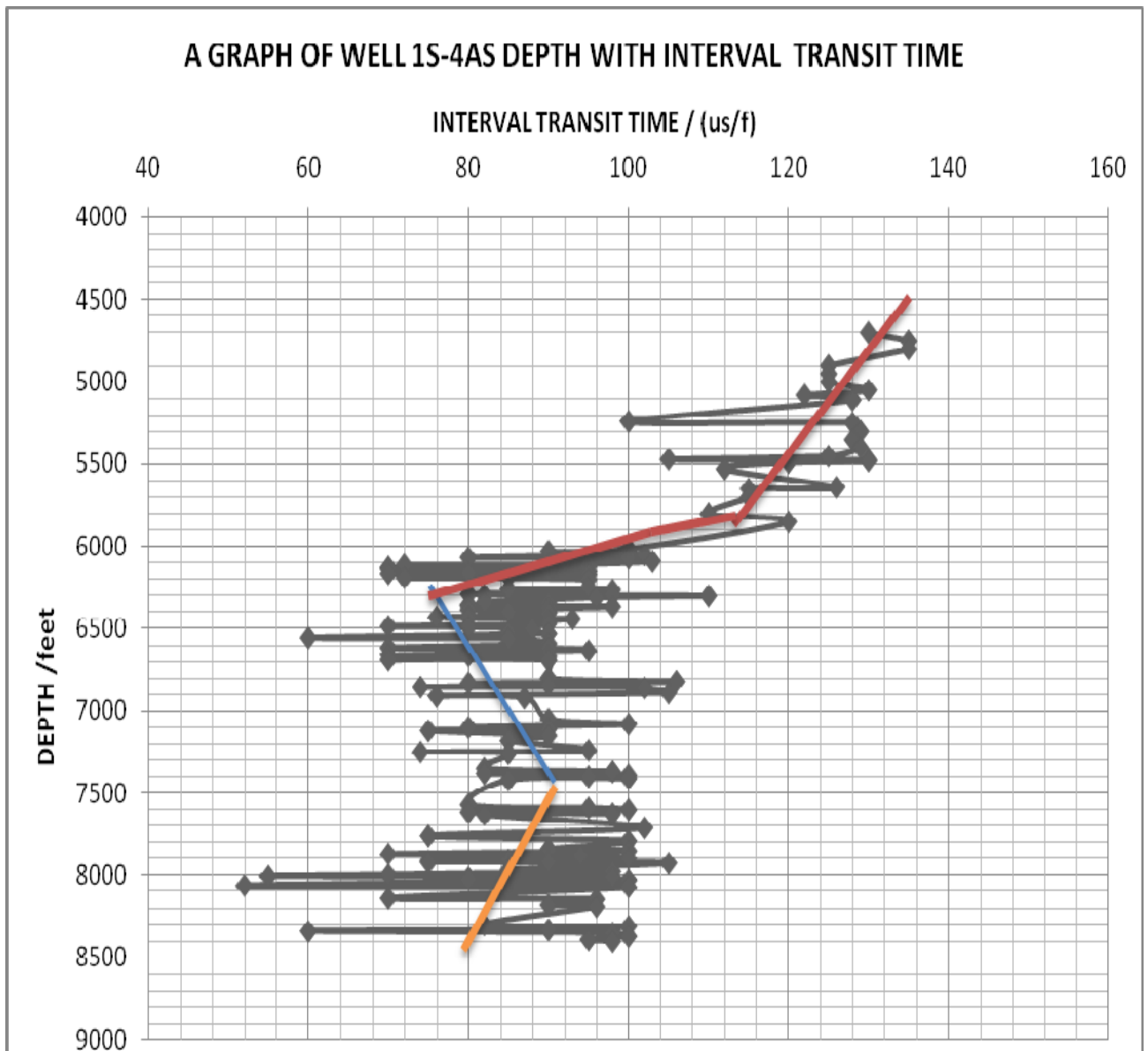


Fig.4.9, shows the depth plot of well 1S-4AX with interval transit time

From figure 4.9, the only over pressured section detected is shown by the blue trend line and lies at interval depth of about 6000 -7500 ft of the reservoir formation of well 1S-4AX

4.14.4 Depth Plot of Well ST-05 with Interval Transit Time

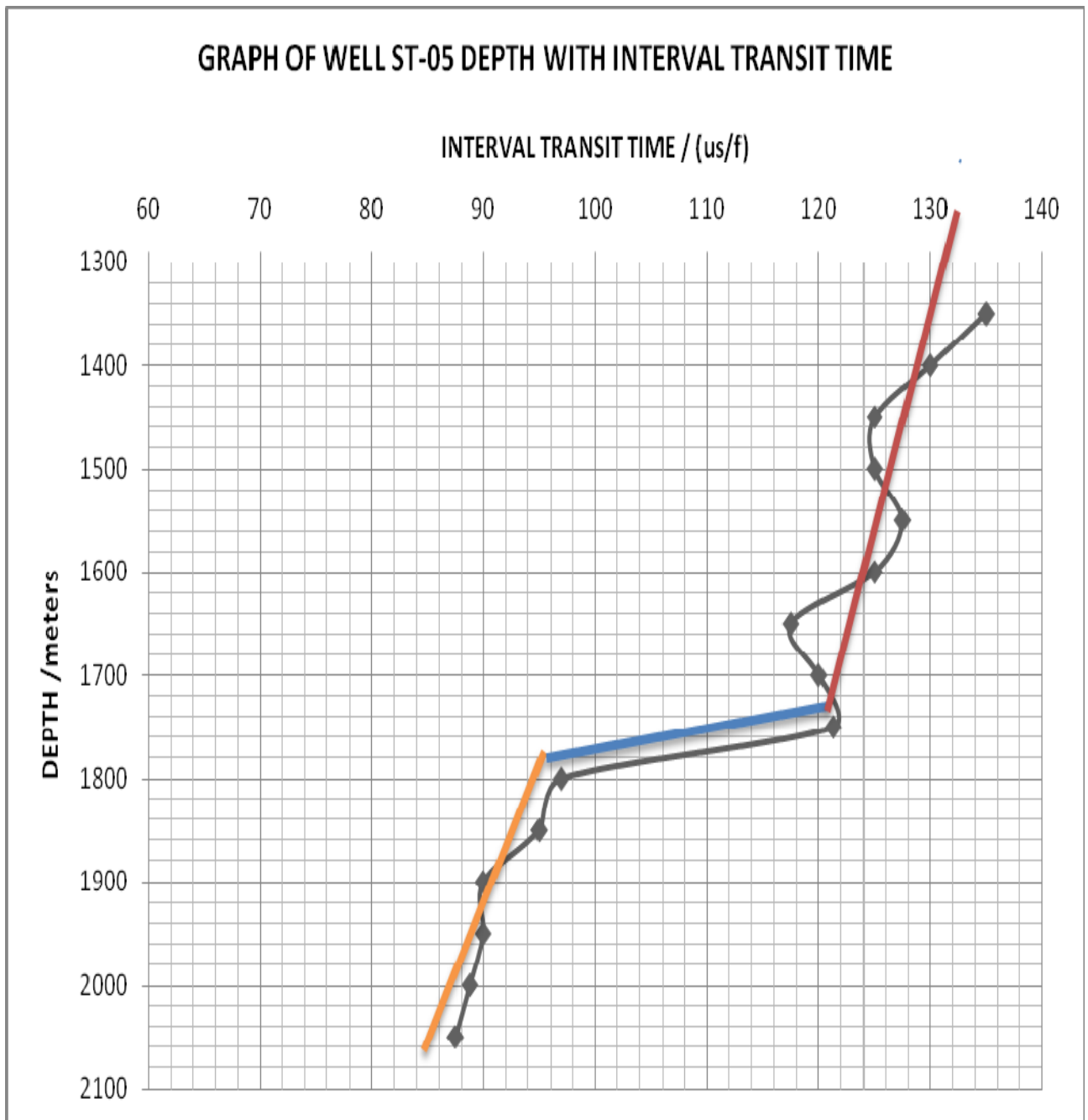


Fig.4.10, shows the depth plot of well ST-05 with interval transit time

Figure 4.10, shows normal compaction trend of well ST-05 with no over pressured sections detected. There is no increase in interval transit time at deeper depths and this suggests that low porosity formations, where pore volume is low and compaction pressure is high, contributes little to rock rigidity. The same results show in ST-06.

4.14.5 Depth Plot of Well ST-06 with Interval Transit Time

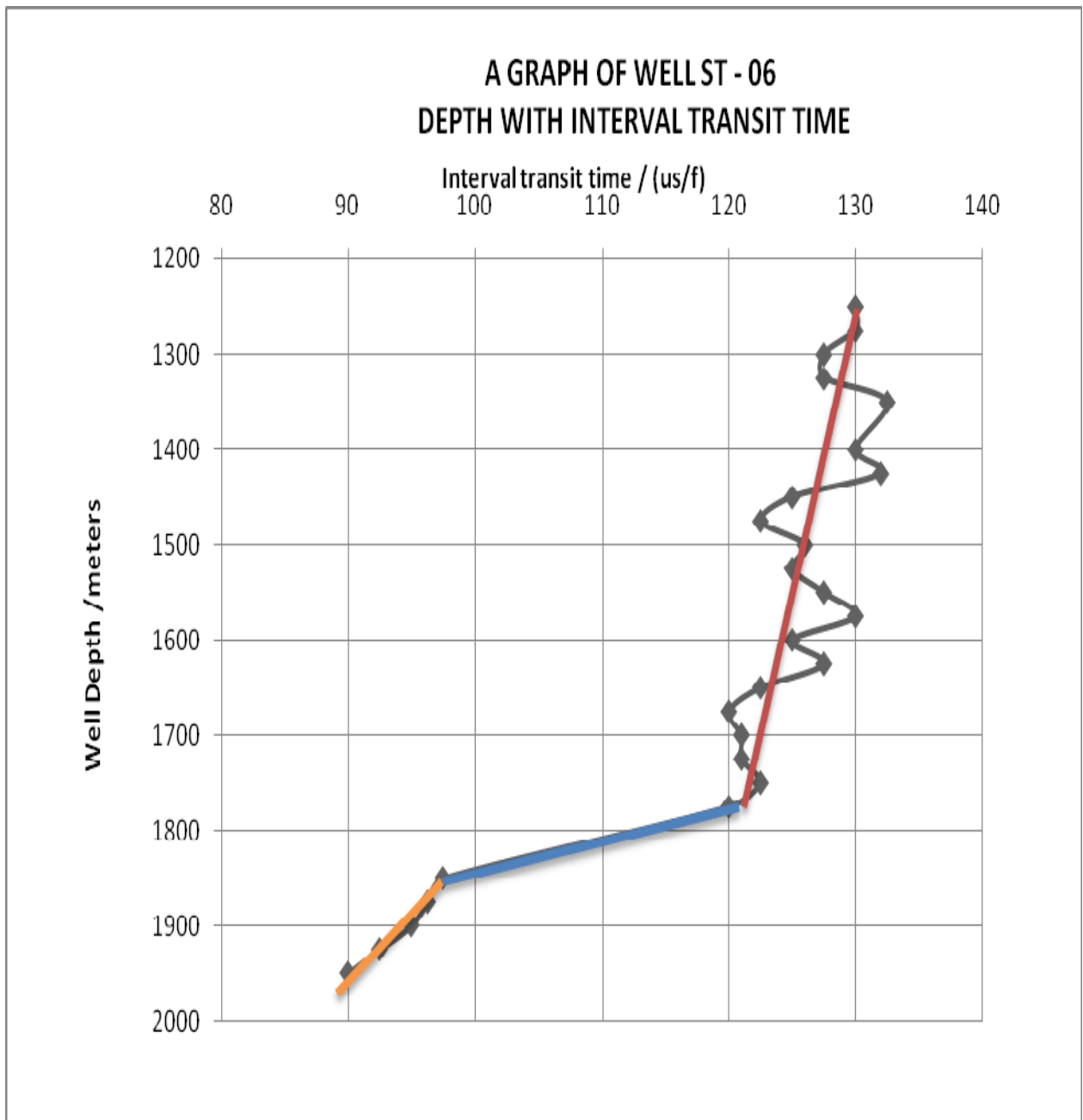


Fig. 4.11, shows the depth plot of well ST-06 with interval transit time

Figure 4.11, shows normal compaction trend of well ST-06 with no over pressured sections detected.

4.14.6 Depth Plot of Well ST-7H with Interval Transit Time

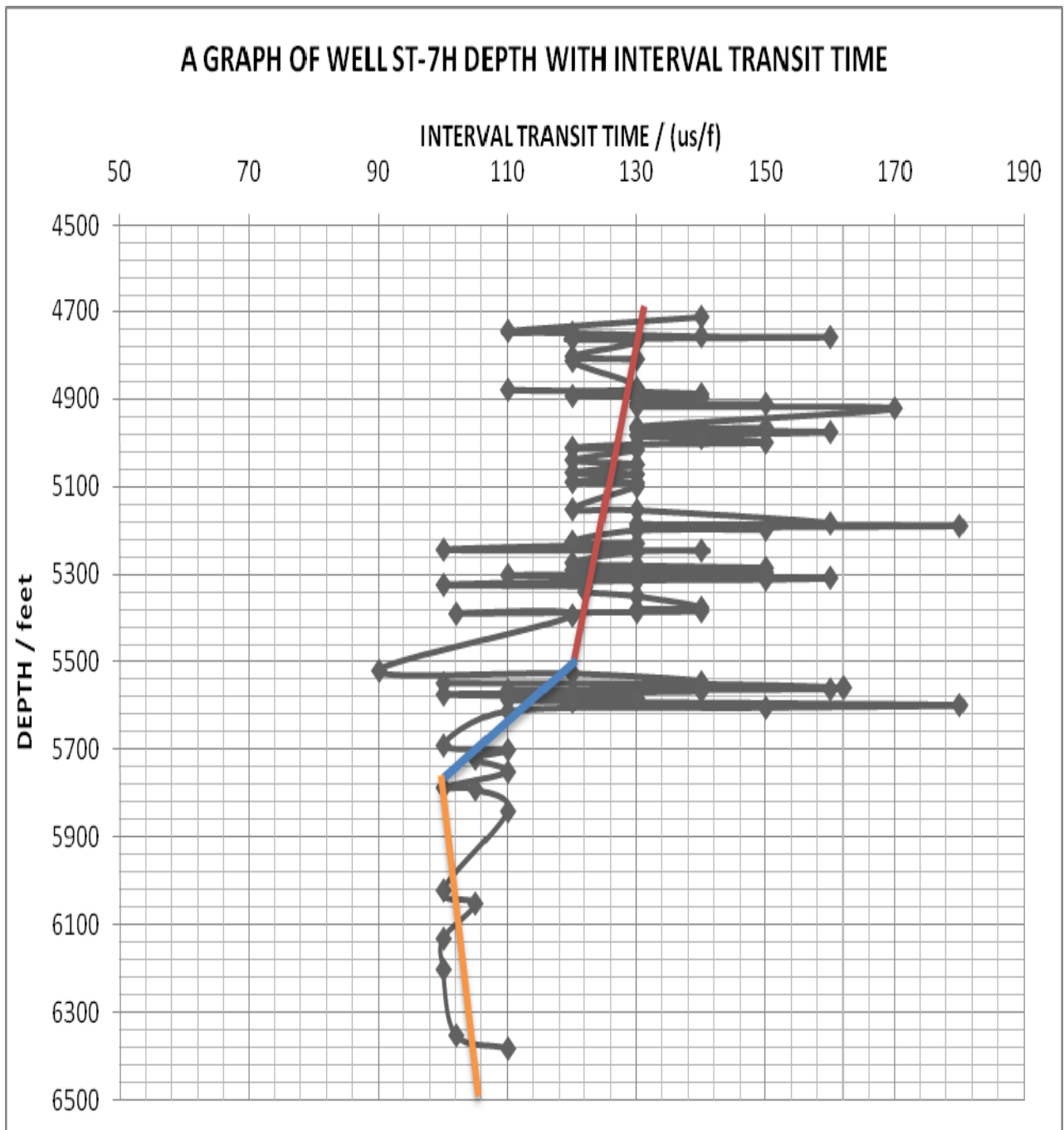


Fig.4.12, shows the depth plot of well ST-7H with interval transit time

From figure 4.12, the only over pressured section detected is shown by the orange trend line and lies at interval depths of about 5800 -6500 ft of the reservoir formation of well ST-7H.

4.15 Problems with results and interpretation

In the area of data presentation and interpretation there were no petrophysical models based on any previous study done on the area. Also there were no previous results to compare to, and interpretation of the data had to be done in isolation.

Therefore, any interpretation of the logs or any recommendation based on such interpretation is an opinion based upon inferences from log measurements, empirical factors and assumptions, which inferences are not necessarily infallible.

CHAPTER 5

CONCLUSIONS AND RECOMMENDATIONS

5.1 Conclusions

Well log analysis methods were applied successfully to wireline log data from six exploratory wells in the Western Basin, formerly called South Tano basin.

Composite well logs of the six exploratory wells studied, revealed that all the reservoir formations drilled lied in the local geology consisting of sandstone and shally silstone of the upper Albian as reported by Davies (1986) and RRI (1998).

The petrophysical parameters estimated, porosity, permeability, water saturation, reservoir thickness (pay zone) and volume of shale were used to characterize the reservoir's potential of the basin.

The resulting distribution of these estimated parameters from the log interpretation allowed the following conclusions to be drawn:

- Western Basin has a potential field for oil and gas.
- Almost all the wells studied encountered oil and gas in their formations.
- Hydrocarbon-bearing zones were between 1795 m and 2371 m.
- Over pressured formation sections were encountered in almost all the wells except two ST-05 and ST-06.
- Oil-bearing zones were more saturated, porous and permeable compared to the gas-bearing zones.
- The low porosity/low permeability of gas-bearing zones suggests tight reservoir section.
- Hydrocarbon pay zones were between 6 m and 40 m.
- Oil-bearing zones recorded estimated high pay zone than the gas-bearing zones.

- Hydrocarbon potential of the wells was not sufficient for economic viability.
- The specific objectives of the study as stated in section 1.3 have been achieved to a very large extent.

The results and interpretations show that oil-bearing zones delineated were more porous and permeable than the gas-bearing zones which perfectly agreed with theory. Gas usually has a considerably lower hydrogen concentration which varies with temperature and pressure.

Therefore when gas is present near enough the borehole to be within its zone of investigation, the neutron log and formation density logs read too low a porosity. The low hydrocarbon pay zones estimated suggest an insufficient potential for hydrocarbon accumulation in the wells, which goes to prove the researched hypothesis stated at section 1.4.

Though petrophysical parameters such as porosity, permeability and water saturation were looking promising the results was inconclusive. This may be due to the severe reservoir compartmentalization, suggested by Philips and PetroCanada. The reservoir quality of the western basin is affected by numerous faults with varying throws, these faults appear to be sealing causing compartmentalization in areal sense (Williams, 1995).

In the past, G.N.P.C has drilled two horizontal well such as ST-7H, which is part of wells studied, in an attempt to develop these reserves and overcome the problem of compartmentalization. All the studied vertical wells drilled appear to drain very limited areas due to the fault blocks (Williams, 1995). However the solution of employing horizontal wells to connect fault blocks may cause some of the reservoir sandstone layers to be missed.

The abnormal pressure zones detected in almost all the wells studied posed a difficulty challenge in trying to economically develop the Tano fields. Its major challenge lies in the safety of drilling tools and cost-effective of well design.

The well log analysis methods employed, is efficient and less expensive in prospecting for hydrocarbons and can be relied upon, when combined with other geophysical methods such

as seismic and core analysis, for further exploratory work and development of the basin. A reservoir simulation based on this new reservoir description will have greater predictive power because reservoir flow capacity is better defined in this study.

5.2 Suggestions for Further Work.

A review of the literature reveals that an analysis of this type of work has not been done in any great detail, considering the number of log interpretation methods and wireline logs available. More importantly there were no core and reservoir area data available to compare and compute the hydrocarbon reserves in place respectively.

It is opinion of this author that the petrophysical data obtained is of sufficient quality and that, further verification of this work can be done by performing similar types of analysis on these reservoirs, such future work is a worthwhile pursuit and therefore recommended.

REFERENCES

1. Alger, R. P. (1980). Geological use of wireline logs: in Developments in Petroleum Geology – 2, G.D Hobson ea, Applied Science Publ London pp.207-272.
2. Allaud, L.A and Martin, M.H. (1977) Schlumberger: The history of well log technique. Publishers: John Wiley & sons Inc.
3. Allen, D et al., (1989). Logging while Drilling: Oilfield Review, April, Pp. 4 -17.
4. Archie, G. E. (1942). The electrical resistivity log as an aid in determining some reservoir characteristics: Petroleum Technology, V.S, p.54-62.
5. Asquith, G and Gibson. C. (1982). Basic Well Log Analysis for geologists: A.A.P.G Publ., Tulsa, p.216
6. Bloch, S. (1993). Empirical Prediction of Porosity and Permeability A.A.P.G Bulletin 77
7. Brown.R.J.S and Gamson, G.W.(1960).Nuclear magnetic logging, AIME,vol 219 pp 199-207
8. Chapman, R. E. (1983). The logging of Boreholes: Petroleum Geology, Concise study, Elsevier, Amsterdam, p.107-157.
9. Chopra.S and Huffman A.R. (2006). Velocity determination for pore-pressure prediction. The Leading Edge, December 2006 Vol.25, No.12 © 2006 Society of Exploration Geophysicists. pg.1502
10. Coats, G.R. and Dumanoir, J.L. (1974). A New Approach to Improved Log- Derived Permeability. The Log Analyst, (January-February 1974), pp. 17
11. Crain E. R. (1986).The Log Analysis Handbook. Publishers: Pennwell,Publishing Company Tulsa, Oklahoma, USA.
12. Crook, L. (1975). Oil terms – a dictionary of terms used in oil exploration and development: Wilton House Publications, London, p.160.

13. Davies, D.W. (1986). The Geology and Tectonic Framework of the Republic of Ghana and the Petroleum Geology of the Tano Basin, Southwestern Ghana. Internal Report, G.N.P.C.
14. Desbrandes, R. (1985). Encyclopedia of well logging: Graham & Trotman, London, p.584.
15. Dewan J.T.(1983). Modern Open Hole log Interpretation: Pennwell Publ. Co.,Tulsa Oklahoma, p. 361.
16. Doveton J. H. (1986). Log Analysis of Subsurface Geology – Concepts and computer methods; John Wiley and sons, p.273.
17. Doveton, J., H.: (1994).”Geological Log Analysis Using Computer Methods, AAPG Computer Applications in Geology, No. 2, AAPG, Tulsa, pp.169.
18. Dresser Atlas, (1982). Well logging and Interpretation Techniques. The Course for Home Study, 2nd Ed.
19. Dullien, F. (1992). Porous Media - Fluid Transport and Pore Structure. Publ: Academic press, San Diego
20. Elliott, H. W., (1983). Some Pitfalls’ In Log Interpretation: Log Analyst, V. 24, p.10-24.
21. England, R.E, (1975). Well log Interpretation: Birdwell Div., Seismograph Service Corp., Tulsa, Oklahoma.
22. Fertl, W. H. (ed), (1976). Abnormal Formation Pressures – Implications to Exploration, Drilling and Production of Oil and Gas Resources: Elsevier, Amsterdam.
23. Hansen, R.R. and white, J., (1991). Features of logging while Drilling: SPE//ADC Conf., Amsterdam, Paper 21989.

24. Heslop, A., (1974). Gamma – ray response of shaly sandstones: SPWLA 15th Ann. Symp. Trans. Paper M, p.11.
25. Hilchie, D.W. (1982). Advanced Well Log Interpretation: D.W. Hilchie Inc., Golden, Colorado.
26. Hobson, G.D. (1984). The occurrence and origin of oil and gas: in Modern Petroleum Technology, G.D. Hobson ea. Applied Science Publ., London, p. 1 – 28.
27. Jackson, J.A. (2001). The history of NMR well logging, publishers: John Wiley & Sons Inc. pg 340-342.
28. Jenkins, R.E., (1960). Accuracy of porosity determinations: First SPWLA Logging Symp., Tulsa, Oklahoma.
29. Johnson, H.M. (1962). A history of well logging, SEG Geophysics, Volume 27, p 507.
30. Labo J., (1986). A practical Introduction to Borehole Geophysics. Tulsa, Okla. Society of Exploration Geophysicists.
31. Levorsen, A., (1967). Geology of Petroleum: W.H. Freeman & Co., San Francisco, p.724.
32. Lynch, Edward S., (1962). Formation Evaluation. New York, Harper and Row.
33. Mah, G. (1987). Geological Evaluation of the onshore North Tano Basin. PCIAC/GNPC Internal Report.
34. Mario, A. Neil.R.B., and Brent, A.C., (2006). Calibration and ranking of pore-pressure prediction models - The Leading Edge, December 2006 Vol. 25, No. 12, pp. 1516–1523.
35. Merkel, R.H., (1979). Well Log Formation Evaluation: A.A.P.G. Continuing Education Series, No. p 14, 82.

36. Misk, A., Mowat, G., Goetz, J. and Vivet, B. (1977). Effects of hole conditions on log measurements and formation evaluation: SAID 5th Ann. European Symp. Trans., Paris, Comm.22, p16.
37. Mitchell J. (1960) Limestones of Ghana. Ghana Geological Survey Bulletin No. 23
38. Morris, R.L. and Briggs, W.P. (1967). Using Log Derived Values of Water Saturation and Porosity. Well Log Analysts, 8th Ann. Logging Symp.
40. Osborne, D.A. (1992). Permeability Estimation Using a Neural Network: A Case Study from the Roberts Unit, Wasson Field, Yoakum County, Texas,” AAPG South West Section Transactions, pp. 125-132.
41. Patchett, J.G. and Coalson, E.B., (1979). The determination of porosity in sandstones and shaly sandstones: Part 1. Quality control: SPWLA 20th Ann. Symp.Trans. Paper QQ. p17.
42. Pirson, S. J., (1983). Geologic well log analysis: 3rd ea. Gulf Pub. Corp.,Houston, p.475.
43. Pirson, S.J.: (1963). Handbook of Well Log Analysis. Englewood Cliffs, N.J.,
44. Ransom, R.C., (1977). Methods based on density and neutron well logging responses to distinguish characteristics of shaly sandstone reservoir rock: Log Analyst, v.18, p. 47-63.
45. Raymer, LL. Hunt, E.R. and Gardner, G.H.F., (1980). Improved Sonic Transit Time-to-Porosity Transform: SPWLA Logging Symp. Trans., July, 1980.
46. Rider, M.H., (1996). The Geological Interpretation of Well Logs: 2nd Ed, Gulf Pub Corp, Houston, p. 280.
47. Robinson, E.S., (1988). Basic exploration geophysics, publishers: John Wiley & Sons Inc, pp. 501-539.

48. RRI (1998). Southern Ghana regional Biostratigraphic and Geochemical Review
.Volume 1. Report Number 5322/1b
49. Sagesman, F.F., (1980). Well logging method, Geophysics, 45, p 1667-1668.
50. Schlumberger Ltd.: "Log Interpretation Charts," Houston, Texas, (1987).
51. Schlumberger, (1989). Log Interpretation charts, Well Services, Houston.
52. Schlumberger, (1989).Log Interpretation Principles/Applications, Well Services,
Houston.
53. Seever, D.O. (1966). A nuclear Magnetic method for determining the permeability of
sandstone, Trans. 7th Ann. SPWLA logging Symp, Tulsa Ok.
54. Sengel, E.W., (1983). Basic Well Logging: The Institute for Energy Development
(IED), Oklahoma City, p.91.
55. Serra, O., (1984). Fundamentals of Well Log Interpretation: 1, The Acquisition of
Logging Data, Elsevier, Amsterdam, p.423.
56. Serra, O. (1986). Fundamentals of Well Log Interpretation: 2, The Interpretation of
Logging Data, Elsevier, p.684.
57. Snyder, Donald D, and David B. Fleming, (1985). Well logging – A 25 year
perspective, Geophysics, V.50, n. 12 p.2504-2529,(December 1985).
58. Thomas, D.H., (1977). Seismic applications of sonic logs: SPWLA 5th European
Symp. Trans., Paris, Paper 7, p.24.
59. Threadgold, P., (1971). Some problems and uncertainties in log interpretation:
SPWLA 12th Ann. Symp. Trans., Paper W. p.19.
60. Turcan, A.N., Jr., (1966). Calculation of water quality from electrical logs-- Theory
and practice. Department of Conservation, Louisiana Geological Survey

61. Timur, A.: (1968). An Investigation of Permeability, Porosity, and Residual Water Saturation Relationship for Sandstone Reservoirs. The Log Analyst, Vol. 9, No. 4, (July-August 1968), pp. 8.
62. Tixier, M.P.: (1949). Evaluation of Permeability from Electric-Log Resistivity Gradients. Oil & Gas Journal, (June 1949), pp. 113.
63. TROY IKODA GROUP (2001). Republic of Ghana North Tano Exploration License Prospective Analysis. Volume No. 1 Text and Composite Logs. Internal Report G.N.P.C.
64. Trompette, R. (1994) Geology of Western Gondwana, A.A. Balkema Publishers.
65. Welex, (1978). An Introduction to Well Log Analysis: Houston, Texas, p.46.
66. Wiener, J., M., et al.: (1991). Predicting Carbonate Permeabilities from Wireline Logs Using a Back-Propagation Neural Network, CM2.1, Society of Exploration Geophysicists, Expanded Abstracts with Biographies, 1991 Technical Program, Vol. 1.
67. Winsauer, W. (1952), Resistivity of brine-saturated sands in relation to pore geometry, AAPG Bulletin, 32, p253-277,
68. Williams, E. (1995). Evaluation of the Seismic Data for the South Tano Reservoir Area In preparation of doctoral thesis work. School of Mines Colorado USA.
69. Worthington, P.E., (1985). The Evolution of Shaly-Sand Concepts in Reservoir Evaluation: The Log Analyst, v.26, No. 1, p. 23-40.
70. Wycoff, R.D., Botset, H.G., Muskat, M. and Reed, D.W., (1934). Measurement of permeability of porous media: A.A.P.G. Bull., v. 18, p.161-90.
71. Wyllie, M.R.J. and Rose, W.D. (1950). Some Theoretical Considerations Related to the Quantitative Evaluation of the Physical Characteristics of Reservoir Rock from Electric Log Data, Trans., AIME, Vol. 189, pp. 105.

APPENDIX A

Table 1a shows WELL 1S - 1X reservoir section petrophysical raw data

ZONES	Depth / Meters	Reservoir Thickness / M	GR / API	Msfl	R_{llm} shallow	R_{lld} Deep	Density / g/cc	CNL / ØN
1	1838 - 1841	3.00	30	10.00	20.00	40.00	2.45	6
2	1841 - 1844	3.00	50	3.00	6.00	6.00	2.275	21.6
3	1844 - 1847	3.00	52	3.10	3.00	5.00	2.3	21.6
4	1847 - 1850	3.00	55	2.70	4.00	4.00	2.31	23
5	1850 - 1853	3.00	42	4.00	7.00	7.00	2.325	23
6	1853 - 1855	2.00	63	2.20	4.00	4.00	2.31	25
7	1855 - 1856	1.00	63	8.00	10.00	10.00	2.475	12
8	1856 - 1857	1.00	45	3.50	9.00	9.00	2.275	22.5
9	1857 - 1859	2.00	45	2.20	7.00	7.00	2.275	22.5
10	1859 - 1861	2.00	40	6.00	9.80	9.80	2.25	25.5
11	1861 - 1864	3.00	35	7.00	10.00	20.00	2.4	12
12	1864 - 1867	3.00	45	3.00	8.00	8.00	2.275	24
13	1867 - 1868	1.00	45	10.00	17.00	17.00	2.425	13.5
14	1868 - 1870	2.00	50	4.00	7.00	7.00	2.3	19.5
15	1870 - 1871	1.00	50	2.50	5.00	5.00	2.4	16.5
16	1871 - 1872	1.00	50	4.00	7.00	7.00	2.366	22.5
17	1872 - 1873	1.00	45	6.00	8.00	8.00	2.366	22.5
18	1873 - 1875	2.00	45	3.50	4.00	4.00	2.4	12
19	1875 - 1878	3.00	55	4.00	3.00	3.00	2.3	24
20	1878 - 1881	3.00	65	4.00	4.00	4.00	2.375	25.8
21	1881 - 1882	1.00	65	1.00	2.00	2.00	2.37	24.6
22	1882 - 1883	1.00	65	2.00	2.00	2.00	2.37	24.6
23	1883 - 1884	1.00	40	8.00	8.00	8.00	2.4	25.5
24	1884 - 1885	1.00	40	5.00	4.00	4.00	2.4	25.5
25	1885 - 1886	1.00	50	2.00	3.00	3.00	2.4	25.5
26	1886 - 1887	1.00	45	1.00	4.00	4.00	2.4	25.5
27	1887 - 1889	2.00	45	2.00	2.50	3.00	2.4	25.5
28	1889 - 1890	1.00	45	3.00	4.00	5.00	2.4	25.5
29	1890 - 1893	3.00	40	2.00	2.50	3.00	2.3	26.4
30	1893 - 1896	3.00	55	1.00	1.50	1.50	2.315	23.1
31	1896 - 1898	2.00	45	2.00	1.50	1.50	2.35	24
32	1898 - 1900	2.00	35	5.00	4.00	4.00	2.35	24
33	1900 - 1904	4.00	48	1.00	1.00	1.10	2.325	24
34	1904 - 1905	1.00	35	2.00	1.00	1.00	2.375	25.5
35	1905 - 1907	2.00	65	2.00	1.00	1.00	2.35	24.9
36	1907 - 1908	1.00	65	4.00	3.00	3.00	2.35	24.9
37	1908 - 1909	1.00	70	3.00	1.50	1.50	2.39	27
38	1909 - 1913	4.00	55	2.00	2.00	2.00	2.39	27
39	1913 - 1916	3.00	72	0.90	1.00	1.00	2.375	30
40	1916 - 1917	1.00	58	3.00	3.00	3.00	2.45	24

41	1917 - 1920	3.00	60	5.00	4.00	4.00	2.35	30
42	1920 -1927	7.00	60	0.60	1.00	1.30	2.25	27

Table 2b shows WELL 1S - 3AX reservoir section petrophysical raw data

ZONE	Depth / Meters	Reservoir Thickness / m	GR / API	Msfl	R_{llm} shallow	R_{lld} Deep	CNL (Ø_N)	FDC (Ø_D)
1	2030 - 2034	4.0	30	1.50	2.00	2.50	33.0	2.35
2	2034 - 2035	1.0	30	3.00	3.00	9.50	32.0	2.40
3	2035 - 2037	2.0	30	1.00	1.50	1.50	32.0	2.40
4	2037 - 2038	1.0	30	0.60	1.00	1.00	28.5	2.35
5	2038 - 2040	2.0	30	1.50	1.50	1.50	28.5	2.35
6	2040 - 2041	1.0	33	0.60	1.00	1.00	33.0	2.20
7	2041 - 2042	1.0	33	1.50	1.50	2.00	36.0	2.43
8	2042 - 2043	1.0	50	2.00	2.00	8.00	33.0	2.45
9	2043 - 2047	4.0	50	0.95	0.96	0.98	36.0	2.30
10	2047 - 2048	1.0	38	10.00	0.50	5.00	39.0	2.45
11	2048 - 2060	12.0	65	0.90	0.95	0.95	43.0	2.26
12	2060 - 2063	3.0	40	3.00	2.00	2.00	44.0	2.33
13	2063 - 2065	2.0	32	0.90	0.95	0.98	45.0	2.25
14	2065 - 2068	3.0	32	5.00	5.00	5.00	40.5	2.28
15	2068 - 2082	14.0	55	0.90	0.95	0.95	40.0	2.30
16	2082 - 2085	3.0	35	1.00	2.00	2.50	43.5	2.31
17	2085 - 2095	10.0	50	0.90	1.00	1.00	39.0	2.35
18	2095 - 2096	1.0	50	4.00	4.00	4.00	39.0	2.35
19	2096 - 2098	2.0	50	1.00	2.00	2.50	39.0	2.40
20	2098 - 2099	1.0	50	4.00	4.00	4.00	37.5	2.28
21	2151 - 2158	7.0	46	1.00	1.50	1.50	41.0	2.40
22	2158 - 2164	6.0	30	1.50	4.00	5.00	36.8	2.31
23	2164 - 2173	9.0	34	1.50	2.00	2.50	29.0	2.34
24	2173 - 2179	6.0	60	0.90	1.00	1.00	29.0	2.38
25	2179 - 2182	3.0	60	0.90	1.50	1.50	37.5	2.36
26	2182 - 2184	2.0	22	2.50	2.00	2.00	39.0	2.40
27	2184 - 2186	2.0	22	1.00	1.50	1.50	37.5	2.23
28	2186 - 2188	2.0	22	20.00	20.00	20.00	33.8	2.36
29	2188 - 2190	2.0	40	1.00	1.50	1.50	30.0	2.33
30	2190 - 2192	2.0	40	3.00	3.00	3.00	30.0	2.33
31	2192 - 2204	12.0	50	3.50	1.00	1.50	26.6	2.44
32	2204 - 2207	3.0	40	1.00	1.20	1.20	31.5	2.46

33	2207 - 2210	3.0	40	0.90	1.00	1.00	33.8	2.45
34	2210 - 2213	3.0	55	2.00	1.50	1.50	34.5	2.44
35	2213 - 2218	5.0	55	0.95	1.00	1.20	34.5	2.44
36	2218 - 2222	4.0	22	1.00	1.10	1.10	35.3	2.43
37	2222 - 2223	1.0	22	3.00	4.00	6.00	36.0	2.45
38	2223 - 2225	2.0	22	10.00	90.00	90.00	36.0	2.45
39	2225 - 2229	4.0	40	2.50	2.00	2.00	28.2	2.40
40	2237 - 2240	3.0	58	0.90	0.98	0.98	36.0	2.43
41	2240 - 2246	6.0	35	0.80	0.95	0.95	32.3	2.34
42	2246 - 2252	6.0	35	30.00	9.00	9.00	33.0	2.58
43	2252 - 2259	7.0	60	0.91	0.95	0.96	27.8	2.40
44	2259 - 2270	11.0	61	0.94	0.95	0.96	34.5	2.38
45	2270 - 2271	1.0	35	10.00	4.00	4.00	33.0	2.40
46	2271 - 2274	3.0	58	6.00	3.00	3.00	36.0	2.47
47	2274 - 2277	3.0	60	0.90	0.95	0.96	27.0	2.35
48	2277 - 2295	18.0	60	0.95	0.97	0.97	31.0	2.39
49	2295 - 2313	18.0	45	9.50	6.00	6.00	30.0	2.38
50	2313 - 2316	3.0	68	0.95	0.95	0.96	21.0	2.45
51	2316 - 2317	1.0	68	6.00	3.00	3.00	33.0	2.50
52	2317 - 2318	1.0	65	0.90	0.96	1.00	33.0	2.50
53	2318 - 2320	2.0	65	2.00	1.50	2.00	33.0	2.50
54	2334 - 2338	4.0	35	5.00	5.00	6.00	36.0	2.48
55	2338 - 2340	2.0	35	3.00	4.00	5.00	19.5	2.48
56	2340 - 2341	1.0	35	5.00	4.00	4.00	19.5	2.48
57	2341 - 2342	1.0	40	6.00	4.00	4.50	20.5	2.43
58	2342 - 2343	1.0	40	2.00	3.00	3.50	20.5	2.43
59	2343 - 2347	4.0	40	3.00	4.00	4.50	22.5	2.45
60	2347 - 2351	4.0	50	5.00	3.00	3.50	21.0	2.45
61	2351 - 2352	1.0	50	2.00	3.00	3.00	21.0	2.45
62	2353 - 2354	1.0	50	4.00	4.50	5.00	21.0	2.45
63	2354 - 2355	1.0	50	0.60	0.95	1.00	22.0	2.38
64	2355 - 2356	1.0	50	5.00	4.00	4.00	22.0	2.38
65	2356 - 2357	1.0	30	0.60	0.95	0.95	24.0	2.38
66	2357 - 2360	3.0	30	5.00	9.00	9.00	24.0	2.38
67	2360 - 2363	3.0	30	1.50	5.00	7.00	30.0	2.38
68	2363 - 2364	1.0	30	6.00	7.00	10.00	15.0	2.35
69	2364 - 2365	1.0	30	2.50	6.00	8.00	15.0	2.35

70	2365 - 2366	1.0	30	6.00	7.00	9.00	15.0	2.35
71	2366 - 2367	1.0	30	1.50	5.00	7.00	21.0	2.35
72	2367 - 2370	3.0	30	2.00	5.00	7.50	21.0	2.35
73	2370 - 2371	1.0	30	2.00	4.50	7.50	21.0	2.35
74	2371 - 2373	2.0	30	10.00	6.00	8.00	22.5	2.33
75	2373 - 2375	2.0	30	2.00	4.00	4.20	22.5	2.33
76	2375 - 2377	2.0	30	6.00	5.00	5.00	21.0	2.33
77	2377 - 2393	16.0	65	0.90	0.95	0.95	28.0	2.39
78	2393 - 2396	3.0	72	2.00	0.96	0.96	31.0	2.42

Table 3c shows WELL 1S - 4AX reservoir section petrophysical raw data

Zone	Depth / Meters	Reservoir Thickness / M	GR / API	M_{sfl}	R_{llm shallow}	R_{lld Deep}	CNL	FDC
1	1833 - 1837	4.00	50	6.00	4.00	4.00	28.00	2.48
2	1838 - 1841	3.00	51	9.50	9.50	9.50	24.00	2.53
3	1841 - 1849	8.00	57	4.00	2.50	3.00	30.00	2.50
4	1849 - 1850	1.00	40.5	9.00	10.00	9.00	24.00	2.53
5	1850 - 1854	4.00	52.5	4.00	5.00	5.00	27.00	2.45
6	1854 - 1856	2.00	52.5	5.00	6.00	7.00	25.50	2.43
7	1856 - 1859	3.00	67.5	3.00	3.00	3.00	30.00	2.40
8	1859 - 1862	3.00	67.5	3.00	4.00	4.00	28.50	2.43
9	1862 - 1864	2.00	45	4.00	9.00	9.00	24.00	2.38
10	1864 - 1865	1.00	37	60.00	30.00	40.00	21.00	2.45
11	1865 - 1867	2.00	37	5.00	10.00	15.00	25.50	2.32
12	1867 - 1868	1.00	37	40.00	20.00	30.00	18.00	2.40
13	1868 - 1870	2.00	37	5.00	9.70	10.00	18.00	2.40
14	1870 - 1871	1.00	37	60.00	20.00	30.00	18.00	2.40
15	1871 - 1878	7.00	45	5.00	9.50	9.70	24.00	2.35
16	1878 - 1879	1.00	37.5	5.00	20.00	30.00	21.00	2.38
17	1879 - 1881	2.00	37.5	40.00	30.00	30.00	18.00	2.40
18	1881 - 1885	4.00	45	3.00	7.00	8.00	27.00	2.34
19	1885 - 1887	2.00	45	9.50	9.00	9.00	27.00	2.40
20	1887 - 1889	2.00	45	4.00	7.00	7.00	28.00	2.35
21	1889 - 1890	1.00	45	9.00	9.00	9.00	24.00	2.40
22	1890 - 1893	3.00	52.5	4.00	3.00	3.00	31.00	2.44
23	1893 - 1905	2.00	52.5	2.50	2.00	2.50	32.00	2.45

Table 4d shows WELL ST - 05 reservoir section petrophysical raw data

ZONE	DEPTH / M	Reservoir Thickness/ m	GR / API	M_{SFL}	R_{LL}_M	R_{LD}	Density Porosity	Neutron Porosity
1	1795 - 1797	2.00	22.5	15.0	9.5	15.0	13.0	14.3
2	1797 - 1798	1.00	52.0	50.0	10.0	20.0	10.5	17.4
3	1798 - 1799	1.00	20.0	9.8	9.2	10.0	4.5	7.8
4	1799 - 1800	1.00	60.0	30.0	9.2	10.0	12.0	18.0
5	1800 - 1801	1.00	40.5	9.8	9.0	9.5	12.0	16.5
6	1801 - 1802	1.00	70.5	9.8	9.0	9.5	10.0	28.5
7	1802 - 1804	2.00	15.0	20.0	9.5	9.5	1.5	7.5
8	1804 - 1805	1.00	97.0	3.0	3.0	3.0	18.0	45.0
9	1805 - 1807	2.00	25.0	20.0	40.0	60.0	4.5	6.0
10	1807 - 1810	3.00	35.0	9.2	5.5	9.2	23.3	24.5
11	1810 - 1815	5.00	24.0	20.0	9.4	25.0	27.0	19.5
12	1815 - 1819	4.00	33.0	9.5	7.0	9.3	22.0	21.0
13	1819 - 1821	2.00	33.0	10.0	9.0	10.0	23.3	22.3
14	1821 - 1822	1.00	33.0	5.0	3.0	4.0	16.5	30.6
15	1822 - 1823	1.00	36.0	5.0	3.0	4.0	21.6	25.0
16	1823 - 1825	2.00	36.0	8.0	6.0	8.0	19.5	19.5
17	1825 - 1826	1.00	49.5	3.0	2.0	2.5	23.4	25.5
18	1827 - 1828	1.00	22.5	3.0	2.0	2.5	24.6	18.0
19	1828 - 1829	1.00	27.0	20.0	10.0	50.0	7.5	9.0
20	1829 - 1830	1.00	30.0	20.0	10.0	50.0	24.9	20.4
21	1830 - 1832	2.00	36.0	9.2	6.0	9.2	21.0	24.6
22	1832 - 1834	2.00	30.0	35.0	10.0	2000.0	28.2	18.0
23	1835 - 1837	2.00	22.5	10.0	9.0	15.0	22.5	21.0
24	1837 - 1842	5.00	30.0	25.0	9.5	50.0	24.4	21.2
25	1842 - 1850	8.00	41.0	4.0	4.0	5.0	14.5	30.0
26	1850 - 1852	2.00	52.0	3.5	2.5	3.0	15.0	31.6
27	1852 - 1854	2.00	30.0	9.7	9.7	10.0	7.5	13.5
28	1856 - 1860	4.00	54.0	2.0	1.5	1.5	15.3	35.0

Table 5e shows WELL ST - 06 reservoir section petrophysical raw data

ZONE	DEPTH / m	Reservoir Thickness/m	GR / API	M_{SFL}	R_{LLM}	R_{LLD}	Ø_D	Ø_N
1	1811 - 1812	1.00	52.00	0.95	0.90	0.80	18.0	37.5
3	1813 - 1815	2.00	52.00	7.00	3.00	5.00	5.0	13.0
4	1815 - 1818	3.00	75.00	6.00	4.00	4.00	14.5	25.5
6	1818 - 1819	1.00	180.00	20.00	9.50	15.00	18.0	17.4
7	1819 - 1820	1.00	22.50	70.00	15.00	18.00	3.0	7.8
8	1820 - 1821	1.00	52.50	10.00	9.50	10.00	3.0	15.0
9	1821 - 1822	1.00	40.50	55.00	10.00	17.00	13.5	12.0
10	1822 - 1823	1.00	49.50	9.80	9.10	9.50	6.0	22.5
11	1823 - 1824	1.00	30.00	20.00	9.50	9.50	12.6	9.0
12	1824 - 1825	1.00	30.00	40.00	9.50	15.00	14.0	16.2
13	1825 - 1826	1.00	82.50	8.00	4.00	5.00	15.0	27.0
14	1826 - 1827	1.00	39.00	8.00	4.00	5.00	3.0	42.0
15	1827 - 1828	1.00	20.00	35.00	9.50	9.50	33.0	9.0
16	1828 - 1829	1.00	82.50	35.00	9.50	9.50	33.0	45.0
17	1829 - 1830	1.00	45.00	2.50	1.80	2.00	27.0	45.0
19	1831 - 1832	1.00	63.00	2.50	1.80	2.00	18.0	10.5
20	1832 - 1833	1.00	20.00	95.00	20.00	95.00	9.6	10.5
21	1833 - 1834	1.00	33.00	95.00	20.00	95.00	22.5	9.6
23	1834 - 1837	1.00	29.00	9.00	10.00	10.40	22.5	22.5
24	1837 - 1838	1.00	25.00	60.00	30.00	150.00	22.5	13.5
25	1838 - 1839	1.00	30.00	60.00	30.00	150.00	22.3	21.0
26	1841 - 1842	1.00	30.00	9.50	8.00	9.10	15.0	16.5
27	1843 - 1848	5.00	52.50	60.00	5.00	6.00	15.0	31.5
28	1848 - 1850	2.00	52.50	5.00	4.00	5.00	15.0	31.5

Table 6f shows Well ST - 7H reservoir section petrophysical raw data

ZONE	DEPTH / Meters	Reservoir Thickness/m	GR / API	R_{ILM} / Ohm.m	R_{ILD} / Ohm.m	RHOB / g/cm3
1	2012 - 2014	2.00	28.0	20.00	25.00	2.540
2	2014 - 2016	2.00	62.0	9.10	9.10	2.350
3	2016 - 2017	1.00	36.0	15.00	15.00	2.540
4	2017 - 2021	4.00	62.0	9.50	9.00	2.385
5	2021 - 2022	1.00	42.0	10.00	10.00	2.300
6	2022 - 2024	2.00	60.0	9.10	9.10	2.350
7	2024 - 2026	2.00	40.0	9.35	9.35	2.380
8	2026 - 2027	1.00	61.0	9.60	9.60	2.400
9	2027 - 2029	2.00	60.0	9.60	9.60	2.375
10	2029 - 2031	2.00	35.0	10.00	10.20	2.680
11	2031 - 2032	1.00	55.0	9.00	9.00	2.380
12	2032 - 2033	1.00	62.0	9.20	9.10	2.450
13	2033 - 2035	2.00	58.0	7.00	6.00	2.440
14	2035 - 2037	2.00	48.0	9.20	9.20	2.450
15	2037 - 2039	2.00	52.0	7.00	7.00	2.380
16	2039 -2040	1.00	69.0	7.00	8.00	2.460
17	2040 - 2042	2.00	47.0	9.20	9.20	2.440
18	2042 - 2045	3.00	60.0	8.00	9.00	2.430
19	2045 - 2047	2.00	58.0	7.00	7.00	2.380
20	2047 - 2048	1.00	60.0	9.00	9.00	2.380
21	2048 - 2049	1.00	45.0	7.00	7.00	2.480
22	2049 - 2051	2.00	65.0	6.00	6.00	2.370
23	2051 - 2053	2.00	60.0	7.00	7.00	2.420
24	2053 - 2057	4.00	40.0	9.20	9.20	2.380
25	2057 - 2065	8.00	68.0	5.50	5.50	2.420
26	2065 - 2067	2.00	70.0	4.60	4.60	2.400
27	2067 - 2074	7.00	75.0	4.00	4.00	2.440
28	2074 - 2076	2.00	70.0	4.50	4.50	2.400
29	2076 - 2083	7.00	40.0	9.20	9.20	2.352
30	2083 - 2085	2.00	70.0	5.00	5.00	2.400
31	2085 - 2088	3.00	55.0	6.50	6.50	2.350

APPENDIX B

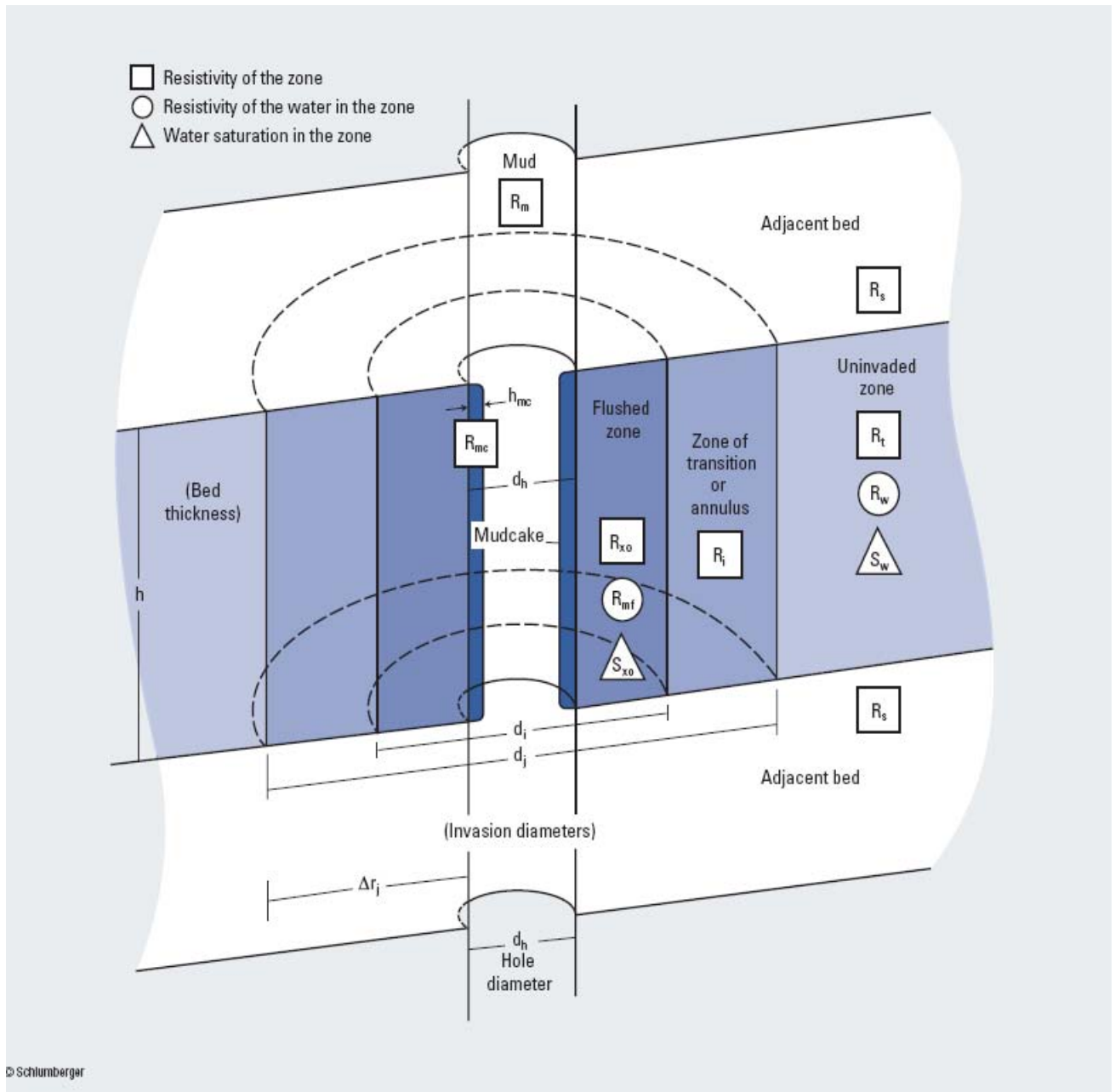


Fig.2.2 Distribution of resistivity in an invaded formation (Schlumberger, 1989)

Stratigraphic Column West Africa - Tano Basin

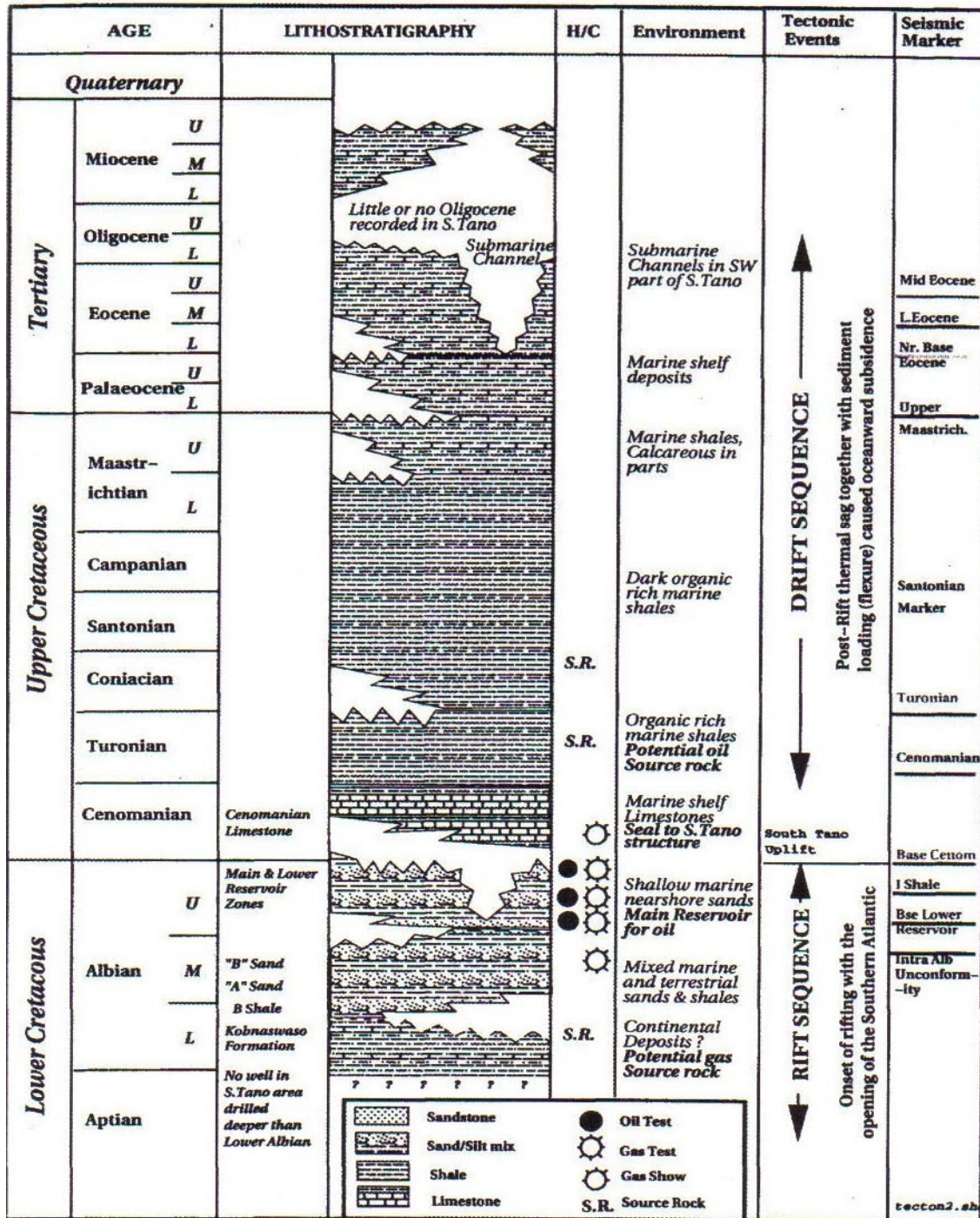


Fig.2.3, shows stratigraphic column of West Africa – Tano basin

South Tano Field Type Curve

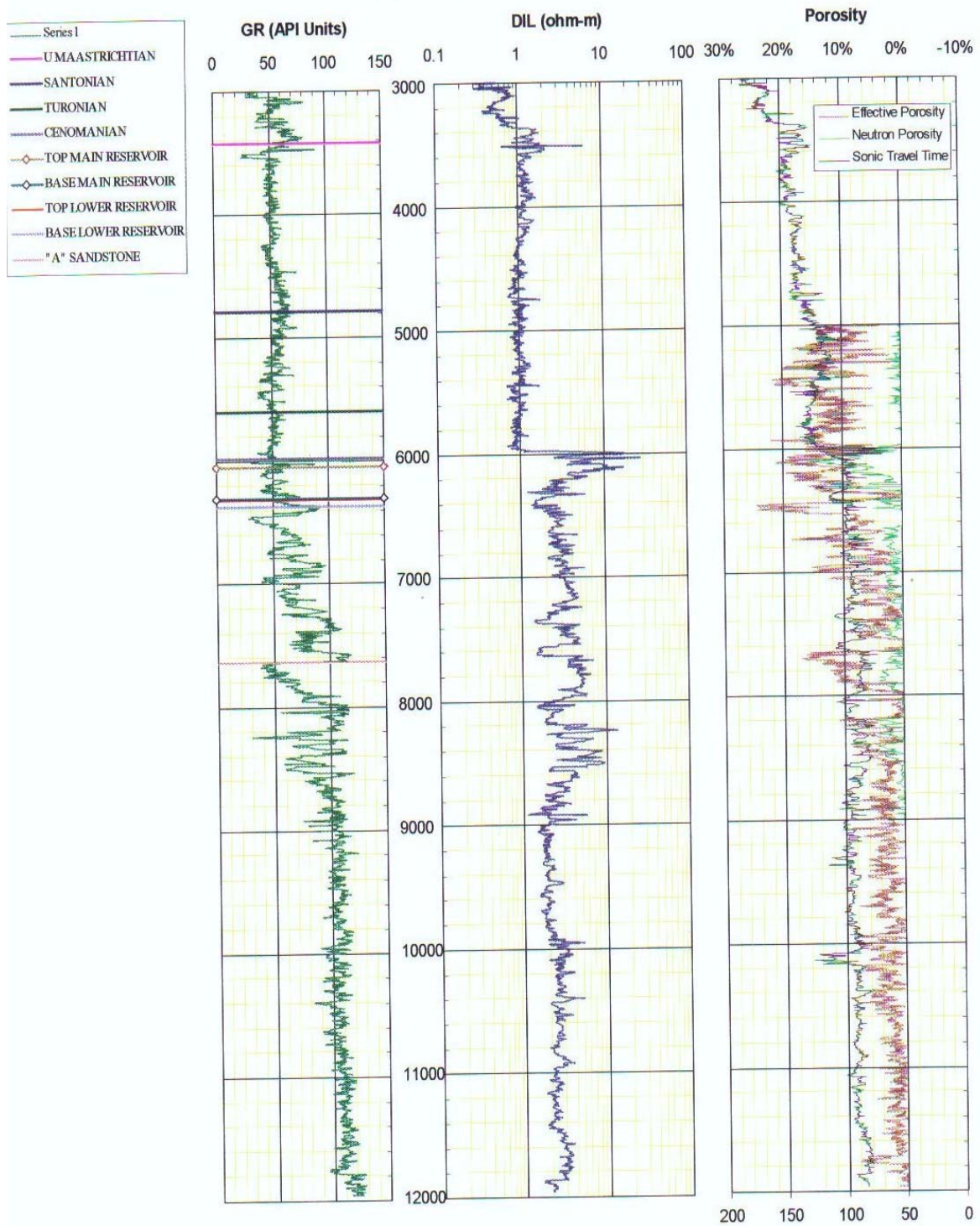


Fig.2.4 shows South Tano Field 1S-1X well log response Curve

CNL* Compensated Neutron Log and Litho-Density* Tool
(fresh water in invaded zone)

Porosity and Lithology—Open Hole

Por-11
(former CP-1e)

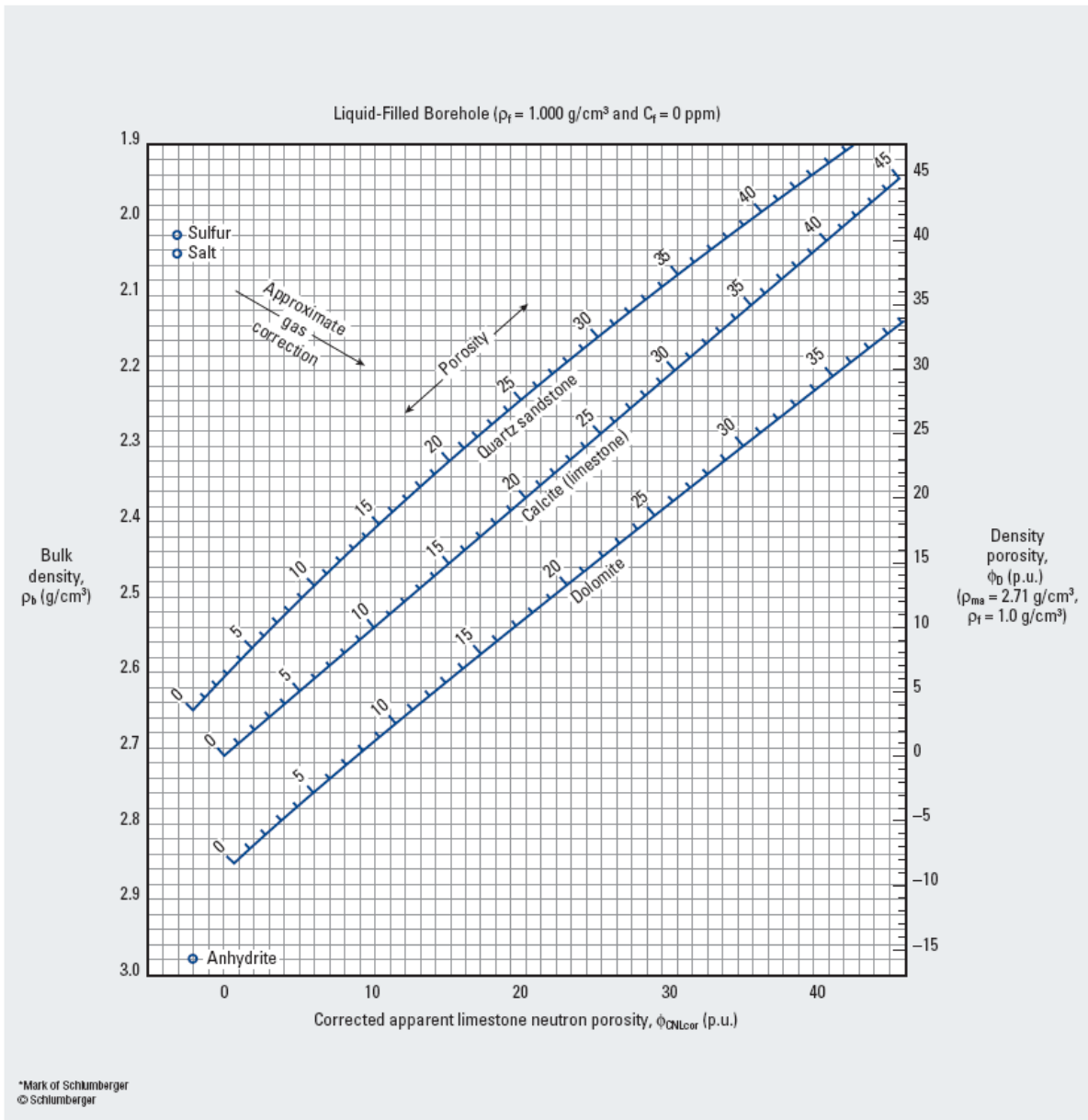


Fig.3.1 Porosity and lithology determination chart

(after schlumberger, 1989)

Permeability from Porosity and Water Saturation

Open Hole

Perm-1
(former K-3)

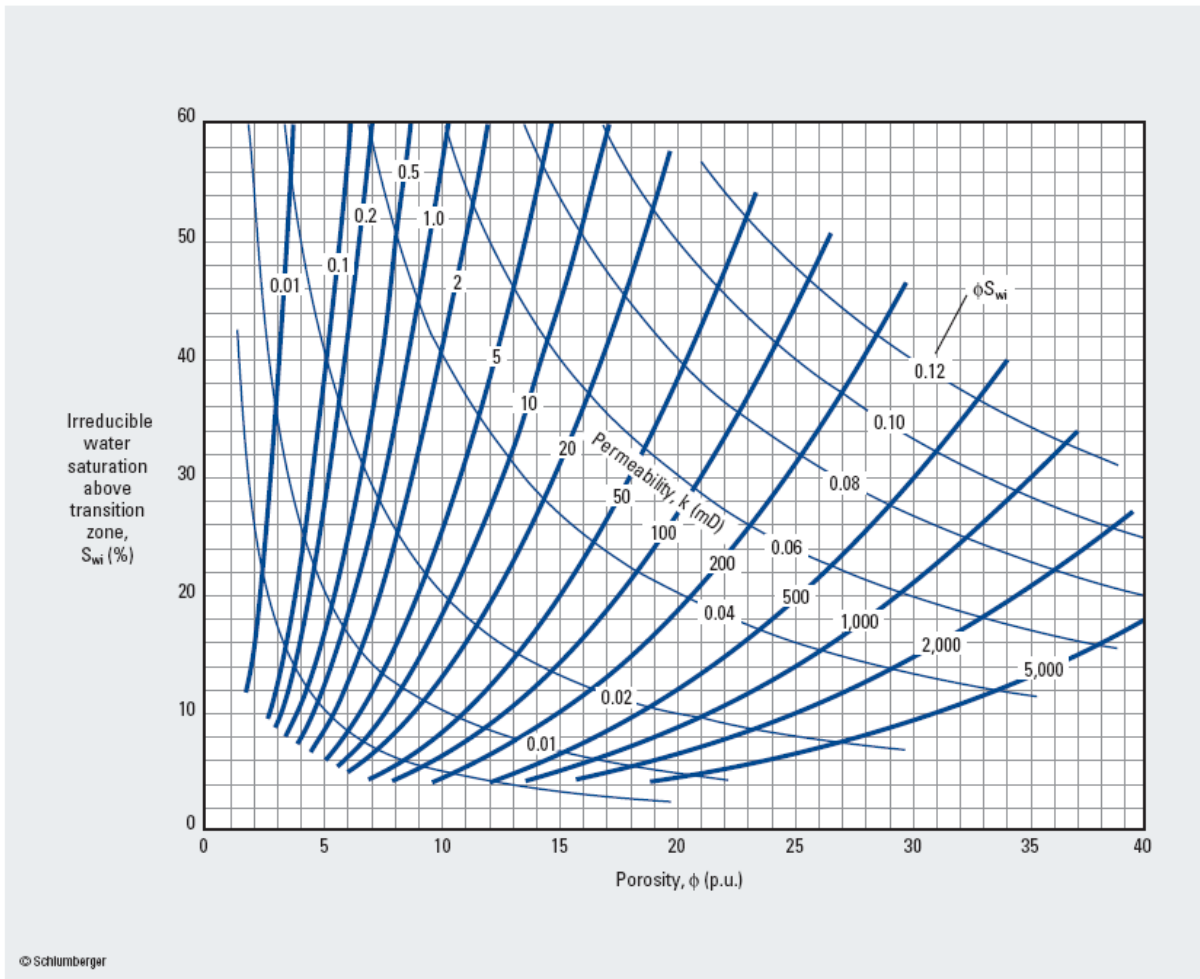


Fig.3.2, permeability from porosity and water saturation (Schlumberger, 1989)

FLOWCHART FOR LOG INTERPRETATION

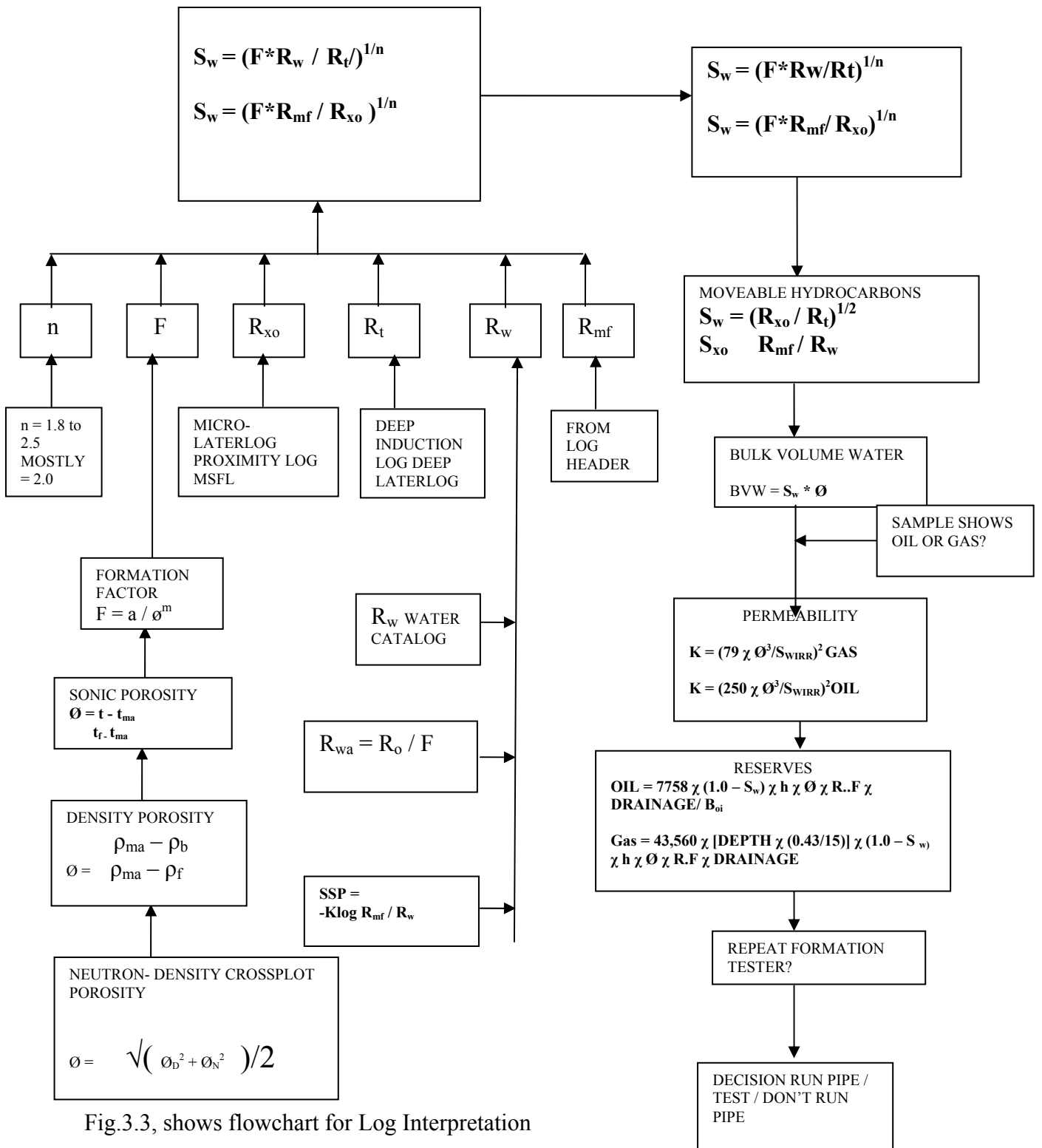


Fig.3.3, shows flowchart for Log Interpretation

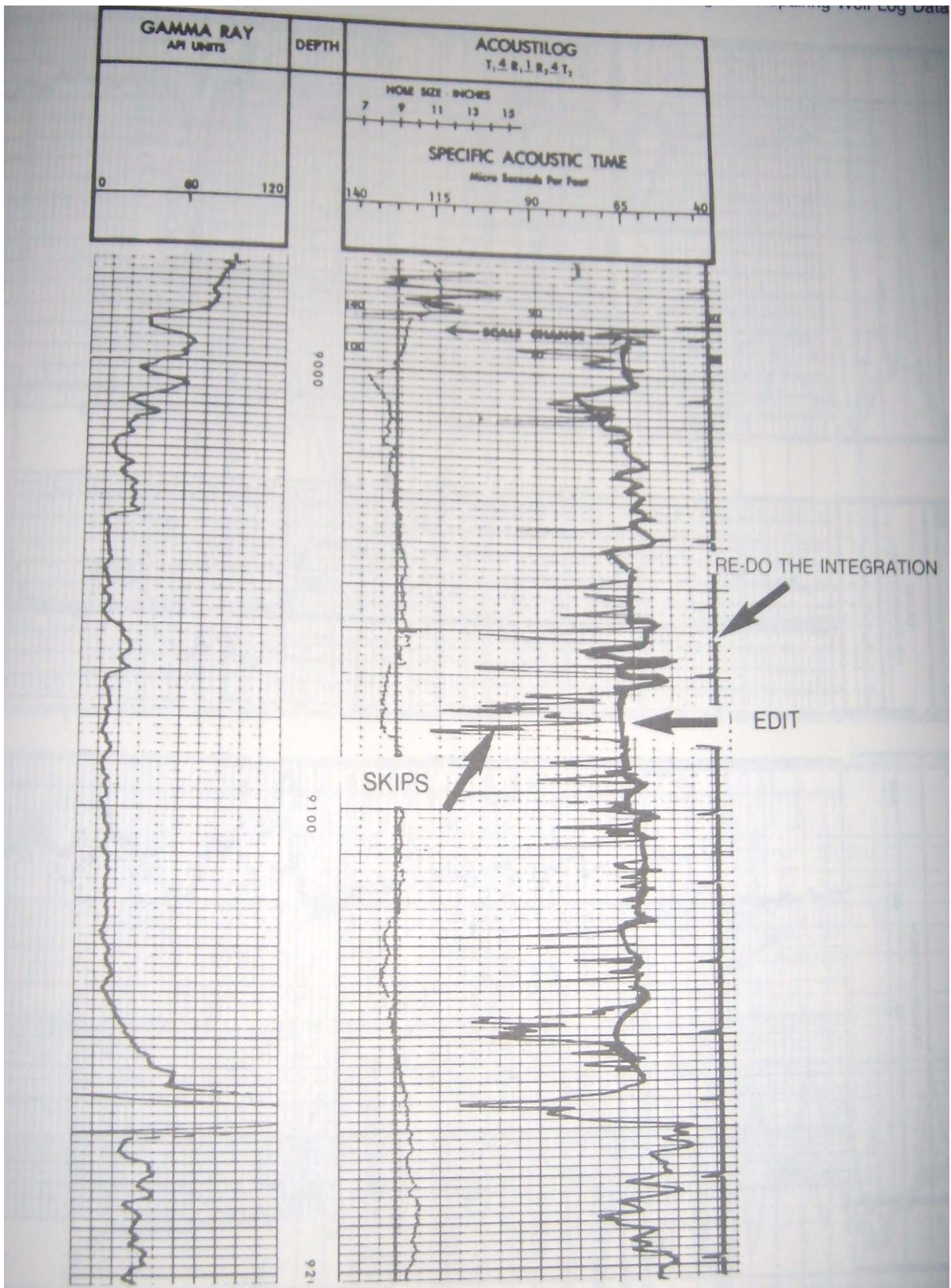


Fig.3.4, Sonic log editing

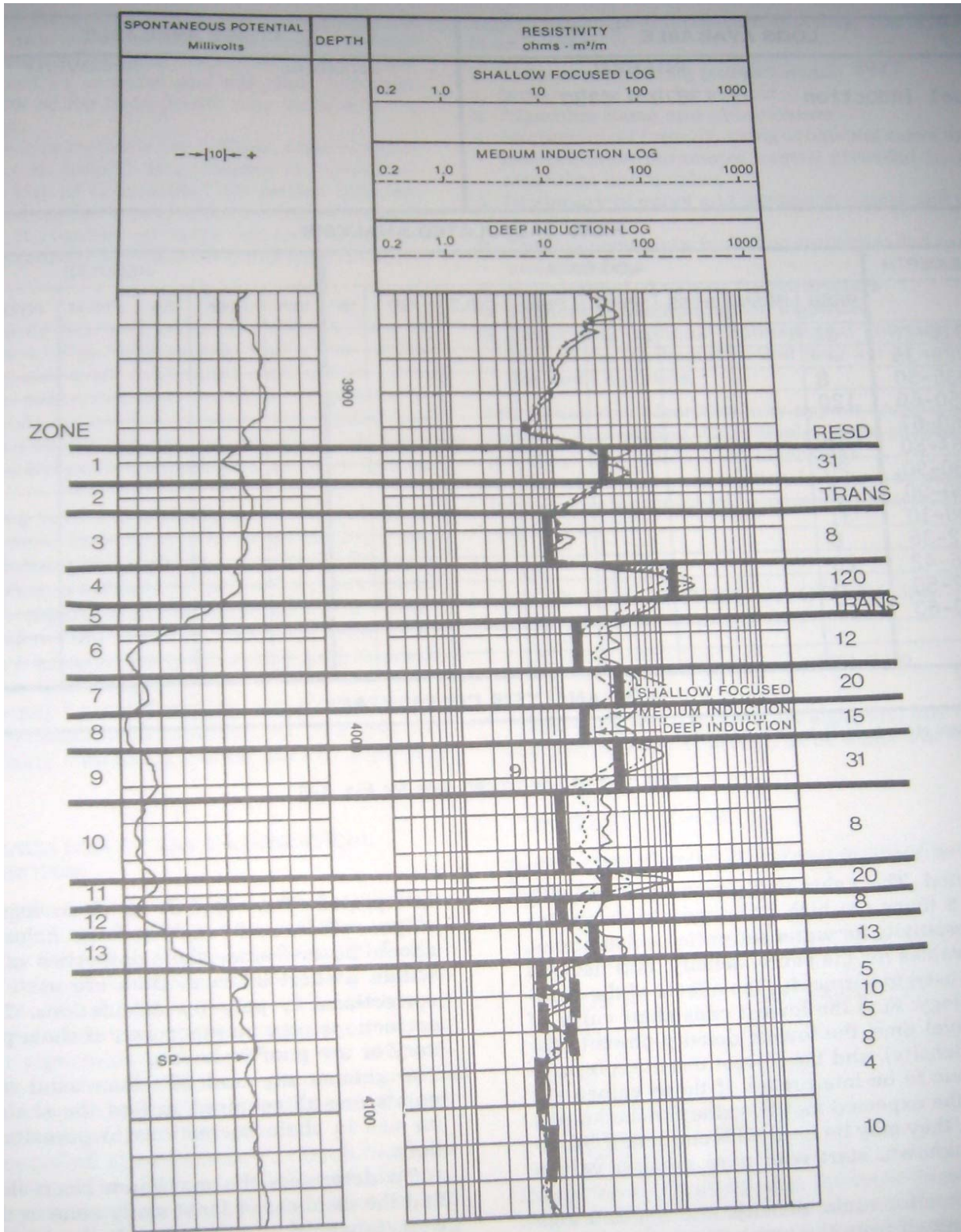


Fig.3.5 making log picks